N° d'ordre

THESE

présentée à

L'UNIVERSITE DES SCIENCES ET TECHNOLOGIES DE LILLE

Pour obtenir le grade de

DOCTEUR DE L'UNIVERSITE

Spécialité: Spectroscopies et Réactivité des systèmes chimiques

par

Vladimir ERMOCHINE

Apport de la chimie quantique à l'étude des aluminosilicates et de surfaces de silice et silicium.

Contribution of quantum chemistry to the study of aluminosilicates and of silica and silicon surfaces.

soutenue le 28 octobre 1996 devant la commission d'examen:

Président	J. SCHAMPS
Rapporteur	P. BOPP
Rapporteur	H. JOBIC
Examinateur	C. BREMARD
Examinateur	K.S. SMIRNOV
Examinateur	D. BOUGEARD

Je dédie ce travail à mes parents.

REMERCIEMENTS

Le travail présenté dans ce mémoire a été réalisé au Laboratoire de spectroscopie infrarouge et Raman de Lille (LASIR UPR 2631L) du CNRS dirigé par Monsieur J.CORSET, Directeur de recherche, et à l'Institut de Physique de l'Université de Saint–Petersbourg (Russie), dirigé par Monsieur A.RUMTSEV, Professeur.

Cette thèse a été co–dirigée par Messieurs D.BOUGEARD, Directeur de recherche au CNRS et K.S.SMIRNOV, Directeur de recherche. Je leur adresse ici mes remerciements pour m'avoir fait bénéficier de leur expérience et de leur disponibilité.

Monsieur J.SCHAMPS, Professeur, me fait le grand honneur d'accepter de présider le jury de cette thèse. Je le prie de bien vouloir trouver ici l'expression de ma grande gratitude.

Monsieur P.BOPP, Professeur à l'Université de Bordeaux I et Monsieur H.JOBIC, Directeur de Recherches à l'Institut de Recherches sur la Catalyse de Villeurbanne ont jugé ce mémoire. Je leur témoigne ma reconnaissance d'avoir accepté cette charge.

Je remercie Monsieur C.BREMARD, Directeur de recherche, d'avoir accepté de faire partie du jury.

Je remercie le Ministère des Affaires Etrangères pour la bourse, qui a permis mes séjours en France, et le personnel du DEE au CROUS de Lille pour sa disponibilité et son aide.

Je remercie l'OTAN pour son soutien financier dans le cadre du programme "High Technology" (projet crg 941422).

Je remercie Philippe FAYE et Laurence VRIELYNCK pour leurs remarques constructives pendant la préparation du manuscript.

Je remercie A.A.TSYGANENKO et A.K.KAZANSKY, Professeurs à l'Université de Saint–Petersbourg et Dr. Peter BORNHAUSER pour les discussions au sujet de ce mémoire, ainsi que Kirill , Olga, Maria, Sacha, Valera pour leur amitié.

Enfin je tiens à remercier le personnel du laboratoire pour son aide et sa bonne humeur et plus particulièrement Chantal, Denis, Gabrielle, Gaëlle, Claude, Franck, Jean–Claude, Jacky, Laurence, Marielle, Nathalie, Philippe, Polo, Sylvia,Thierry, Valérie ...

SOMMAIRE.

CHAPITRE 1
INTRODUCTION

Les silicates et aluminosilicates sont des matériaux très importants pour leurs applications industrielles et leur intérêt technologique augmente régulièrement. Il y a une grande diversité de formes structurales et cristallographiques parmi ces cristaux et de nouvelles structures apparaissent comme résultat de la synthèse chimique. Le quartz et les verres ont de nombreuses applications en optique et électronique. Les zéolithes jouent un rôle très important dans l'industrie du pétrole comme adsorbants et catalyseurs sélectifs. Cette importance pratique appelle à comprendre les propriétés chimiques et physiques de ces matériaux.

Il existe différentes méthodes expérimentales pour étudier les propriétés structurales et la nature des centres catalytiques. La spectroscopie vibrationnelle et la RMN sont très utiles, car on peut associer les caractéristiques spectroscopiques aux propriétés des liaisons chimiques et aux mécanismes des mouvements atomiques. Mais les structures compliquées, la diversité des formes (présence de cations différents et polymorphisme crystallographique) (Chapitre 2) gênent l'interprétation quantitative des données expérimentales et la compréhension de la nature des processus chimiques. Les méthodes théoriques sont complémentaires des méthodes expérimentales. Ces dernières années, le progrès de l'outil informatique autorise le calcul de structures compliquées par les méthodes de la chimie quantique même au niveau *ab initio*[1]. La dynamique moléculaire est une méthode indispensable dans la modélisation du comportement des grands ensembles d'atomes. Les méthodes théoriques appliquées dans ce travail sont présentées dans le Chapitre 3.

L'intérêt pour la compréhension des mécanismes des réactions se produisant pendant la fabrication des silicates et zéolithes est motivé par la possibilité d'obtenir des produits purs et homogènes ainsi que des cristaux avec une structure déterminée. Les méthodes de spectroscopie vibrationnelle et RMN sont appliquées pour élucider la nature des réactions chimiques pendant la synthèse. La difficulté dans l'étude de ces processus

tient au fait que les méthodes spectroscopiques ne sont capables de suivre le processus chimique qu'après la formation d'unités suffisamment grandes, alors que les premiers pas de réaction peuvent être importants pour l'optimisation des conditions de la synthèse. La chimie quantique peut aider à comprendre les étapes de la réaction sol-gel et de la synthèse hydrothermale de zéolithes. Un tel calcul conduisant à une hypothèse pour le chemin de réaction est présenté au Chapitre 4.

L'utilisation des méthodes de modélisation moléculaire est nécessaire pour étudier les processus compliqués de la diffusion des molécules dans les pores des zéolithes, de l'adsorption et de l'interaction avec le réseau. C'est une branche de la science des matériaux qui se développe très rapidement. La plupart des auteurs considèrent le réseau des zéolithes rigide. Cependant, la description correcte du comportement des molécules adsorbées (diffusion, fixation d'une molécule à un centre d'adsorption) nécessite la prise en compte des vibrations du réseau. Un grand progrès a été obtenu dans la modélisation des vibrations des silicates et aluminosilicates [2].

A chaque calcul de dynamique moléculaire se trouve une information sur le potentiel. Au début du développement de la dynamique moléculaire pour la modélisation des silicates et aluminosilicates, on a utilisé des potentiels empiriques et différents modèles de champ de force ont été appliqués [3]. Le progrès dans les méthodes de chimie quantique ab initio nous permet d'obtenir des potentiels de meilleur qualité à partir des calculs quantiques.

Les simulations de dynamique moléculaire fournissent non seulement des données structurales, mais aussi des données dynamiques. Après la transformation de Fourier d'une fonction d'autocorrélation, on peut simuler les spectres infra-rouge et Raman [3], les densités d'états vibrationels et les spectres de diffusion de neutrons [4]. L'information concernant des vibrations des atomes peut donc être obtenue et les maxima observés sur les spectres peuvent être attribués à un mouvement atomique spécifique. Les méthodes d'analyse en coordonées normales sont aussi utiles dans l'interprétation des spectres car elles donnent des valeurs quantitatives de la participation de chaque atome dans un mode de vibration. Le champ de forces *ab initio* développé et testé par simulation des

spectres infra-rouges et Raman des zéolithes est le sujet du Chapitre 5.

L'origine de l'acidité catalytique est connectée avec l'acidité de Brönsted des groupes hydroxyles des ponts $Si - OH - Al$. La substitution d'un atome de silicium par un atome d'aluminium induit la création d'une charge négative, compensée par l'apparition du proton. Celui-ci est localisé sur un des atomes d'oxygène voisin de l'aluminium. Puisque la concentration de ces centres est faible et qu'ils sont distribués dans le cristal au hasard, un modèle structural et dynamique ne peut pas être obtenu directement à partir des seules données expérimentales. Une approche théorique devient donc indispensable. Un calcul des propriétés structurales et vibrationnelles du centre de Brönsted par les méthodes de la chimie quantique *ab initio* et par la dynamique moléculaire est présenté dans le Chapitre 5.4.

Les réactions catalytiques sont des processus compliqués qui incluent différentes étapes. Actuellement, des réactions élémentaires telles que la fixation d'un proton du réseau par une molécule adsorbée peuvent être étudiées quantitativement. Le premier problème est de calculer la surface d'énergie potentielle par les méthodes de chimie quantique. Puisqu'on considère des régions du potentiel loin de l'équilibre, l'énergie de corrélation doit être prise en considération. Le problème suivant est de calculer la dynamique causée par ce potentiel. Elle est essentiellement quantique, car l'hydrogène est un atome léger. Mais l'énergie vibrationnelle des niveaux excités se relaxe et il est important de connaître les mécanismes de ce processus parce que le temps de relaxation est souvent comparable au temps de réaction. Le développement des techniques experimentales résolues dans le temps a donné beaucoup d'informations sur les temps de relaxation des états excités dans différents systèmes [5]. Tandis que la théorie de la relaxation a une longue histoire [6], les résultats théoriques obtenus sur la dynamique d'énergie vibrationnelle des atomes ou groupes moléculaires de surface ne sont pas encore très satisfaisants [7]. Une méthode quantitative pour étudier le problème de la relaxation est développée et appliquée à un système modèle simple $H/Si(111)$ dans le Chapitre 6 qui devrait être utilisée ultérieurement pour l'étude de la relaxation des vibrations des groupes OH et OD sur des surfaces de silice et dans les zéolithes.

REFERENCES

1. J.Sauer, P.Ugliengo, E.Garrone, and V.R.Saunders, Chem. Rev. **94** (1994) 2095
2. C.Brémard and D.Bougeard Adv.Materials **7** (1995) 10
3. K.S.Smirnov and D.Bougeard J.Phys.Chem. **97** (1993) 9434
4. W.P.J.H.Jacobs, J.H.M.C.Wolput, R.A.van Santen, and H.Jobic Zeolites **14** (1994) 117
5. A.Laubereau and W.Kaiser Rev.Mod.Phys. **50** (1978) 607
6. D.W.Oxtoby Adv.Chem.Phys. **47** (1981) 487
7. H.Gai and G.Voth J.Chem.Phys. **99** (1993) 740

CHAPITRE 2

LES STRUCTURES ET LES MODELES

Les zéolithes sont des aluminosilicates qui se présentent dans la nature sous différentes formes cristallographiques. De nombreuses structures ont été synthétisées dans les conditions du laboratoire. Les aluminosilicates possèdent la formule chimique $[Si_nAl_mO_{2(m+n)}]^{m-}$. Ils sont composés de tétraèdres SiO_4 et AlO_4 et les deux atomes nommés $T(T = Al, Si)$ sont connectés par un oxygène. Les atomes d'aluminium sont distribués aléatoirement dans le réseau en respectant la règle de Löwenstein: deux atomes Al ne peuvent pas être connectés par un atome d'oxygène. Dans les zéolithes, les groupements TO_4 sont arrangés dans l'espace en créant des cavités reliées par des fenêtres ou des systèmes de canaux. La charge négative causée par les tétraèdres AlO_4^- est compensée par des cations situés dans les cages des zéolithes. Les zéolithes sont caractérisées par le rapport Si/Al et la nature des cations. Les zéolithes dont la charge négative est compensée par l'introduction de protons sont appelées les zéolithes protonées. Les zéolithes avec le rapport $Si/Al = \infty$ sont appelées siliciques; ce cas idéal ne peut pas être obtenu dans les conditions du laboratoire, mais on peut produire des échantillons avec un rapport Si/Al compris entre 50 et 70 et les considérer comme zéolithes siliciques.

Les zéolithes ont une propriété structurale importante pour les applications industrielles: leur porosité. En changeant la taille de ces pores on peut contrôler les conditions des réactions chimiques. Dans les zéolithes, les pores sont normalement bien définis spatialement. Ils définissent des canaux linéaires, sinusoïdaux ou des réseaux de cages.

Dans ce travail, nous étudions les structures des zéolithes siliciques suivantes: la sodalite, la faujasite et la silicalite. Elles sont présentées dans la Figure 1. La première structure consistant en un empilement cubique de blocs sodalites est simple, alors que les deux autres, composées d'empilements tétraédriques (faujasite) ou de systèmes de canaux rectilignes et sinusoïdaux (silicalite), sont plus compliquées. Cette différence crystallographique se manifeste dans les spectres de vibrations. Comme nous le montrons

dans le Chapitre 5, les spectres de faujasite sont plus riches que les spectres de sodalite.

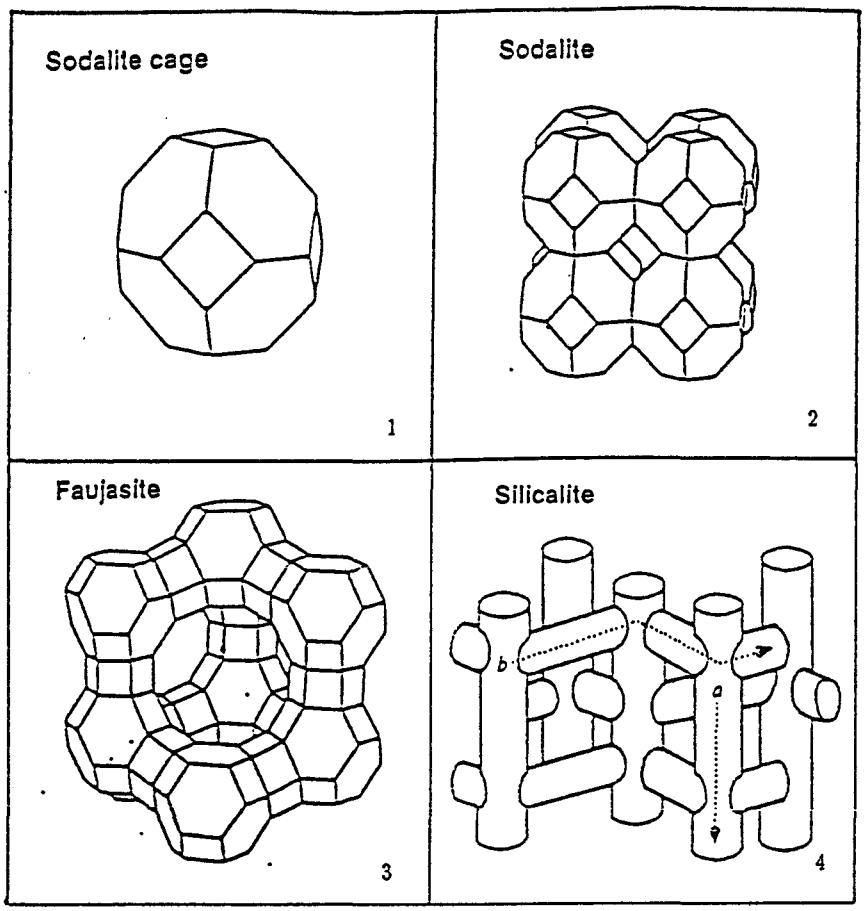

Figure 1. Les structures des réseaux de zéolithes. Dans 1, 2 et 3 les atomes T sont localisés aux intersections des arêtes, les atomes O (non représentés) se trouvent entre deux atomes T en général localisés hors du trait joignant les atomes T. Dans 4 sont représentés les deux types de canaux: a) le canal direct, b) le canal sinusoïdal.

Nous avons choisi la faujasite pour étudier la substitution des atomes de Si par Al et l'hydratation. Puisque les cations assurant l'électroneutralité n'influencent pas les vibrations dans la région $300 - 1200\ cm^{-1}$, nous nous sommes limités à cette région spectrale et avons négligé , dans ce travail, les modes de réseau de basse fréquence et la dynamique des cations. Une description plus détaillée de ce sujet peut être trouvée par exemple en [1,2]. En outre, nous nous sommes interessés à la dynamique des protons dans les zéolithes hydratées. Les données de diffraction des neutrons [3] montrent que

les protons dans les zéolithes sont localisés sur des atomes d'oxygène de pont et forment un centre de Brönsted acide (Fig. 2).

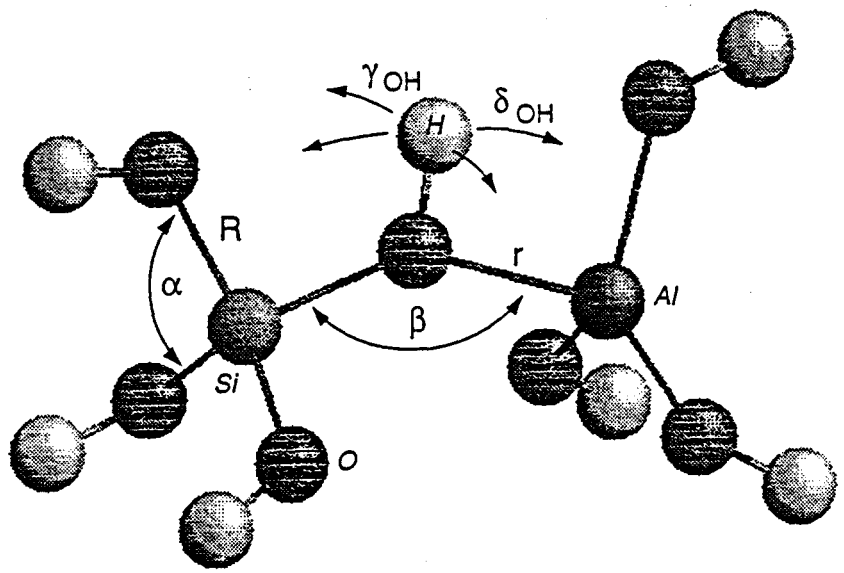

Figure 2. Le modèle moléculaire $(OH)_3SiOHAl(OH)_3$ du groupe OH du pont dans les zéolithes hydratées. Définition des coordonnées internes.

Dans le chapitre 4, nous étudions des réactions qui se produisent pendant la synthèse hydrothermale des zéolithes et les réactions sol-gel. Dans les calculs de molécules modèles par les méthodes de chimie quantique, tous les degrés de liberté ont été relaxés pendant la recherche de la géométrie correspondant à l'énergie minimale. Nous avons étudié les molécules avec le *Si* tétra- et pentavalent $Si(OH)_4$ et $Si(OH)_5^-$ permettant les calculs avec une bonne base (DZP) alors que les molécules de grosse taille $(OH)_3SiOSi(OH)_4^-$ et $(OH)_3SiOSi(OH)_3$ ont été calculées avec une base plus petite 3-21g*. L'aluminium tri- et tétravalent a été étudié avec la base DZP pour les petites molécules $Al(OH)_3$ et $Al(OH)_4^-$, et avec la base 3-21g* pour les molécules $(OH)_3SiOAl(OH)_2$ et $(OH)_3SiOAl(OH)_3^-$. Les géométries optimisées des molécules calculées sont présentées sur la Figure 3.

Dans le chapitre 5, les champs de forces pour la modélisation des propriétés vibrationnelles des zéolithes ont été obtenus par des calculs de chimie quantique. La nature

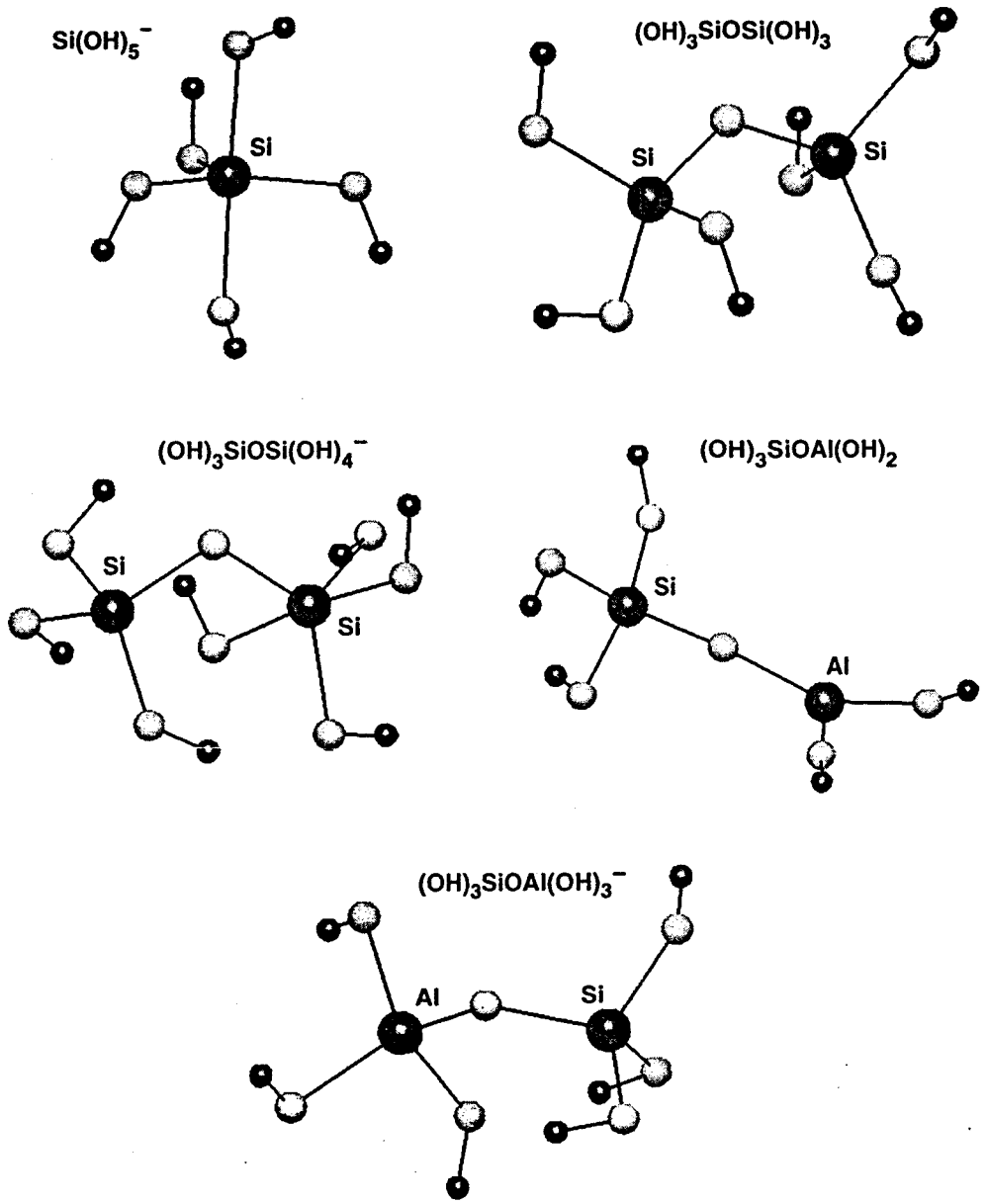

Figure 3. Géométries optimisées des molécules étudiées comme modèles de la réactivité en synthèse hydrothermale.

partiellement covalente des liaisons SiO et AlO justifie le calcul des propriétés structurales et dynamiques des zéolithes en utilisant des molécules de petite taille comme modèles [4]. Pour reproduire correctement la structure électronique de ces fragments on sature les atomes d'oxygène terminaux par des atomes d'hydrogène. Nous devons remarquer que les torsions des groupes OH terminaux dans les molécules avec deux atomes T ont été bloquées lors du calcul des propriétés vibrationnelles pour éviter la formation de liaisons hydrogènes intramoléculaires qui n'existent pas dans les zéolithes.

Pour calculer le champ de forces pour les zéolithes siliciques nous avons choisi comme modèles la molécule $Si(OH)_4$ dont la relativement petite taille permet de faire des calculs à un bon niveau de théorie (DZP/MP2) et la molécule $(OH)_3SiOSi(OH)_3$ qui sert de modèle de pont; nous l'avons étudiée avec la base 3-21g*. La molécule $(OH)_3SiOSi(OH)_3$ est présentée en Figure 4 où les coordonnées internes sont aussi définies.

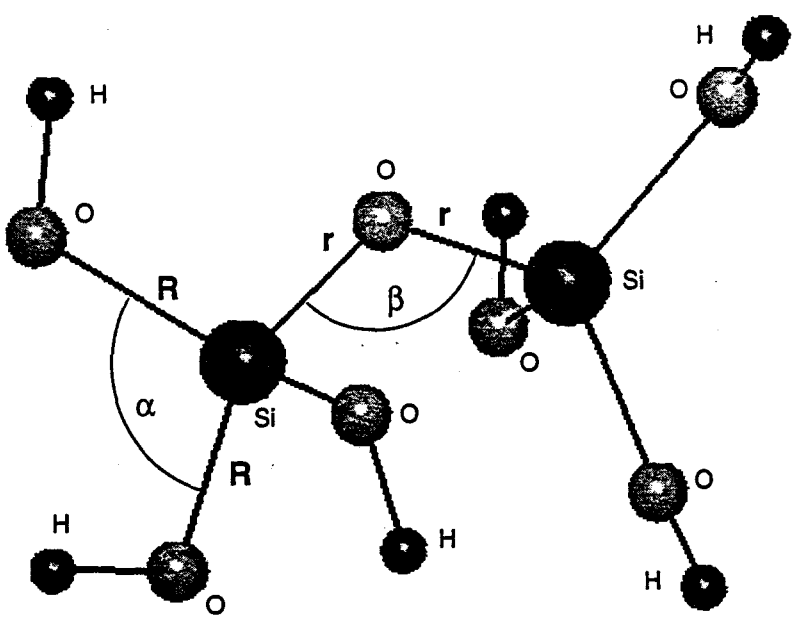

Figure 4. Le modèle moléculaire $(OH)_3SiOSi(OH)_3$ du pont dans les zéolithes siliciques. Définition des coordonnées internes.

Les molécules $Al(OH)_4^-$ (DZP/MP2), $(OH)_3SiOAl(OH)_3^-$ (3-21g*) ont été calculées pour définir le champ de force pour les zéolithes aluminées. Pour étudier les zéolithes

hydratées et les vibrations des groupes OH du pont, nous avons choisi les molécules $H_3SiOHAlH_3$ (3-21g* , DZP/MP2) et $(OH)_3SiOHAl(OH)_3$ (3-21g*). Cette dernière est présentée en Figure 2.

Dans le chapitre 5.4, nous étudions les propriétés vibrationnelles des groupes OH sur la surface de silice. La silice est l'oxyde de silicium SiO_2 dans la phase amorphe. Des groupes OH terminaux couvrent la surface de la silice. Les études vibrationnelles montrent que les deux types de groupes OH - isolés et géminaux - peuvent exister. Le groupe OH isolé est présenté en Figure 5 avec la définition des coordonnées internes. Le modèle des groupes OH sur une surface de la silice considéré dans ce travail est la molécule $Si(OH)_4$. Elle a été traitée par la chimie quantique au niveau DZP/MP2. Mais la différence possible dans le comportement vibrationel [5] entre les groupes isolés et géminaux peut être révélée par le calcul du cluster plus gros : $OH - Si(OSiH_3)_3$.

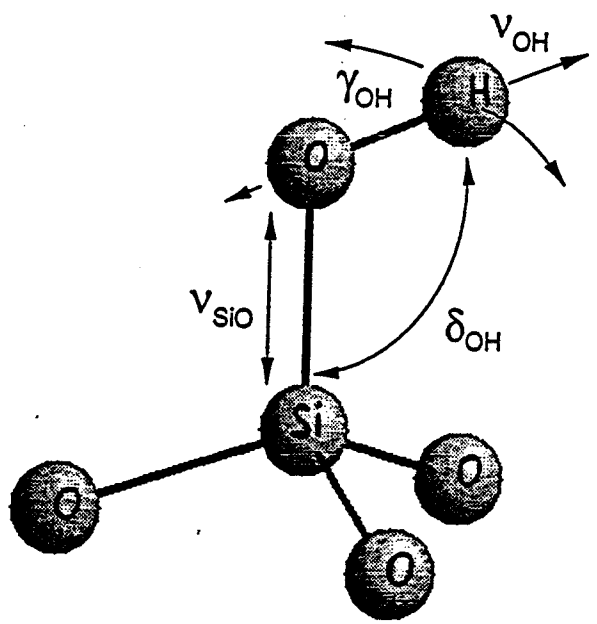

Figure 5. La définition de coordonnées internes du groupe OH terminal sur la surface de la silice

Les structures cristallographiques des zéolithes présentées seront utilisées ensuite dans l'étude des spectres vibrationels par la dynamique moléculaire (Chapitre 5). Les modèles moléculaires de fragments de zéolithes et de surface de la silice, précédemment

introduits, seront traités par des méthodes de chimie quantique (Chapitres 5).

REFERENCES

1. K.S.Smirnov, M.Le Maire, C.Brémard, and D.Bougeard Chem.Phys. **179** (1994) 445
2. D.Dumont, Thèse, Université de Lille I, 1996
3. M.Czjzek, H.Jobic, A.N.Fitch, and T.J.Vogt J.Phys.Chem. **96** (1992) 1535
4. J.Sauer Chem. Rev. **89** (1989) 199
5. B.A.Morrow and A.J.McFarlan, J.Phys.Chem. **96** (1992) 1395

CHAPITRE 3
TECHNIQUES DE CALCUL

Dans ce chapitre, nous présentons les méthodes théoriques utilisées pour étudier la dynamique des solides (réseaux de zéolithes et silicium) et des espèces adsorbées sur des surfaces (les groupes OH et OD sur la surface de la silice et dans les zéolithes et les atomes d'hydrogène sur la surface du silicium).

Dans l'approximation adiabatique les fonctions potentielles pour le mouvement atomique peuvent être obtenues à partir des calculs de la structure électronique par des méthodes de chimie quantique au niveau *ab initio* qui sont présentées dans le Chapitre 3.1.

La méthode rapide et efficace pour l'analyse du mouvement vibrationel mais limitée par l'approximation harmonique est l'analyse en coordonnées normales (Chapitre 3.2).

La dynamique moléculaire est une approche plus générale qui permet de traiter des problèmes non-harmoniques; elle peut donner une information dynamique et structurale et permet de considérer des paramètres externes comme la pression ou la température. Elle est présentée dans le Chapitre 3.3.

Une approche combinant les dynamiques quantique et classique basée sur la théorie de perturbation permet l'étude de la dynamique hors-équilibre d'espèces adsorbées sur des surfaces excitées par laser. Cette technique est introduite dans le Chapitre 3.4.

L'objectif des calculs de la structure électronique des atomes et des molécules est de trouver des solutions à l'équation de Schrödinger. Dans les approximations non-relativistes et de Born-Oppenheimer on obtient:

$$H\Psi(\mathbf{x_1},...,\mathbf{x_n}) = E\Psi(\mathbf{x_1},...,\mathbf{x_n}). \tag{1}$$

où $\mathbf{x_i}$ représente la coordonnée spatiale $\mathbf{r_i}$ et de spin s_i d'un électron i. L'Hamiltonien en (1) est:

$$H = -\sum_i \frac{\nabla^2}{2} + \sum_i v(\mathbf{r_i}) + \sum_{i<j} \frac{1}{|\mathbf{r_i} - \mathbf{r_j}|} = \sum_i h_i + \sum_{i<j} \frac{1}{r_{ij}}. \tag{2}$$

où

$$v(\mathbf{r_i}) = \sum_\alpha \frac{Z_{\alpha i}}{r_{i\alpha}} \tag{3}$$

est un potentiel appliqué à l'électron i et créé par les charges nucléaires. Nous utilisons les unités atomiques dans ce chapitre.

Le problème principal provient du terme biélectronique en (2) qui ne permet pas de diagonaliser l'Hamiltonien et entraine différentes approximations. L'une d'entre elles est l'approximation d'Hartree - Fock, qui présente la fonction d'onde multiélectronique Ψ_{HF} comme un déterminant composé de fonctions d'ondes monoélectroniques

$$\Psi_{HF} = \frac{1}{\sqrt{N!}} det[\psi_1, \psi_2, ..., \psi_N]. \tag{4}$$

L'application du principe variationel avec les conditions d'orthogonalité pour les fonctions ψ_i donne les équations d'Hartree - Fock

$$F\psi_i(\mathbf{x}) = \sum_j^N \epsilon_{ij}\psi_j(\mathbf{x}) \tag{5}$$

où l'opérateur de Fock F est défini par

$$F = h + j - k \tag{6}$$

où

$$hf(\mathbf{x_1}) = [-\frac{1}{2}\nabla^2 + v(\mathbf{r_1})]f(\mathbf{x_1}), \tag{7}$$

$$jf(\mathbf{x_1}) = \sum_{k=1}^{N} \int \psi_k^*(\mathbf{x_2})\psi_k(\mathbf{x_2})\frac{1}{r_{12}} f(\mathbf{x_1})d\mathbf{x_2}, \tag{8}$$

$$kf(\mathbf{x_1}) = \sum_{k=1}^{N} \int \psi_k^*(\mathbf{x_2})\psi_k(\mathbf{x_1})\frac{1}{r_{12}} f(\mathbf{x_2})d\mathbf{x_2}. \tag{9}$$

Puisque les fonctions ψ_i apparaissent dans l'opérateur de Fock, l'équation (5) est non-linéaire, et on doit la résoudre par iterations. Pour les couches fermées on peut simplifier cette équation (5) sous la forme [1]

$$F\psi_i(\mathbf{r}) = \epsilon_i\psi_i(\mathbf{r}). \tag{10}$$

Dans l'implémentation de la théorie d'Hartree-Fock, les orbitales s'expriment sous la forme d'une combinaison de fonctions de base $\phi_p(\mathbf{r})$. On transforme ainsi le problème mathématique en un problème de valeurs propres pour une matrice de grande dimension

$$\mathbf{FC} = \mathbf{ESC} \tag{11}$$

où le vector C est composé de coefficients issus du développement des fonctions d'onde dans la base des fonctions $\phi_p(\mathbf{r})$. Le système des équations (11) est appelé: *les équations de Roothaan.* On calcule les éléments matriciels à partir des intégrales de base. Les intégrales nécessaires sont alors:

les intégrales de recouvrement,

$$S_{pq} = \int \phi_p^*(\mathbf{r})\phi_q(\mathbf{r})d\mathbf{r} \tag{12}$$

les intégrales de l'énergie cinétique ,

$$T_{pq} = \int \phi_p^*(\mathbf{r})(-\frac{1}{2}\nabla^2)\phi_q(\mathbf{r})d\mathbf{r} \tag{13}$$

les intégrales de l'attraction entre les électrons et les noyaux,

$$(A|pq) = \int \phi_p^*(\mathbf{r})\frac{Z_A}{r_{1A}}\phi_q(\mathbf{r})d\mathbf{r} \tag{14}$$

les intégrales de la répulsion entre les électrons,

$$(pq|rs) = \int \phi_p^*(\mathbf{r_1})\phi_q(\mathbf{r_1})\frac{1}{r_{12}}\phi_r(\mathbf{r_2})\phi_s^*(\mathbf{r_2})d\mathbf{r_1}d\mathbf{r_2}. \tag{15}$$

Quand on calcule ces intégrales de manière exacte, la méthode est appelée *ab initio.*

Il est clair que si on augmente la base, on obtient une solution plus proche de la solution exacte, cependant les conditions matérielles (capacité des machines et temps de calcul) deviennent limitantes. Il existe des bases composées de fonctions de type $\zeta = exp(-\zeta_i r)$ qui ont le bon comportement à longues distances, mais pour des raisons pratiques (facilité de calculer les intégrales) on utilise les fonctions ζ composées par des combinaisons linéaires de fonctions gaussiennes $exp(-\eta_i r^2)$. Parmi ces différentes bases les plus usuelles seront utilisées dans ce travail, plus précisément les bases du groupe de Pople (6-31g** par exemple [2]) et celles de Dunning (DZP [double-ζ + polarisation], par exemple [3]). Les fonctions de polarisation (fonctions de type p pour l'hydrogène et fonctions d pour les élements p) sont ajoutées pour donner une flexibilité à la base.

Mais l'approximation d'Hartree - Fock néglige une quantité d'énergie assez importante, qui est appelée *l'énergie de correlation* $E_{cor} = E_{exacte} - E_{HF}$, car la fonction d'onde exacte n'est pas composée d'un déterminant unique. Une des méthodes pour tenir compte de cette énergie est la méthode de l'interaction de configurations (CI).

On peut aussi appliquer la théorie de perturbation de Möller-Plesset. Dans cette théorie l'Hamiltonien (2) est composé par:

$$H = H_0 + V \tag{16}$$

où H_0 est la somme des opérateurs de Fock et la perturbation est

$$V = \sum_{i \neq j} \frac{1}{r_{ij}} - \sum_i (j_i - k_i). \tag{17}$$

Au premier ordre, la fonction d'onde est

$$\Psi^{(1)} = \sum_{i>j,a>b} \frac{< \Phi_{ij}^{ab} | V | \Phi_0 >}{\epsilon_i + \epsilon_j - \epsilon_a - \epsilon_b} \Phi_{ij}^{ab}. \tag{18}$$

La fonction Φ_{ij}^{ab} est une fonction propre de l'opérateur H_0 où deux orbitales i et j occupées sont substituées par deux orbitals a et b inoccupées. Au deuxième ordre, l'énergie est

$$E^{(2)} = \sum_{i>j,a>b} \frac{| < \Phi_{ij}^{ab} | V | \Phi_0 > |^2}{\epsilon_i + \epsilon_j - \epsilon_a - \epsilon_b}. \tag{19}$$

Une description plus détaillée des méthodes post - Hartree-Fock peut-être trouvée en [4]. La théorie de Möller-Plesset au second ordre (MP2) est appliquée dans ce travail.

L'énergie vibrationnelle des systèmes moléculaires dans leur état d'équilibre est partiellement dispersée sur des mouvements atomiques spécifiques caractérisés par leurs fréquences et appelés *les modes normaux*. L'analyse en coordonnées normales nous permet d'étudier ce phénomène. Etant donnée la quantité d'ouvrages [5,6] traitant de ce sujet, nous ne présenterons que les principales étapes.

L'énergie cinétique d'une molécule s'exprime en coordonnées cartésiennes sous la forme simple:

$$2T = \sum_{i=1}^{3N} m_i \dot{x}_i^2 = \sum_{i=1}^{3N} \dot{q}_i^2 \tag{20}$$

où x_i est le déplacement d'un atome i de masse m_i parmi les N atomes de la molécule. On introduit les coordonnées pondérées par la masse $q_i = \sqrt{m_i} x_i$. Au voisinage de la position d'équilibre on peut développer l'énergie potentielle en série de Taylor par rapport aux déplacements x_i.

$$2V = 2V_0 + 2\sum_{i=1}^{3N} (\frac{\partial V}{\partial x_i})_0 x_i + \sum_{i,j}^{3N} (\frac{\partial^2 V}{\partial x_i \partial x_j})_0 x_i x_j + ... \tag{21}$$

Au minimum le terme d'ordre 1 est nul. Si les termes d'ordre supérieur à 2 ne sont pas pris en compte (approximation harmonique), la relation (21) devient alors

$$2V = \sum_{i,j}^{3N} (\frac{\partial^2 V}{\partial x_i \partial x_j})_0 x_i x_j = \sum_{i,j}^{3N} f_{ij} x_i x_j = \sum_{i,j}^{3N} m_i^{-1/2} f_{ij} m_j^{-1/2} q_i q_j, \tag{22}$$

les facteurs f_{ij} sont appelées les constantes de force.

On peut simplifier le problème en utilisant la forme matricielle pour les équations (20) et (22).

$$2T = \mathbf{q}^+ \mathbf{q} \tag{23}$$

$$2V = \mathbf{q}^+ \mathbf{M}^{-1/2} \mathbf{F} \mathbf{M}^{-1/2} \mathbf{q} = \mathbf{q}^+ \mathbf{F_q} \mathbf{q} \tag{24}$$

où $\mathbf{q}$ est un vecteur à $3N$ composantes, $\mathbf{F}$ est la matrice symétrique de constantes de force de dimension $3N$ x $3N$, $\mathbf{M}$ est une matrice $3N$ x $3N$ diagonale contenant les masses

des atomes. $\mathbf{A}^+$ indique une matrice $\mathbf{A}$ transposée. La solution du problème vibrationel est de trouver une transformation $\mathbf{L}$ orthogonale ($\mathbf{L}^+ = \mathbf{L}^{-1}$)

$$\mathbf{q} = \mathbf{LQ} \tag{25}$$

qui diagonalise les deux formes quadratiques (23,24)

$$2T = \mathbf{Q}^+\mathbf{L}^+\mathbf{LQ} = \mathbf{Q}^+\mathbf{Q} \tag{26}$$

$$2V = \mathbf{Q}^+\mathbf{L}^+\mathbf{F_q}\mathbf{LQ} = \mathbf{Q}^+\mathbf{\Lambda}\mathbf{Q}, \tag{27}$$

où $\mathbf{\Lambda}$ est une matrice diagonale composée d'éléments λ_i, et les nouvelles coordonnées $\mathbf{Q}$ sont appelées *les coordonnées normales.* Tenant compte de l'orthogonalité de la matrice $\mathbf{L}$ on obtient l'équation aux valeurs propres de la matrice $\mathbf{F_q}$.

$$\mathbf{L}^{-1}\mathbf{F_q}\mathbf{L} = \mathbf{\Lambda} \tag{28}$$

L'équation de Lagrange

$$\frac{d}{dt}\left(\frac{\partial T}{\partial \dot{Q}_i}\right) + \frac{\partial V}{\partial Q_i} = 0 \tag{29}$$

en coordonnées normales a une forme diagonale

$$\ddot{Q}_i + \lambda_i Q_i = 0 \qquad (i = 1, 3N), \tag{30}$$

et on peut voir que les valeurs propres λ_i déterminent les fréquences des vibrations ω_i^2 d'un système moléculaire.

L'énergie potentielle s'exprime pourtant plus naturellement en coordonnées internes telles que les élongations de liaisons, les déformations d'angles plans et dièdres. La transformation qui lie les coordonnées cartésiennes $\mathbf{x}$ et internes $\mathbf{R}$ définit la matrice $\mathbf{B}$

$$\mathbf{R} = \mathbf{Bx}. \tag{31}$$

La matrice $\mathbf{B}$ a pour dimension S x $3N$, où S est le nombre de coordonnées internes. On peut alors redéfinir l'énergie potentielle par:

$$2V = \mathbf{R}^+\mathbf{F_R}\mathbf{R} = \mathbf{x}^+\mathbf{B}^+\mathbf{F_R}\mathbf{Bx} = \mathbf{q}^+\mathbf{M}^{-1/2}\mathbf{B}^+\mathbf{F_R}\mathbf{B}\mathbf{M}^{-1/2}\mathbf{q} \tag{32}$$

L'association des équations (27) et (32) fournit une nouvelle manière pour calculer la matrice $\mathbf{F_q}$

$$\mathbf{F_q} = \mathbf{M^{-1/2} B^+ F_R B M^{-1/2}}. \tag{33}$$

Pour trouver la solution d'un problème vibrationel on doit donc calculer les matrices $\mathbf{B}$, puis $\mathbf{F_q}$ et résoudre le problème de valeurs propres (28) pour cette dernière.

La méthode décrite [7] suppose le travail dans l'espace $3N$ x $3N$ des coordonées cartésiennes. Les calculs de chimie quantique produisent également les matrices de constantes de forces exprimées aussi en coordonées cartésiennes. Mais pour des raisons évidentes, un champ de forces en coordonnées internes est souhaitable. C'est un problème difficile en principe, car la transformation correspondante

$$\mathbf{F_R} = (\mathbf{B^{-1}})^+ \mathbf{F B^{-1}}. \tag{34}$$

entraine l'inversion de la matrice $\mathbf{B}$ non-carrée. Même si on ajoute 6 coordonnées internes ($M = S + 6$), qui satisfont aux conditions d'Eckart - Sayvetz et décrivent les translations et rotations de la molécule [5], la nouvelle matrice $\mathbf{B}$ ne sera toujours pas carrée. C'est une conséquence de la redondance d'assemblage de coordonnées internes: *le nombre de coordonnées internes M est généralement plus grand que* $3N$, et une coordonnée redondante apparaît à chaque ajout, au système moléculaire, de cycle ou noeud comprenant trois liaisons et plus. Mathématiquement, le problème des redondances se produit du fait que les coordonnées internes ne sont pas indépendantes. Il existe $M - 3N$ relations linéaires entre elles. A cause de ce problème il n'existe pas un choix unique pour la matrice $\mathbf{F_R}$ [8].

Pour trouver un champ de forces en coordonnées redondantes on établit la "pseudo-inversion" de la matrice $\mathbf{B}$ [9] en utilisant la matrice $\mathbf{G}$ définie par:

$$\mathbf{G} = \mathbf{B M^{-1} B^+}. \tag{35}$$

Cette matrice de dimension MxM peut-être diagonalisée par une transformation orthogonale ($\mathbf{W^+} = \mathbf{W^{-1}}$)

$$\mathbf{G} = \mathbf{W \epsilon W^+}, \tag{36}$$

où la matrice ϵ diagonale contient les $3N$ valeurs propres non-nulles et $M - 3N$ zéros. On peut définir une matrice ϵ_1 *pseudo-inverse* dans laquelle seuls les éléments non-nuls sont inversés. Les éléments nuls restent inchangés pendant cette opération. La matrice $\mathbf{G^{-1}}$ est alors définie par:

$$\mathbf{G^{-1}} = \mathbf{W}\epsilon_1\mathbf{W^+} \tag{37}$$

et impose le choix d'un champ de force dit *canonique* [8]. Avec le calcul de la matrice $\mathbf{B^{-1}}$:

$$\mathbf{B^{-1}} = \mathbf{M^{-1}B^+G^{-1}} \tag{38}$$

on obtient la matrice $\mathbf{F_R}$ en coordonnées redondantes. Le programme REDONG [9] utilisé dans ce travail produit à partir d'un champ de forces $\mathbf{F}$ *ab initio* le champ de force défini par les équations (34 à 38)

3.3 La dynamique moléculaire.

Dans la méthode de la dynamique moléculaire on résoud le système d'équations de Newton pour un ensemble suffisamment grand de particules avec des méthodes numériques. La méthode d'intégration des équations de mouvement, choisie dans ce travail, est l' algorithme de vitesse de Verlet [10].

$$\vec{r}(t+\delta t) = \vec{r}(t) + \delta t\vec{v}(t) + \frac{1}{2}\delta t^2\vec{a}(t) \tag{39}$$

$$\vec{v}(t+\delta t) = \vec{v}(t) + \frac{1}{2}\delta t[\vec{a}(t) + \vec{a}(t+\delta t)]. \tag{40}$$

On calcule les accélérations des atomes par la deuxième loi de Newton, utilisant les masses atomiques et les forces dérivées de la fonction potentielle. Ces forces sont évaluées à chaque pas de la dynamique moléculaire.

Pour simuler un système infini on introduit habituellement les conditions périodiques pour le système d'équations de la dynamique moléculaire.

Toutefois les calculs ont été effectués dans l'ensemble NVE: le nombre d'atomes, le volume de la boîte de simulation et l'énergie totale du système sont constants. Afin d'atteindre la température stationnaire désirée, la méthode du bain [11] est utilisée dans la phase d'équilibration: à chaque pas de calcul de cette phase transitoire, les vitesses des atomes sont multipliées par un facteur ζ:

$$\zeta = (1 + \frac{\delta t}{t_T}(\frac{T_{ref}}{T} - 1))^{1/2} \tag{41}$$

où T est la température cinétique actuelle, T_{ref} est la température de référence, δt est le pas temporel et t_T est la constante de relaxation. Cette méthode impose au système d'atteindre la température désirée T_{ref} avec une vitesse déterminée par t_T.

Les calculs de la dynamique moléculaire nous permettent de déterminer des fonctions de corrélation différentes. Après transformation de Fourier on obtient un spectre de la quantité étudiée. Par exemple, la transformation de Fourier de la fonction

d'autocorrélation du moment dipolaire du système moléculaire simule le spectre infrarouge:

$$I(\omega) = \frac{1}{2\pi} \int_{-\infty}^{\infty} dt < \mu(0)\mu(t) > exp(-\imath\omega t) \tag{42}$$

Le moment dipolaire total $\mu(t)$ est décrit comme une somme des positions atomiques pondérées par les charges atomiques. La moyenne de l'ensemble est calculée sur la même trajectoire par la moyenne sur quelques milliers d'origines de temps [12]. Les détails des calculs de spectres par dynamique moléculaire sont décrits dans [12-14].

3.4 La théorie de relaxation.

Les fréquences de vibration d'élongation de la liaison OH des groupes hydroxyles dans les zéolithes et sur les surfaces de silice sont trois à quatre fois plus élevées que toutes autres fréquences de vibration du système. La durée de vie des états vibrationels excités de tels oscillateurs est 10^5 fois plus longue que leur période de vibration [15,16]. Par conséquent, l'étude directe de la relaxation d'énergie vibrationnelle par dynamique moléculaire hors équilibre est difficile à traiter. La faible masse de l'oscillateur H entraine aussi des doutes sur l'aptitude de la mécanique classique à reproduire une dynamique vibrationnelle que l'on attend essentiellement quantique. On peut cependant étudier le phénomène de la relaxation d'énergie de vibrations des groupes OH dans le cadre de la théorie des perturbations en traitant les vibrations de l'atome d'hydrogène par des méthodes de mécanique quantique et les vibrations du solide par la dynamique moléculaire.

La théorie des perturbations suppose la forme suivante d'Hamiltonien

$$H = H_0(\vec{q}) + H_b(\vec{Q}) + V(\vec{q}, \vec{Q}, t) \tag{43}$$

où

$$H_0 = -\frac{\nabla^2}{2M} + U(\vec{q}) \tag{44}$$

est l'Hamiltonien d'un oscillateur anharmonique, H_b est l'Hamiltonien du bain décrivant dans notre cas les vibrations du solide, V exprime le couplage entre l'oscillateur et le bain.

On note les états propres de H_0 $i, j, ...$ et ceux de H_b $\alpha, \beta, ...$ Le bain est supposé être en équilibre thermique, donc, la probabilité que le bain soit dans un état α est $P_\alpha = exp(-E_\alpha/k_BT)$. La vitesse de transition τ_{ij}^{-1} du niveau i au niveau j grâce à la perturbation V est exprimée dans la théorie de perturbation dépendant du temps par la formule "Golden Rule" de Fermi [17]:

$$\tau_{ij}^{-1} = \frac{2\pi}{\hbar Z_R} \sum_\alpha \sum_\beta P_\alpha |V_{i\alpha,j\beta}|^2 \delta(E_i - E_j + E_\alpha - E_\beta), \tag{45}$$

où Z_R est la fonction de partition du bain. Par application de la transformation de Fourier à la fonction δ on obtient:

$$\tau_{ij}^{-1} = \frac{1}{\hbar^2 Z_R}\int_{-\infty}^{\infty} dt \sum_\alpha \sum_\beta P_\alpha |V_{i\alpha,j\beta}|^2 exp[\frac{it}{\hbar}(E_i - E_j + E_\alpha - E_\beta)] \tag{46}$$
$$= \frac{1}{\hbar^2 Z_R}\int_{-\infty}^{\infty} dt exp(i\omega_{ij}t) \sum_\alpha \sum_\beta P_\alpha exp(\frac{it}{\hbar}E_\alpha) V_{i\alpha,j\beta} exp(-\frac{it}{\hbar}E_\beta) V_{j\beta,i\alpha}$$

et en représentation d'Heisenberg

$$\tau_{ij}^{-1} = \frac{1}{\hbar^2 Z_R}\int_{-\infty}^{\infty} dt exp(i\omega_{ij}t) < exp(\frac{iH_b t}{\hbar}) V_{ij} exp(-\frac{iH_b t}{\hbar}) V_{ji} > \tag{47}$$
$$= \frac{1}{\hbar^2}\int_{-\infty}^{\infty} dt exp(i\omega_{ij}t) < V_{ij}(t) V_{ji}(0) > .$$

Dans l'hypothèse d'un couplage faible on suppose

$$V(\vec{q}, \vec{Q}, t) = V(0, \vec{Q}, t) - \vec{\nabla} V(0, \vec{Q}, t)\vec{q}. \tag{48}$$

Le premier terme peut être pris en compte par la renormalisation de la fréquence de transition. Le deuxième terme est le produit de la coordonnée d'oscillateur et de la force dépendante du temps calculée à la position équilibre de l'oscillateur. Avec cette forme du couplage l'équation (47) devient:

$$\tau_{ij}^{-1} = \frac{|<i|q|j>|^2}{\hbar^2}\int_{-\infty}^{\infty} dt exp(i\omega_{ij}t) < \vec{F}(t)\vec{F}(0) >_{qm} \tag{49}$$
$$= \frac{1}{\hbar^2}|<i|q|j>|^2 \zeta_{qm}(\omega_{ij}).$$

Le corrélateur dans l'équation (49) est quantique. Pourtant, dans l'application à un système avec de nombreux degrés de liberté on est obligé de simuler le bain classiquement. Comme pour les basses températures les vibrations du bain ont un comportement quantique, l'utilisation de la formule (49) ne traduira pas, dans ces conditions limites, la dépendence correcte de la vitesse de relaxation avec la température.

Dans l'approximation harmonique, pour le bain, il existe une relation exacte entre les fonctions de corrélation quantique et classique que nous établissons ci-dessous. On peut lier par une transformation unitaire le déplacement d'un atome hors de sa position d'équilibre avec les coordonnées normales et obtenir la fonction d'autocorrélation suivante:

$$< x_i(t) x_i(0) >= \sum_\alpha |L_{i\alpha}|^2 \ < q_\alpha(t) q_\alpha(0) > . \tag{50}$$

Dans la base des coordonnées normales, les équations du mouvement sont indépendantes pour chaque coordonnée. En coordonnées normales, la fonction d'autocorrélation de la force peut par conséquent être reliée à la fonction d'autocorrélation du déplacement en utilisant un facteur dépendant de la fréquence.

La fonction d'autocorrélation classique du déplacement (51) et sa transformée de Fourier (52) peuvent être calculées facilement:

$$< q(t)q(0) >_{cl} = \frac{1}{N}\sum_{\alpha}\frac{1}{\beta\omega_{\alpha}^2}cos(\omega_{\alpha}t) \tag{51}$$

$$\zeta_{cl}(\omega) = \frac{1}{N}\sum_{\alpha}\frac{1}{2\beta\omega_{\alpha}^2}[\delta(\omega-\omega_{\alpha})+\delta(\omega+\omega_{\alpha})] = \frac{1}{2\beta\omega^2}[\rho(\omega)+\rho(-\omega)] \tag{52}$$

où N est le nombre d'atomes dans le réseau et ρ est la densité d'états continue. Cette dernière est définie par

$$\rho(\omega) = \frac{1}{N}\sum_{\alpha}\delta(\omega-\omega_{\alpha}). \tag{53}$$

La fonction d'autocorrélation quantique de l'opérateur de coordonnée q_{α} a la forme suivante [18]:

$$< q_{\alpha}(t)q_{\alpha}(0) >_{qm} = \frac{1}{N}\sum_{\alpha}\frac{1}{2\omega_{\alpha}}[(1+n(\omega_{\alpha}))exp(-it\omega_{\alpha})+n(\omega_{\alpha})exp(it\omega_{\alpha})], \tag{54}$$

où

$$n(\omega) = \frac{1}{exp(\beta\omega)-1} \tag{55}$$

est la fonction de population de Bose. La transformation de Fourier de la fonction de corrélation quantique donne

$$\begin{aligned}\zeta_{qm}(\omega) &= \frac{1}{N}\sum_{\alpha}\frac{1}{2\omega_{\alpha}}[(1+n(\omega_{\alpha}))\delta(\omega-\omega_{\alpha})+n(\omega_{\alpha})\delta(\omega+\omega_{\alpha})] \\ &= \frac{1}{2\omega}[(1+n(\omega))\rho(\omega)-n(-\omega)\rho(-\omega)].\end{aligned} \tag{56}$$

Puisqu'il n'existe pas d'états de fréquence négative, seul un des deux termes du crochet des équations (52) et (56) est non-nul quel que soit le signe de la fréquence de transition intramoléculaire. Nous pouvons réécrire (52) et (56) dans une forme plus facile à manipuler:

$$\zeta_{qm}(\omega) = \frac{1}{2\omega}[1 + n(\omega)]\rho(\omega), \qquad \omega > 0 \tag{57}$$
$$\zeta_{qm}(\omega) = -\frac{1}{2\omega}n(-\omega)\rho(-\omega), \qquad \omega < 0$$

et

$$\zeta_{cl}(\omega) = \frac{1}{2\beta\omega^2}\rho(\omega), \qquad \omega > 0 \tag{58}$$
$$\zeta_{cl}(\omega) = \frac{1}{2\beta\omega^2}\rho(-\omega), \qquad \omega < 0$$

Puisque la densité d'états ne dépend pas de l'amplitude du mouvement et par conséquent de la façon de traîter le système (quantique ou classique), il existe une correspondance directe entre les fonctions de corrélation quantique et classique:

$$\zeta(\omega)_{qm} = \gamma(\omega)\zeta(\omega)_{cl}, \tag{59}$$

où le préfacteur $\gamma(\omega)$ est défini par

$$\gamma(\omega) = \beta\omega[1 + n(\omega)]\rho(\omega), \qquad \omega > 0 \ (emission\ de\ phonons) \tag{60}$$
$$\gamma(\omega) = -\beta\omega n(-\omega)\rho(-\omega), \qquad \omega < 0 \ (absorption\ de\ phonons).$$

Même si l'égalité établie est strictement valable dans l'approximation harmonique, pour les vibrations du solide ce sera une bonne approximation à relativement basses températures, car les déplacements des atomes hors de leur position d'équilibre sont assez petits. Ce facteur additionel peut être appliqué à la fonction de corrélation obtenue par dynamique moléculaire, puisque l'anharmonicité du bain est la cause d'effets normalement plus faibles.

On peut calculer la transformée de Fourier de la fonction de corrélation de la force $\zeta(\omega)$ par dynamique moléculaire avec contraintes pour garder la coordonnée $\vec{q}$ à l'équilibre. Les calculs de dynamique moléculaire (Chapitre 3.3) nous permettent de calculer des fonctions de corrélation différentes. Les fonctions d'autocorrélation peuvent être calculées facilement par le théorème de Wiener - Khinchin [19]

$$\int dt e^{i\omega t} < F(0)F(t) >_{cl} = lim\frac{1}{2T}|\int_{-T}^{T} dt e^{i\omega t}F(t)|^2. \tag{61}$$

Finalement, on obtient par dynamique moléculaire la fonction d'autocorrélation de la force $\zeta_{cl}(\omega)$. Après le calcul des éléments de matrice de l'opérateur de coordonnée $\vec{q}$, on applique les formules (49) et (60) pour obtenir la vitesse de transition. Enfin, après avoir fait la somme des vitesses de transition sur tous les états finaux on obtient la durée de vie de l'état excité.

REFERENCES

1. C.C.J. Roothaan Rev.Mod.Phys. **23** (1951) 69

2. J.S.Binkley, J.A.Pople, and W.J.Hehre J.Am.Chem.Soc. **102** (1980) 939

3. T.H.Dunning,Jr., J.Chem.Phys. **53** (1970) 2823

4. R.J.Bartlett and J.F.Stanton, p.65 in *Reviews in Computational Chemistry*, vol.5, K.B.Lipkowitz and D.B.Boyd, Ed., VCH Publishers, New York, 1994

5. S. Califano, Vibrational States, John Willey and Sons, New York (1976)

6. E.B.,Jr,Wilson,J.C.Decius, and P.C.Cross, Molecular Vibrations, McGraw-Hill, New York (1955)

7. T.Shimanouchi *Programs for the Normal Coordinate Treatment of Polyatomic Molecules*, University of Tokyo, Tokyo, 1968

8. K.Kuczera and R.Czerminski, J.Mol.Structure THEOCHEM, **105** (1983) 269

9. A.Allouche and J.Pourcin, Spectrochimica Acta, **49A** (1993) 571; A.Allouche, RE-DONG, QCPE 628.

10.M.P.Allen and D.J.Tildesley *Computer Simulation of Liquids*, Clarendon Press, Oxford, 1987

11.H.J.C.Berendsen, J.P.M.Postma, W.F.Van Gunsteren, A.Di Nola, and J.R.Haak J.Chem.Phys. **81** (1984) 3684

12.P.H.Berens and K.R.Wilson J.Chem.Phys.**74** (1981) 4872

13.P.H.Berens, S.R.White, and K.R.Wilson J.Chem.Phys. **75** (1981) 515

14.K.S.Smirnov and D.Bougeard J.Raman Spectrosc., **24** (1993) 255

15.M.P.Casassa, E.J.Heilweil, J.C.Stephenson, and R.R.Cavanagh J.Chem.Phys. **84** (1986) 2361

16.M.J.P.Brugmans, M.Bonn, H.J.Bakker, and A.Lagendijk Chem.Phys. **201** (1995) 215

17.D.W.Oxtoby Adv.Chem.Phys. **47** (1981) 487

18.V.M.Kenkre, A.Tokmakkof, and M.D.Fayer J.Chem.Phys. **101** (1994) 10618

19.W.H.Press, B.P.Flannery, S.A.Teukolsky, and W.T.Vettering *Numerical Recipes*, Cambridge University Press, 1986

CHAPITRE 4

ETUDE AB INITIO DES PREMIERES ETAPES DE LA SYNTHESE HYDROTHERMALE DES ZEOLITHES ET DES PROCESSUS SOL-GEL.

Soumis pour publication à Journal of Molecular Structure (THEOCHEM)

AB INITIO STUDY OF THE INITIAL STEPS OF THE HYDROTHERMAL ZEOLITE SYNTHESIS AND OF THE SOL–GEL PROCESSES

Vladimir A.Ermoshin[+#], Konstantin S.Smirnov[+], and Daniel Bougeard[#*]

[#]*Laboratoire de Spectrochimie Infrarouge et Raman du CNRS, Université des Sciences et Technologies de Lille, Bat.C5, 59655 Villeneuve D'Ascq cedex, France*

[+]*Institute of Physics, St.Petersburg State University, St.Petersburg 198904, Russia*

Abstract

The initial steps of the hydrothermal zeolite synthesis and of the sol–gel processes were studied by ab initio calculations of molecular models representing reagents, intermediates, and final products of the reactions. The calculations have shown that anionic compounds are more stable than corresponding neutral ones. It is proposed that the reaction mechanism is a polycondensation involving anionic species with subsequent formation of both linear and cyclic chains.

Received on 17th April 1996;revised version ... September 1996

1. Introduction

The hydrothermal synthesis of zeolites and sol–gel processes for production of aluminosilicates have a common motivation which is related to the purity and homogenity of the products obtained during these reactions at lower temperatures than through melting of silicates and aluminosilicates. In both cases the reaction occurs through a polycondensation of silicon and aluminium hydroxides and it obviously includes similar steps. Investigations of the initial steps of the sol–gel reactions are of significant interest because of the importance of these compounds for many applications and results of such studies can be used to optimize reaction conditions.

Several attempts have already been undertaken to elucidate the mechanism of the reactions by means of spectroscopic methods. ^{27}Si NMR and vibrational spectroscopy have been used to follow the sol–gel process [1–3] or the hydrothermal synthesis of zeolites [4,5] with the aim to characterise the templates or inorganic reaction intermediates. For sol–gel processes where only silicon atoms are present and the reaction is not disturbed by other particles, such as template molecules, the NMR data indicate that at the beginning of condensation a step–by–step assembly occurs that leads to small ordered units such as three– and four– membered rings and chains [3].

The mechanism of the sol–gel processes has also been studied using some theoretical approaches. Several groups postulated the existence of a penta–coordinated silicon atom as an intermediate either of the condensation or of the hydrolysis reactions [8–10]. Such intermediates were also found by Garofalini et al. in their molecular–dynamical studies of the sol–gel polymerisation [11,12]. However, quantum–chemical calculations show that the intermediate pentavalent state is more stable than the final products. This observation leads to the question, why the reaction does not stop at the step where the overall minimum of energy is reached. The question asked is that of the relative stability of neutral and anionic small oligomers in the very first stages of the polycondensation. One way to answer is to perform new more precise calculations of the oligomers in order to identify possible reaction pathways. In this paper we concentrate on the energy levels neglecting eventual barriers along the reaction coordinates.

Obviously this approach suffers of the fact that isolated molecules are treated while the real reactions occur in solutions. Nevertheless one obtains relative stabilities for the components of the reacton mixture and hints about possible reaction channels in the first steps of the polycondensation. The results presented concern mainly hydroxyl derivatives which are particularly relevant for the hydrothermal zeolite synthesis in basic solutions. Pouxviel at al. [13] stated that in the sol–gel polymerisation the overall condensation rate seems to increase with the decreasing of the proton concentration and thus this study can also represent a limit representation of the sol–gel processes. Finally it brings new information in the field

of chemistry of penta–coordinated silicon initiated by DePuy et al. [14] and developed in the last ten years [8–10].

2. Method and models

The calculations of the present work were performed with the CADPAC package [15] either on an SGI workstation or on a CRAY C98 at the IDRIS computing center. The structures and energies of the models were calculated with the 3–21G* and DZP basis sets. These basis sets were chosen in order to compare the results of a small tractable set with those of a more developed set, both containing polarization functions necessary to reproduce structural data. As anions are involved in the course of the reactions, the distribution of the negative charge could necessitate the inclusion of diffuse functions. Further in such polymerisation reactions the interaction energies can be affected by the basis set superposition error (BSSE) [16]. In order to estimate the corresponding influences and the systematic errors we performed for the small entities $Si(OH)_4$, $Si(OH)_5^-$, $Al(OH)_3$ and $Al(OH)_4^-$ complete calculations with diffuse fuctions and BSSE correction with the counterpoise method [17] at the 3–21G* level. The diffuse functions were added on all atom types using the orbital exponents given in ref. 18. These results were qualitatively extrapolated to the calculations of larger clusters necessary for the comprehension of the first steps of the polycondensation: $(OH)_3Si–O–Si(OH)_3$ and $(OH)_3Si–O–Al(OH)_2$ as well as the corresponding monohydroxylated anions.

No restrictions were imposed on the symmetry of the models during the optimization procedure. For the small oligomers (one T atom) the hessian matrix was tested to be positive. This CPU time intensive calculation was not performed for the larger derivatives where several conformations can occur, mainly caused by the rotations of the OH groups which are not relevant for the chemical reactivity.

3. Results and discussion

3.1. Structures at the DZP level

The calculated equilibrium structures of some molecular models which were not reported previously in the literature or which were not calculated at this level of theory are presented in Figure 1. The SiO bond length calculated for the $Si(OH)_4$ molecule is 1.622 Å in good agreement with previous results [19]. The calculated structure of the $Si(OH)_5^-$ species is trigonal–bipyramidal. The SiO bond lengths are equal to 1.791 Å and 1.740 Å for the axial bonds, and to 1.690, 1.690 and 1.695 Å for the planar ones. The difference between the bond lengths for each set is obviously caused by the low symmetry arising from the conformation of the OH groups. Similarly, the AlO bonds increase from 1.674 Å to 1.760 Å when

going from the planar trigonal $Al(OH)_3$ to the tetrahedral $Al(OH)_4^-$ species.

All calculated OH bond lengths are in the range 0.940–0.945 Å, while the TOH angle is between 114.1° and 117.8°.

In the neutral $(OH)_3SiOSi(OH)_3$ dimer the SiO bond lengths of the OH groups have a value of 1.621 Å which is similar to that in $Si(OH)_4$ molecule, while the SiO bond of the SiOSi bridge has a shorter length of 1.613 Å. Substitution of $Si(OH)_3$ by $Al(OH)_3^-$ leads to a decrease of the SiO bond length to 1.578 Å in the Al–O–Si bridge and to a small increase of the SiO bonds to 1.633 Å in the $Si(OH)_3$ groups. On the aluminium side the values of the AlO bonds (1.768 Å) are similar to those in the $Al(OH)_4^-$ molecule (1.760 Å), while the bridge AlO bond has a length of 1.741 Å.

3.2. Energetics and reaction mechanism

The calculated energies of the molecules are gathered in Table 1. As expected a systematic decrease of the energy is observed when going from the 3–21G* to the DZP basis sets. The comparison of the energies for $Si(OH)_5^-$ and $Si(OH)_4 + OH^-$ indicates that the former is more stable for both basis sets. In order to verify this result we have also calculated $Si(OH)_6^{2-}$ at the 3–21G* level, the energy of –737.8929 a.u. indicates that this molecule is less stable than $Si(OH)_5^- + OH^-$. At this point it is necessary to test the influence of diffuse atomic orbitals and BSSE on the result. We therefore performed a complete study of the silicium derivatives which will be qualitatively used to analyze the results of the larger clusters. Table 1 shows that the use of larger bases leads to a decrease of the stabilisation in the reaction

$$Si(OH)_4 + OH^- \text{ ------->} \quad Si(OH)_5^-$$

(59.8 and 60.2 kcal/mole for the 3–21+g* and DZP basis, respectively, versus 105.1 for the 3–21g* basis). The BSSE corrected stabilisation is of the same order for all basis sets: 50.9, 53.9 and 48.5 kcal/mole for 3–21g*, 3–21+g* and DZP, respectively. We can conclude that $Si(OH)_5^-$ really corresponds to a stable state. This statement is valid for isolated molecules. It is also reasonable under the conditions of hydrothermal synthesis where an hydroxyl excess is always present. Although this stability of pentacoordinated silicon is surprising in view of the usual four–fold coordination of silicon in presence of OH ligands, it is in agreement with the results of Gordon et al. on silanes in the gas phase [20] and on hexacoordinated dianions [22]. These results suggest that the tetra– and hexacoordinated silicon atoms experimentally observed are stabilized by the intermolecular forces of their environment. In the case of strong chelating ligands the silicon–ligand interaction could compensate the energy difference between tetra– and pentacoordination. For hexacoordinated derivatives we can expect a stabilization of a state which

is already a minimum of the energy surface with a significant barrier [21].

Similarly, $Al(OH)_4^-$ is more stable than $Al(OH)_3$. The stabilisation energy here is −147.5, −99.9 and −107.9 kcal/mole for the 3–21g*, 3–21+g* and DZP basis, respectively and it is thus larger than for $Si(OH)_4$. The BSSE analysis performed leads to corrected values of 93.9 and 95.8 kcal/mole for the stabilisation with the 3–21g* and 3–21+g* basis, respectively. Therefore the BSSE decreases from 53.6 kcal/mole for the 3–21g* basis to 4.1 kcal/mole after inclusion of diffuse functions.

In order to check the generality of this stabilisation upon hydroxylation, we replaced the hydroxyl groups by fluorine atoms. In Table 1 we see that at the 3–21G* level hexacoordinated silicon (SiF_6^{2-}: −881.4107 a.u.) is slightly more stable than pentacoordinated silicon (SiF_5^- + F^-: −881.4025 a.u.) while the contrary is true with the more precise DZP basis set (−885.9873 vs. −886.0394 a.u for SiF_6^{2-} and SiF_5^- + F^-, respectively). This inversion is caused by the BSSE which amounts to 63.4 kcal/mole for the 3–21g* basis. Further the increase of stability of SiF_5^- by comparison with SiF_4 is 61.7 kcal/mole after correction of BSSE. Therefore pentacoordinated trigonal–bipyramidal SiF_5^- is the most stable fluorinated species in this series.

Finally in analogy to the known existence of oxo derivatives for hydroxylated transition metals, the energy of $(OH)_3Si{=}O^-$ + H_2O was calculated at the 3–21+g* level. The value of −663.1633 a.u. shows that this derivative is clearly less stable than $Si(OH)_5^-$, that the energy difference is large enough to avoid the necessity of a DZP calculation and that pentahydroxylated silicon is the most stable species in the series $Si(OH)_4$, $Si(OH)_5^-$, $Si(OH)_6^{2-}$ and $(OH)_3Si{=}O^-$.

From the calculation of the dimer $(OH)_3SiOSi(OH)_3$ at the STO3G level by Johnson et al.[9] it is possible to calculate a stabilisation energy of 153 Kcal/mol upon hydroxylation with one OH group. An energy gain of 118.7 Kcal/mol for $(OH)_3SiOSi(OH)_3$ and of 177.4 Kcal/mol for $(OH)_2AlOSi(OH)_3$ upon the hydroxylation was calculated at the 3–21G* level in the present work. As the hydroxylation of these clusters is basically identical to the reactions previously discussed, the inclusion of the OH^- groups can be expected to give rise to a BSSE of the order of 54 kcal/mole at the 3–21g* level. Therefore we can estimate that the stabilisation is of the order of about 65 and 123 kcal/mole for the Si and Al derivative, respectively. Thus, the monohydroxylation leads to an energy decrease and to an increase of the TO bond lengths mainly localised on the hydroxylated T atom (section 3.1.).

Table 1 leads to the conclusion that the anionic species have a higher stability than the corresponding neutral ones: $Si(OH)_5^-$ and $Al(OH)_4^-$ are more stable than $Si(OH)_4$ + OH^- and $Al(OH)_3$ + OH^-, respectively; similarly, $(OH)_3SiOSi(OH)_4^-$ and $(OH)_3SiOAl(OH)_3^-$ are more stable than

$(OH)_3SiOSi(OH)_3 + OH^-$ and $(OH)_3SiOAl(OH)_2 + OH^-$, respectively. Further, the energy stabilisation is larger when an anionic aluminium is involved instead of a silicic anion. All these conclusions are based on calculations of isolated molecules which contain intramolecular hydrogen bonds (Fig. 1) replaced in the liquid state or in solutions by intermolecular hydrogen bonds. In fact as hydrogen bonds are known to have enthalpies of formation smaller than 5 kcal/mole [22] the energies discussed are larger than hydrogen bonds energies and the developments presented are not limited by the gas phase approximation.

All these results show that the mechanism of the first dimerisation cannot lead to neutral species as it was proposed by several authors [9,10] because the intermediate pentavalent state of Si is more stable in the presence of hydroxide excess. The most probable mechanism arising from the data of the present work is a polycondensation involving anionic species with an initiation step corresponding to the creation of pentacoordinated silicon or tetracoordinated aluminium, particularly in basic solutions; the propagation corresponds to a step in which one anion condenses with one neutral monomer yielding an anionic dimer under elimination of water

$$Al(OH)_4^- + Si(OH)_4 \longrightarrow H_2O + (OH)_2Al\text{–}O\text{–}Si(OH)_3^-$$

The results obtained at the 3–21G* level also show that an increase of the chain length leads to an increase of the energy stabilisation upon hydroxylation of the T atom.

The products ratios usually used in hydrothermal synthesis lead to a solution containing $Si(OH)_4$,$Al(OH)_3$ and NaOH in the ratios 10:2:4 [6, 7]. As $Al(OH)_4^-$ is more stable than $Si(OH)_5^-$ we can assume that all aluminium atoms are present as $Al(OH)_4^-$; therefore the remaining OH^- can react with $Si(OH)_4$ to produce a mixture of $Si(OH)_5^-$ and $Si(OH)_4$ in the ratio 1:4. Since the observed Si/Al ratio is usually of the order of 4 [6, 7] the most probable mean reaction mechanism is the reaction of $Al(OH)_4^-$ with $Si(OH)_4$, i.e. a reaction of tetrahedral entities corresponding to a shielding of the negatively charged $Al(OH)_4$ by the neutral silicium hydroxyde. This interpretation is in line with the experimental data obtained by ^{29}Si NMR [23] and ^{29}Si, ^{17}O, ^{13}C and ^{27}Al NMR [24] indicating that in the first steps of the gel formation from Al_2O_3–SiO_2 mixtures self–polymerization between Si species is not observed and that aluminosilicates species are formed containing tetrahedral aluminium surrounded by four silicate ligands,"similar to zeolite precursors".

Further propagation of the reaction can occur through formation of either linear or cyclic active chains according to similar reactions involving the simply charged anionic dimer with the neutral monomer. The cyclisation effect should become active after the building of trimers. Recently, Hill and Sauer have shown that the strain energy in rings significantly decreases for the building of four– and

higher–membered rings [25]. When the chain becomes longer the energy stabilisation obtained from the chain prolongation competes with the energy gain from cyclisation, which can lead to the creation of the complicated substructures encountered in zeolites and glasses. At this point of the reaction an influence of template molecules in the hydrothermal synthesis becomes important in order to orientate the subunits into the three–dimensional structure. This way of polymerisation explains the NMR data which show the presence of short linear oligomers before the appearance of small rings and eventually of pentacoordinated silicon during the hydrothermal synthesis of zeolites [26]. In previous NMR works the observation of pentacoordinated silicon was not addressed because the frequency range was usually not broad enough and the signals expected for pentacoordinated silicon fall around 103 ppm with respect to TMS [24] where silicon atoms of longer chains and complicated substructures are assigned. Further these NMR results do not give information about the anionic or neutral nature of the species observed.

4. Conclusions

The data of the present work indicate that the initial steps of the hydrothermal zeolite synthesis and of the sol–gel process could occur through a polymerisation process involving anionic species. It is shown that the gain of energy upon the hydroxylation is increased with the increase of chain length. In addition, the stabilisation energy is larger if the aluminium compound is involved in the process. This observation corresponds to the conclusion of Thomson et al. [27] who found that tetrahedral aluminiun centers possess a good Lewis acid character using STO3G on several clusters. The results presented are in good agreement with the available NMR data and supported by the similarity of the results on fluoride derivatives corresponding to the experimental development of the fluoride way of zeolite synthesis [28].

Acknowledgements

The authors gratefully aknowledge the financial support of the NATO Scientific and Environmental Affairs Division (Grant Number HITECH.CRG 941422) and IDRIS computing center for allocation of time (project 940148). V.A.E. thanks the Ministère des Affaires Etrangères for a fellowship.

References

1. G.Engelhardt, W.Altenburg, D.Hoebbel and W.Wieker, Z.Anorg.Allg.Chem. 428 (1977) 43.
2. I.Artaki, M.Bradley,T.W.Zerda and J.Jones, J.Phys.Chem. 89 (1985) 4399.
3. F.Devreux, J.P.Boilot, F.Chaput and A. Lecomte, Phys.Rev.A 41 (1990) 6901.
4. K.F.M.G.J.Scholle, W.S.Veeman, P.Frenken and G.P.M.van der Velden, J.Phys.Chem. 88 (1984) 3395.
5. P.K.Dutta and M.Puri, J.Phys.Chem. 91 (1987) 4329.
6. F.Delprato,L.Delmotte,J.L.Guth and L.Have, Zeolites 10 (1990) 546.
7. J.Weitkamp, R.Schumacher, U.Weib, Chem.–Ing.–Tech. 64 (1992),1109.
8. R.Damrauer,L.W.Burggraf,L.P.Davis and M.S.Gordon, J.Am.Chem.Soc.110 (1988) 6601.
9. S.E.Johnson, J.A.Deiters,R.O.Day and R.R.Halmes, J.Am.Chem.Soc. 111 (1989) 3250.
10. J.K.West and S.Wallace, J.Non–Cryst.Solids 152 (1993) 109.
11. G.E.Martin and S.H.Garofalini, J.Non–Cryst.Solids 171 (1994) 68.
12. S.H.Garofalini and G.Martin, J.Phys.Chem. 98 (1994) 1311.
13. J.C. Pouxviel, J.P. Boilot, J.C. Beloeil and J.Y. Lallemand, J. Non–Cryst. Solids 89 (1987) 345.
14. C.H. Depuy, V.M. Bierbaum and R.J. Damrauer, J. Am. Chem. Soc. 106 (1984) 4051.
15. R.D.Amos and J.E.Rice, "CADPAC: The Cambridge Analytic Derivatives Package", issue 4.0,Cambridge ,1987.
16. N.R. Kestner, J. Chem. Phys, 48 (1968) 252.
17.S.F. Boys and F. Bernardi, Mol. Phys. 19 (1970) 553.
18.W.J. Hehre, L. Radom, P. v.R.Schleyer and J.A. Pople, "Ab initio molecular orbital theory", Wiley, New York, (1986).
19 B.J.Teppen,D.M.Miller,S.Q.Newton and L.Schäfer J.Phys.Chem. 98 (1994) 12545.
20. M.S. Gordon, L.P. Davis, L.W. Burggraf and R. Damrauer, J. Am. Chem. Soc. 108 (1986) 7889.
21. M.S. Gordon, M.T. Carroll, L.P. Davis and L.W. Burggraf, J. Phys. Chem. 94 (1990) 8125.
22. A. Novak, Struct. Bond. 18 (1974) 177.
23. J.C. Pouxviel and J.P. Boilot in "Ultrastructure processing of advanced ceramics", J.D. MacKenzie and D.R. Ulrich, Eds., Wiley, New York, p.197 (1987).
24. G.A. Pozarnsky and A.V. McCormick, J. Non–Cryst. Solids 190 (1985) 212.
25. J.R.Hill and J.Sauer, J.Phys.Chem. 98 (1994) 1238.
26. B.Herreros and J.Klinowski J.Phys.Chem. 99 (1995) 1025.
27. J. Thomson, G. Webb, B.C. Webster, and J.M. Winfield, J. Chem. Soc. Faraday Trans. 91 (1995) 155.
28. J.L.Guth, H. Kessler and R. Wey, Pure Appl. Chem. 58 (1986) 1389.

Table 1. Energies of the molecules at the optimized geometries (All energies are in atomic units:1 a.u= 1 Hartree = 627.71 kcal/mole = 2623.83 kJ/mole).

	3-21G*	3-21+G*	DZP
OH^-	-74.8924	-75.0227	-75.3723
H_2O	-75.6316	-75.6650	-76.0470
$Si(OH)_4$	-587.9963	-588.0818	-591.0137
$Si(OH)5^-$	-663.0561	-663.1997	-666.4938
$(OH)_3SiOSi(OH)_3$	-1100.3665	-	-1105.9838
$(OH)_3SiOSi(OH)_4^-$	-1175.4482	-	-
$Al(OH)_3$	-466.0213	-466.0958	-468.4932
$Al(OH)_4^-$	-541.1487	-541.2776	-544.0374
$(OH)_2AlOSi(OH)_3$	-978.3895	-	-
$(OH)_3AlOSi(OH)_3^-$	-1053.5608	-	-1059.0358
F^-	-98.7887	-	-99.4153
SiF_4	-683.6095	-	-687.0666
SiF_5^-	-782.6138	-	-786.6240
SiF_6^{2-}	-881.4107	-	-885.9873
$(OH)_3Si{=}O^-$	-587.3658	-587.4983	-

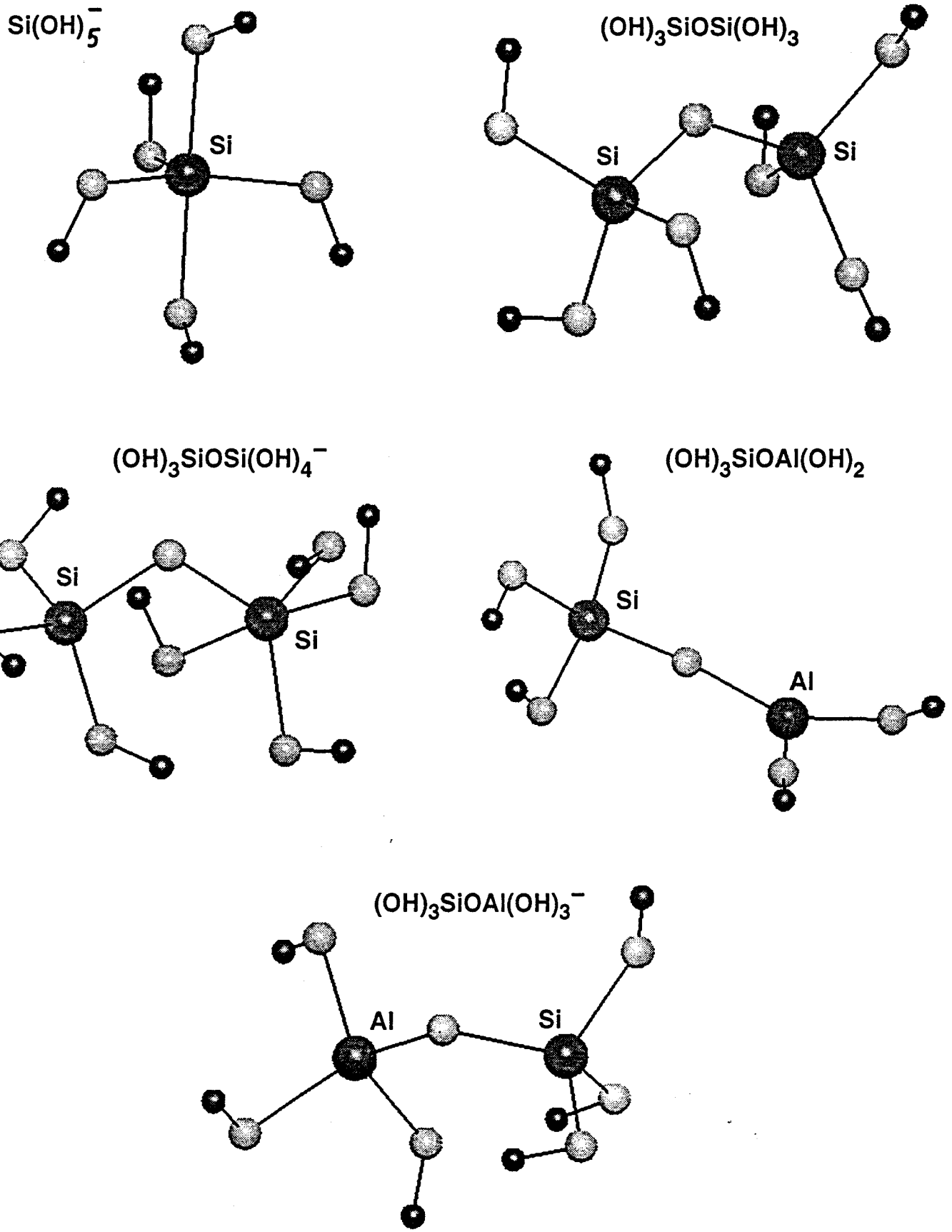

Spatial representation of the structure of some molecules calculated and gathered in Table 1

CHAPITRE 5

CHAMP DE FORCES DE VALENCE AB INITIO. APPLICATION A LA MODELISATION DES ZEOLITHES ET DE LA SILICE.

5.1. Introduction

L'étude de la dynamique du réseau et des groupes OH des zéolithes et de la silice est très importante pour les applications industrielles de ces matériaux. Par exemple, les processus catalytiques dans les zéolithes se produisent généralement avec la participation de l'hydrogène des centres de Brönsted dont la dynamique et les interactions avec le réseau influent notablement sur la vitesse de réaction. La spectroscopie vibrationnelle est une source d'information sur la dynamique des particules et des solides. Toutefois la complexité des zéolithes et de la silice nécessitent des méthodes théoriques afin d'interpréter les données expérimentales.

Deux approches sont essentiellement utilisables pour les calculs des spectres vibrationels des zéolithes: l'analyse en coordonnées normales et la dynamique moléculaire. La première est plus rapide, mais est limitée à l'approximation harmonique. La dynamique moléculaire permet de traiter les problèmes non-harmoniques, donne une information dynamique et structurale et permet de considérer des paramètres externes comme la pression et la température.

Les propriétés dynamiques dépendent fortement du choix des fonctions potentielles. La difficulté d'obtention des paramètres empiriques est liée à la taille importante de la maille élémentaire et au désordre structural. La mise en oeuvre de méthodes de chimie quantique au niveau *ab initio* est un chemin prometteur pour l'obtention de potentiels utiles en modélisation des matériaux.

Quelques essais ont été faits afin d'obtenir les fonctions potentielles à partir de calculs *ab initio* [1-7]. Comme les liaisons $T - O$ dans les zéolithes sont partiellement covalentes, des champs de forces qui prennent en compte l'orientation spatiale de ces liaisons sont nécessaires. Un potentiel de la mécanique moléculaire a été développé par Hill et Sauer [5,6]; il reproduit bien les propriétés structurales, mais la dynamique fournie par ce potentiel n'est pas correcte [7]. Il faut noter que le potentiel plus récent, utilisé dans le modèle de couche [7] reproduit bien la dynamique des zéolithes siliciques et hy-

dratées. Les interactions électrostatiques prises en compte dans ce travail permettent de distinguer les groupes OH dans différents sites cristallographiques, mais les modes de déformation "dans le plan" et "hors-du-plan" du groupe OH n'y sont pas discutés.

Dans ce travail nous introduisons l'approche qui permet, à partir de calculs *ab initio*, d'obtenir les paramètres du champ de force de valence largement utilisé dans l'analyse en coordonnées normales. L'aptitude de ce champ de forces à reproduire la dynamique de différents réseaux de zéolithes et la dynamique des groupes OH dans les zéolithes ou sur la surface de la silice est prouvée par la simulation à l'aide de la dynamique moléculaire des spectres vibrationels.

REFERENCES.

1. S.Tsuneyuki, M.Tsukada, H.Aoki, and Y.Matsui Phys.Rev.Lett. **61** (1988) 869
2. B.W.H.van Beest, G.J.Kramer, and R.A.van Santen Phys.Rev.Lett. **64** (1990) 1955
3. G.J.Kramer, N.P.Farragher, B.W.H.van Beest, and R.A.van Santen Phys.Rev. **B43** (1991) 5068
4. K.de Boer, A.P.J.Jansen and R.A.van Santen Studies Surf.Sci.Catal. **84** (1994) 2083
5. J.-R.Hill and J.Sauer J.Phys.Chem. **98** (1994) 1238
6. J.-R.Hill and J.Sauer J.Phys.Chem. **99** (1995) 9536
7. K.-P.Schröder and J.Sauer J.Phys.Chem. **100** (1996) 11043

5.2. Silicates.

Article publié dans Chemical Physics 202 (1996) 53-61

ELSEVIER

Chemical Physics 202 (1996) 53–61

Chemical Physics

Ab initio generalized valence force field for zeolite modelling. 1. Siliceous zeolites

Vladimir A. Ermoshin [a,b], Konstantin S. Smirnov [b], Daniel Bougeard [a,*]

[a] *Laboratoire de Spectrochimie Infrarouge et Raman du CNRS, Université des Sciences et Technologies de Lille, F-59655 Villeneuve d'Ascq Cedex, France*

[b] *Institute of Physics, St. Petersburg State University, St. Petersburg 198904, Russia*

Received 1 August 1995

Abstract

A new potential permitting the molecular dynamics study of the structural and dynamical properties of siliceous zeolites is presented and tested. It is based on a quantum-chemical derivation of the Cartesian force constants which are transformed into an internal coordinate system and corrected for systematic errors. The calculated vibrational spectra for three siliceous zeolites (sodalite, faujasite and silicalite) show a very satisfactory agreement with the experimental ones and the force field is very similar to a potential recently derived from experimental data.

1. Introduction

Zeolites and other microporous materials attract much attention due to their important role as selective catalysts, adsorbents, and ion exchangers [1]. Many processes in zeolites occur at a short time scale and thus, knowledge of the zeolite dynamics is required for understanding their role in underlying processes. This information can be obtained by infrared [2] and Raman spectroscopy [3]. However, due to the complexity of the zeolite framework the complete lattice dynamics cannot be directly derived from experimental data. Thus, the interpretation of zeolite spectra necessitates an implementation of computational methods which are able to assign a particular spectral feature to a certain atomic motion and to describe the latter at the microscopic level.

Two main approaches are possible for the calculation of the vibrational spectra of zeolites: normal mode analysis (NMA) and molecular dynamics (MD) techniques. The former is quicker but restricted to the harmonic approximation, while the latter is more flexible in the treatment of non-harmonic problems and yields information on both structural and time-dependent characteristics. In addition, MD enables the study of the dependence of properties on external parameters such as temperature and pressure. As a consequence, MD simulations have been applied to investigate framework and cation dynamics, and diffusion of adsorbed molecules in zeolites [4–10].

The reliability of all simulation methods strongly depends on the potential functions. Because of the large size of the zeolite unit cell and the lack of sufficient experimental data, the functional form and the parameters of potentials cannot be determined unambiguously. The implementation of quantum-mechanical calculations especially at the ab initio

* Corresponding author.

SSDI 0301-0104(95)00313-4

level is a promising way in order to derive potentials for zeolite modelling.

Several attempts have already been undertaken in order to obtain potential functions for zeolitic systems from ab initio calculations. Tsuneyki et al. [11], Van Beest et al. [12], and Kramer and co-workers [13] have reported ion pair potentials based on calculations of small clusters representing TO_4 tetrahedra (T = Si, Al). Despite the fact that these potentials could reproduce structural characteristics and elastic constants of crystalline silicates, the vibrational spectra of the compounds were only approximately described [14]. An ab initio shell model potential was recently reported by de Boer et al. [15]. The authors noted that in spite of a reasonable agreement between calculated and observed structures and elastic constants for silica compounds, the potential needs some further improvement necessitated by the absence of an appropriate Si–O–Si term in the model.

As T–O bonds in zeolites are partially covalent, one can expect that potential functions which take explicitly into account the spatial orientation of the bonds will be appropriate for zeolitic systems. Such a force field is widely used in molecular mechanics and NMA. Recently, Hill and Sauer [16] have reported a consistent approach where parameters of molecular mechanics potentials were determined on the basis of calculations of relatively small molecular models representing zeolite subunits. The force field obtained was then verified in energy minimization calculations of structural characteristics of dense and microporous silicates. The authors have shown that this approach yields an accurate and transferable force field for solids based on ab initio data from cluster models. The calculated structural characteristics were in a good agreement with experimental data. However, to our knowledge the ability of this force field to reproduce the vibrational spectra of zeolites has not been proved yet.

Another version of the force field type potential set is the generalized valence force field (GVFF) used in NMA. In our previous publications [5,7] it was shown that MD calculations using a simplified version of the GVFF were able to describe the main features of both the infrared and Raman spectra of zeolite lattices very well. For a problem containing n atoms the GVFF contains at least $(3n-5)(3n-6)/2$ force constants while only a maximum of $3n-6$ frequencies can be observed. Therefore the values of the parameters usually cannot be determined unambiguously. One way out of this dilemma is the use of experimental data originating from several isotopic substituted derivatives in a fitting procedure. This method was applied by Bärtsch et al. [17] to develop a GVFF appropriate for the reproduction of the vibrational spectra of zeolite A. However, being suitable for silicates it may fail in the case when parameters for more complicated compounds have to be determined.

In the present paper we report an alternative approach to the calculation of GVFF parameters for zeolite modelling. As a first step it includes ab initio quantum-chemical calculations of small model clusters models representing zeolite units. Thereafter the strategy developed by Allouche and Pourcin [18] is applied to calculate the parameters of the force field in terms of internal coordinates taking into account the redundancies existing between the coordinates of the internal coordinates basis set. Finally, the potentiality of this force field to reproduce the vibrational spectra of zeolites is verified in molecular dynamics calculations. In the present paper this approach is applied to siliceous zeolites. The extension to aluminosilicates will be reported in a forthcoming publication.

2. Method and computational procedure

A scheme of the approach used in the present work is shown in Fig. 1. It is supposed that the dynamics of the zeolite lattice can be described in terms of vibrations of small subunits such as SiO_4 tetrahedra and $O_3Si–O–SiO_3$ shared tetrahedra. These units were treated with quantum-chemical calculations at ab initio level and as a result of such calculations a matrix of second derivatives of the total energy in Cartesian coordinates (F_x) was calculated. As the matrix cannot be directly transferred in MD (or NMA) calculations, it was transformed into the matrix of second derivatives in internal coordinates (F_r) taking into account the redundancies existing between the coordinates [18]. Finally, the obtained force field was used in MD calculations of three siliceous zeolites (sodalite, silicalite, and faujasite).

The ab initio calculations were performed with the help of the CADPAC package [19] using the basis set 3-21G* at the Hartree–Fock level as a suitable combination for the calculation of larger clusters in a reasonable time and the DZP basis set at the MP2 level as a reference calculation which takes the correlation into account and is able to reproduce the force constants accurately. $Si(OH)_4$ was calculated with both basis sets. Calculations of the $(OH)_3Si–O–Si(OH)_3$ cluster were carried out with

Table 1
Force constants of $Si(OH)_4$, disilicic acid arid zeolites in mdyn/Å, mdyn Å/rad^2 and mdyn/rad (italic digits indicate the mean value of the force constants located above them

Internal coordinate or interaction	$Si(OH)_4$		Disilicic acid	Zeolites
	DZP/MP2	3-21G*	3-21G*	
			7.20 6.50	
SiO (R)			7.06 6.50	
	5.38	6.66	*6.66*	5.38
OSiO (α)	0.703 (117°)	0.874 (115°)	0.847/0.975 [a]	0.78
	0.817 (106°)	0.946 (107°)	(Fig. 3)	
SiO/SiO (R/R)	0.162 (117°)	0.220 (115°)	0.286/0.330	0.19
Si common	0.213 (106°)	0.254 (107°)	(Fig. 4)	
SiO/SiO (r/r)			0.31	0.25
O common				
SiO/OSiO (R/α)	0.067/0.249	0.091/0.260	−0.07/0.282	0.13
SiO common	*0.132*	*0.156*	*0.160*	
SiO/OSiO (R/α)	−0.099/−0.167	−0.119/−0.197	−0.096/−0.204	−0.13
Si common	*−0.132*	*−0.156*	*−0.160*	
OSiO/OSiO (α/α)	−0.074/−0.161	−0.105/−0.177	−0.066/−0.183	−0.11
SiO common	*−0.113*	*−0.135*	*−0.135*	
OSiO/OSiO (α/α)	−0.319/−0.331	−0.374/−0.390	−0.355/−0.404	−0.32
Si common	*−0.325*	*−0.382*	*−0.389*	
SiOSi (β)			0.013	0.12
SiO/SiOSi (r/β)			−0.07/0.02	0.00
			0.00	
OH	8.86	9.44		
SiOH	0.376	0.412		
OH/SiOH	0.215	0.270		
SiO/OH	−0.077	−0.035		
SiOH/SiO	0.285	0.340		

[a] Digits separated by slash stand for the minimum and the maximum values of the force constant.

the 3-21G* basis set. In the calculation of $(OH)_3Si-O-Si(OH)_3$ it was necessary to block several torsion coordinates in order to avoid the building of internal hydrogen bonds which would have led to relaxed structures much too far from the structure of Si–O–Si bridges in zeolites and silicates. The transformations of the F_x into the F_r matrix were performed with the REDONG program [18] using the set of internal coordinates defined in Fig. 2. Finally the force constants of these molecules were used to extract a force field for zeolites which was used in the MD runs in order to simulate the vibrational spectra.

The molecular dynamics simulations were carried out with programs developed in our group. All the MD runs and spectra calculations were performed under conditions identical to those reported in Ref. [5]. The MD simulations were carried out on a Silicon Graphics Indigo2 workstation. CADPAC calculations were performed at the CNRS centre IDRIS on Cray C94.

3. Results and discussion

The harmonic force constants obtained for the two molecules are listed in Table 1. The systematic

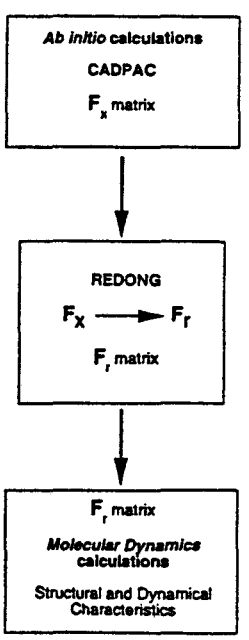

Fig. 1. Scheme of the computational procedure.

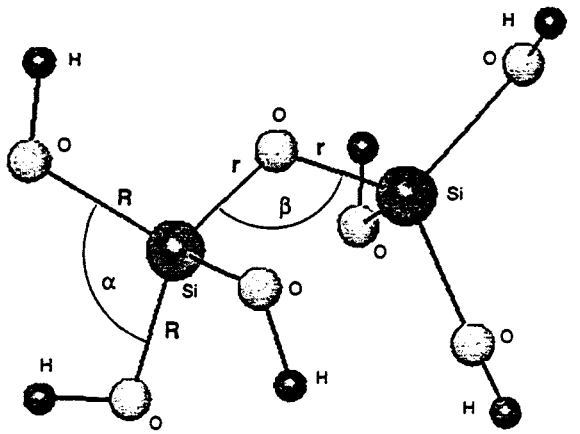

Fig. 2. Definition of used internal coordinates. R and r denote Si–O bond within SiO_4 tetrahedron and in Si–O–Si bridge, respectively.

overestimation of the 3-21G* set by comparison with DZP/MP2 is observed as expected. As the OH groups are not relevant for the present study of siliceous zeolites they will not be discussed here. For the purpose of extracting force constants for zeolites we will discuss each type of force constant separately and compare their variations with the basis set and the cluster size.

The stretching force constants of disilicic acid give rise to two sets of values, one (7.06, 7.20 mdyn/Å) corresponding to the bridging SiO bonds, the other ones (6.50 mdyn/Å) to the terminal OH groups. The mean value of these eight force constants is exactly equal to the value obtained with the same basis set for $Si(OH)_4$. Therefore the corresponding value of the force constant for the DZP/MP2 calculation of $Si(OH)_4$ (5.38 mdyn/Å) is proposed for zeolites.

Fig. 3 displays all the values of the OSiO bending force constants obtained in the calculation as a function of the OSiO angle. The dependence is linear for the 3-21G* values. Considering the systematic error between DZP/MP2 and 3-21G* and the parallelity of the variation of the force constant with the OSiO angle for both basis sets it is possible to propose a value of 0.78 mdyn Å/rad^2 for OSiO angles supposed to be tetrahedral in zeolites. A similar behaviour is shown in Fig. 4 for the SiO/SiO interaction force constant in the SiO_4 tetrahedra. A similar analysis leads to a value of 0.19 mdyn/Å in zeolites.

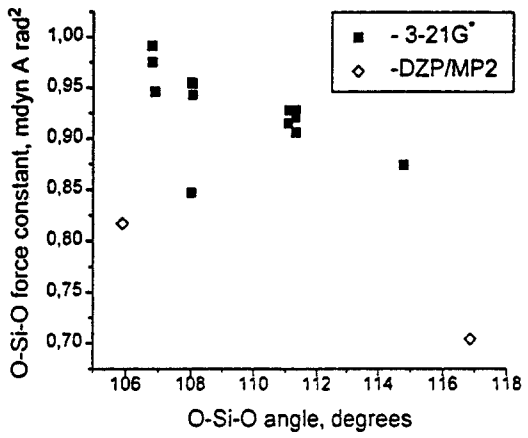

Fig. 3. Calculated values of the O–Si–O force constant versus O–Si–O angle.

The interaction force constant for SiO bonds with common O atoms was obtained by applying the correction factor 0.81 = 5.38/6.66 derived from the SiO bonds in $Si(OH)_4$ to the value calculated with the 3-21G* basis set in disilicic acid.

The interactions between bonds and angles in the SiO_4 tetrahedra can directly be deduced from Table 1. Obviously the interactions SiO/OSiO with common SiO bond ($f_{SiO/\alpha}$) and without common SiO bonds ($f'_{SiO/\alpha}$) have opposed values and as the absolute value is identical for both molecules with the 3-21G* basis it seems judicious to assign the values of the DZP/MP2 calculation of $Si(OH)_4$,

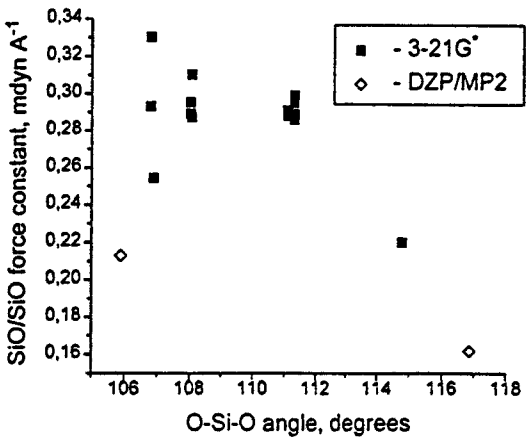

Fig. 4. Calculated values of the SiO/SiO off-diagonal force constant versus O–Si–O angle.

0.13 and −0.13 mdyn/rad for $f_{SiO/\alpha}$ and $f'_{SiO/\alpha}$, respectively.

Due to the great geometrical distance between $Si(OH)_4$ and zeolites for the OSiO angles the analysis of their interaction force constants is more complicated. For α/α interactions three types of terms exist: large/large, small/small and large/small. For each parameter all interactions were represented by one single value which was derived from the mean values obtained for disilicic acid by a correction estimated from the calculations performed on $Si(OH)_4$. Thus using a correction factor of 0.83, for $f_{g\alpha}$ the force constant was calculated to −0.11 mdyn Å/rad^2; for $f'_{\alpha\alpha}$ the value is −0.32 mdyn Å/rad^2.

As the optimized structure of disilicic acid obtained is far from the zeolite value for the bridging SiOSi angle (178°) the corresponding diagonal force constant is certainly underestimated. We therefore chose to transfer the value 0.12 mdyn Å/rad^2 from a RHF/TZ + 2d/Cl calculation of disiloxane [20]. Finally, as the 3-21G* calculation of the SiO/SiOSi interaction force constant of disilicic acid led to small positive and negative values, we decided to set this constant to zero for zeolites.

These force constants deduced from ab initio calculations are compared with literature data in Table 2. For the comparison with Bärtsch et al. [17]

Table 2
Values of the force constants for the GVFF of zeolites (units: see Table 1)

Force constant [a]	This work	Ref. [17]	Ref. [21]	Ref. [16] [b]
F_R	5.38	5.100	5.94	5.76
$f_{R/R}$	0.19	0.153	0.711	0.94
F_α	0.78	0.948 [c]	0.729	1.87
$f_{R/\alpha}$	0.13	−0.080 [c]	0.00	0.522
$f'_{R/\alpha}$	−0.13	0.080 [c]	−0.263	0.522
$f_{\alpha/\alpha}$	−0.11	−0.172 [c]	0.00	0.00
$f'_{\alpha/\alpha}$	−0.32	−0.500 [c]	−0.167	0.00
F_β	0.12	0.091	0.126	0.064
$f_{r/r}$	0.25	0.275	0.843	0.94
$f_{r/\beta}$	0.00	0.036	0.398	0.085

[a] $f_{x/x}$ and $f'_{x/x}$ denote off-diagonal force constants for internal coordinates with or without common bond, respectively. R denotes SiO bonds considered in the SiO_4 tetrahedra, r the same bonds in the SiOSi bridges.

[b] Only the harmonic force constants from Ref. [16] were used.

[c] Data of the present work were used to calculate this force constant (see text).

we had to make some assumptions because they derived three linear relations between five constants:

$f_\alpha - f_{\alpha\alpha} = 1.12,$

$f_{\alpha\alpha} - f'_{\alpha\alpha} = 0.328,$

$f_{r\alpha} - f'_{r\alpha} = -0.16.$

In order to determine the force constants we added two relations from the quantum-chemical treatment of disilicic acid

$f_{\alpha\alpha}/f'_{\alpha\alpha} = -0.11/-0.32 = 0.344,$

$f_{r\alpha}/f'_{r\alpha} = 0.13/-0.13 = -1.00.$

These equations lead to the digits given in the second column of Table 2 and were used to generate the spectra represented in Fig. 5 and 6.

Table 3 and 4 compare the calculated frequencies of the bands in the infrared and Raman spectra of

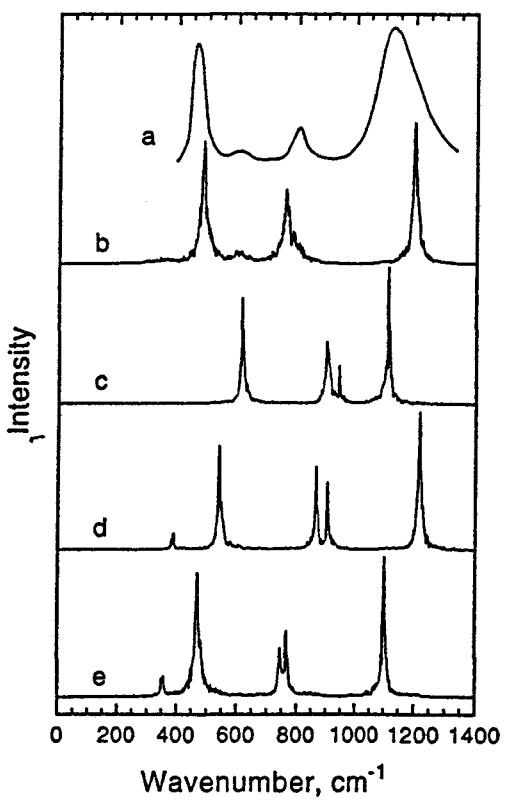

Fig. 5. Infrared spectra of siliceous sodalite calculated with different parametrizations of the GVFF. (a) Experimental spectrum from Ref. [22], (b) this work, (c) Ref. [16], (d) Ref. [17], (e) Ref. [21].

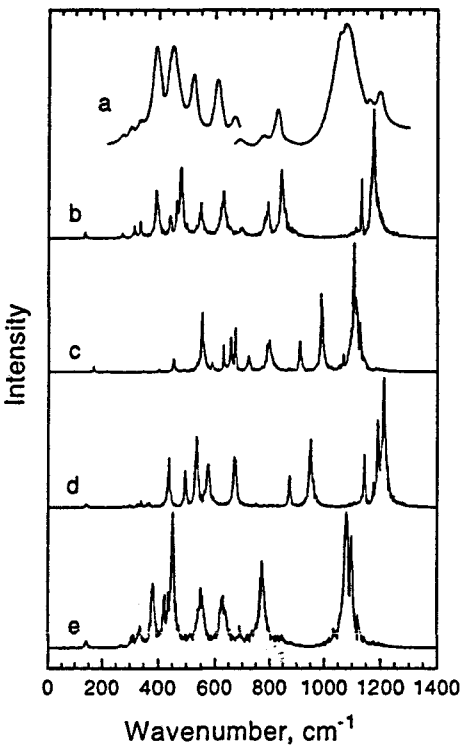

Fig. 6. Infrared spectra of siliceous faujasite calculated with different parametrizations of the GVFF. (a) Experimental spectrum from Ref. [22], (b) this work, (c) Ref. [16], (d) Ref. [17], (e) Ref. [21].

Table 3
Calculated and experimental positions of the bands (cm^{-1}) in the infrared spectra of zeolites

Sodalite		Silicalite		Faujasite	
Calc.	Exp. [a]	Calc.	Exp. [a]	Calc.	Exp [b]
1183	1107	1176	1100		1208
				1156	1174
					1090
				835	834
749	787	785	800	786	794
				700	684
				636	612
513	450	590	550	556	528
		492	420	498	482
				457	462
				410	401
				350	352
318	289			328	325
				281	289

[a] Ref. [23]. [b] Ref. [24].

Table 4
Calculated and experimental positions of the bands (cm^{-1}) in the Raman spectra of zeolites

Sodalite		Silicalite		Faujasite	
Calc.	Exp.	Calc.	Exp. [a]	Calc.	Exp. [b]
1123		1167	1083		1180
			977	1138	1090
777			806	840	820
627		784	799		
		480	467	536	510
468			432		493
367		363	375	356	360
		295	290	314	312
				292	298
				112	105
78		66–205 [c]		89	95
					70
					60

[a] Ref. [25]. [b] Ref. [26].
[c] A wide band within the indicated limits.

three siliceous zeolites with those measured experimentally. A systematic difference between the calculated and experimental positions is observed for the region of asymmetric stretching SiO vibrations above 1000 cm^{-1}. Three factors can explain such a discrepancy. Firstly, it is conceivable that the SiO force constant calculated for such small clusters is still too large compared with that in silicates. Secondly, the anharmonicity of the SiO bonds which would shift the frequencies to lower values is neglected in the present study. Finally, the calculated spectra are related to perfect zeolite lattice, while the experimental spectra are measured for powdered microcrystalline samples of partially aluminated compounds. Except in this spectral region the mean square deviation of the theoretical and experimental positions does not exceed 23 cm^{-1} and even approaches 14 cm^{-1} in the case of faujasite. Taking into account that no experimental information (except structural data for the frameworks) was used in the calculations and that the experimental data also have an uncertainty of up to 10 cm^{-1} depending for example on the sample preparation method, the agreement can be considered as very satisfactory.

Fig. 5 and 6 show the infrared spectra computed for sodalite and faujasite with the four force fields collected in Table 2. The analysis of the spectra and table reveals that obviously our results are a nice confirmation of the data of Bärtsch et al. [17]. This is not surprising, since their force field was obtained as a result of fitting procedure involving information on spectra of isotopically substituted compounds. The results of the present study confirm that using isotopic substitution the indetermination caused by the huge quantity of force constants in large systems can be reduced and that this procedure yields reliable force fields.

The spectra obtained with the force field developed by Etchepare et al. for α-quartz are also in good agreement with those computed with the force fields obtained in this study and reported in Ref. [17] However, the examination of Table 2 shows that this is probably due to a compensation of several force constants that leads to an "accidental" good reproduction of the experimental spectra. In fact, the values of the SiO/SiO and SiO/SiOSi force constants are significantly larger than those calculated in the present work and determined from experiment [17].

The potential developed by Hill and Sauer [16] mainly aimed at a description of the energy of the framework. A trial to calculate the dynamics with the harmonical part of this field led to considerable discrepancies in different regions of the spectrum for siliceous sodalite as well as for faujasite (Fig. 5 and 6). The infrared spectrum shows the deformation modes observed under 600 cm^{-1} at too high frequencies, while the splitting between SiO asymmetric (above 1000 cm^{-1}) and symmetric (around 850 cm^{-1}) stretching modes is much too small (Table 3 and 4). The analysis of the parameters obtained from the refinement process suggests two hypotheses which could have led to these discrepancies. First all interactions between SiO bonds were set equal and reached a very high value although these parameters can be expected to be different depending on the nature of the atom common to the two bonds (Si in the tetrahedra or O in the Si–O–Si bridge). This high value leads to the reduction of the splitting noticed previously and must be compensated by an increase of the diagonal force constant F_R. Secondly, the interaction force field has a very simplified structure with identical values for the bond/angle interactions while our calculation indicates that these constants should have opposite signs.

The results of the present study confirm those of our previous work [5]. The quality of the simulated spectra is slightly improved but the most important result is that this approach enables the systematic derivation of a reliable force field for complicated compounds with a minimal use of experimental information. While our previous work using guessed values of the force constants was successful, in this paper the method indicates the range for start values used to optimize the force field even if some force constants cannot be determined unambiguously. This also allows to simplify the fitting procedure in case experimental spectra of isotopically substituted derivatives are used to obtain the force constant values and to eliminate redundancy relations between some force constants.

In fact, this method is simpler and less time consuming than the commonly used procedure varying atomic coordinates for the calculation of an energy surface which is subsequently fitted by analytical potential functions [16]. Thus it can be recommended for the calculation of valence potential parameters not only for GVFF but also for molecular mechanics force fields. Finally, the approach can readily be applied to systems where a few or no experimental information on the vibrational spectra is available.

4. Conclusion

An ab initio general valence force field for crystalline microporous materials is proposed and tested by calculation of the vibrational spectra for siliceous zeolites. The comparison of the force constants obtained for silicic and disilicic acid leads to the conclusion that the force constants do not strongly depend on the cluster size. Thus, it is possible to calculate force constants for zeolites making calculations on small clusters with good quality basis sets. The comparison shows an excellent agreement of the force field calculated in the present study with the recent force field obtained from experimental data.

The calculated spectra still show some discrepancies but since experimental spectra of purely siliceous zeolite crystals are not available the obtained agreement can be considered as very satisfactory. A first way of improvement will be the introduction of anharmonicity which will improve the calculation of the vibrations of the SiO bonds. In a next step we will perform similar calculations on other small systems in order to derive the force constants necessary to calculate real zeolites containing a certain amount of disordered aluminum atoms and it will be possible to follow the influence of the Si/Al ratio on the spectra.

In the present paper we were able to show that quantum-chemical calculations used to derive force constants yields parameters which are a nice basis for further studies of spectroscopic properties of zeolites and permit a better interpretation of the complicated spectra. Of course, not only zeolites, but also other systems with covalent bonds can be treated in the same way

Acknowledgements

We would like to acknowledge the financial support of NATO (Contract HTECH.CRG 941422), computing time at IDRIS (Project 940148) and support by RFFI (Russian Foundation for Basic Researches) (Grant No. 95-03-9551a). VE acknowledges a grant from the Ministère des Affaires Etrangères. The authors thank Dr. P. Bornhauser for useful discussions.

References

[1] M.E. Davis, Intern. Eng. Chem. Res. 30 (1991) 1675.
[2] E.M. Flaningen, H. Khatami and H.A. Szymanski, Advan. Chem. Ser. 101 (1971) 201.
[3] C. Brémard and D. Bougeard, Advan. Mater. 7 (1995) 10.
[4] P. Demontis and G.B. Suffritti, J. Chem. Soc. Faraday Trans. 91 (1995) 525.
[5] K.S. Smirnov and D. Bougeard, J. Phys. Chem. 97 (1993) 9434, and references therein.
[6] J.M. Shin, K.T. No and M.S. Jhon, J. Phys. Chem. 92 (1988) 4553.
[7] K.S. Smirnov, M. Le Maire, C. Brémard and D. Bougeard, Chem. Phys. 179 (1994) 445.
[8] K.S. Smirnov and D. Bougeard, Zeolites 14 (1994) 203.
[9] P. Demontis and G.B. Suffritti, in: Modelling structure and reactivity in zeolites, ed. C.R.A. Catlow (Academic Press, New York, 1992) p. 79, and references therein.
[10] D. Dumont and D. Bougeard, Studies Surf. Sci. Catal. 84 (1994) 2131.

[11] S. Tsuneyuki, M. Tsukada, H. Aoki and Y. Matsui, Phys. Rev. Lett. 61 (1988) 869.
[12] B.W.H. van Beest, G.J. Kramer and R.A. van Santen, Phys. Rev. Lett. 64 (1990) 1955.
[13] G.J. Kramer, N.P. Farragher, B.W.H. van Beest and R.A. van Santen, Phys. Rev. B 43 (1991) 5068.
[14] R.G.D. Valle and H.C. Andersen, J. Chem. Phys. 94 (1991) 5056.
[15] K. de Boer, A.P.J. Jansen and R.A. van Santen, Studies Surf. Sci. Catal. 84 (1994) 2083.
[16] J.R. Hill and J. Sauer, J. Phys. Chem. 98 (1994) 1238.
[17] M. Bärtsch, P. Bornhauser, G. Calzaferri and R. Imhof, J. Phys. Chem. 98 (1994) 2817.
[18] A. Allouche and J. Pourcin, Spectrochim. Acta 49A (1993) 571;A. Allouche, REDONG, QCPE 628.
[19] R.D. Amos and J.E. Rice, CADPAC: The Cambridge Analytical Derivatives Package, Issue 4.0, Cambridge, 1987.
[20] J.B. Nicholas, R.E. Winans, R.J. Harrison, L.E. Iton, L.A. Curtiss and A.J. Hopfinger, J. Phys. Chem. 96 (1992) 7958.
[21] J. Etchepare, M. Merian and L. Smetankine, J. Chem. Phys. 60 (1974) 1873.
[22] A.J.M. de Man and R.A. van Santen, Zeolites 12 (1992) 369.
[23] J.B. Nicholas, A.J. Hopfinger, F.R. Trouw and L.E. Iton, J. Am. Chem. Soc. 113 (1991) 4792.
[24] W.P.J.H. Jacobs, J.H.M.C. Wolput and R.A. van Santen, J. Chem. Soc. Faraday Trans. 89 (1993) 1271.
[25] G. Deo, A.M. Turek, I.E. Wachs, D.R.C. Huybrechts and P.A. Jacobs, Zeolites 13 (1993) 265.
[26] C. Brémard and M. Le Maire, J. Phys. Chem. 97 (1993) 9695.

5.3. Aluminosilicates.

Article publié dans Chemical Physics 209 (1996) 41-51

ELSEVIER

Chemical Physics 209 (1996) 41–51

Chemical Physics

Ab initio generalized valence force field for zeolite modelling 2. Aluminosilicates

Vladimir A. Ermoshin [a,b], Konstantin S. Smirnov [b], Daniel Bougeard [a,*]

[a] *Laboratoire de Spectrochimie Infrarouge et Raman du CNRS, Université des Sciences et Technologies de Lille, 59655 Villeneuve d'Ascq cedex, France*

[b] *Institute of Physics, St. Petersburg State University, St. Petersburg 198904, Russian Federation*

Received 12 February 1996

Abstract

A generalized valence force field for modelling the vibrational spectra of aluminosilicates is developed on the basis of ab initio calculations (3-21G* and DZP/MP2) performed on small clusters: $Si(OH)_4$, $(OH)_3SiOSi(OH)_3$, $Al(OH)_4^-$, $H_3SiOHAlH_3$, $(OH)_3SiOAl(OH)_3^-$ and $(OH)_3SiOHAl(OH)_3$. The Cartesian force constants from the ab initio calculations are transformed into internal coordinates and used in molecular dynamics simulations of protonated and non-protonated faujasite structures. Calculated positions of the bands in the infrared and Raman spectra of the zeolite are in good agreement with those observed. The force field explains the main features in the vibrational spectra of OH(OD) groups of protonated structures.

1. Introduction

Zeolites are microporous aluminosilicates with a wide range of applications as molecular sieves, ion exchangers and especially as shape-selective heterogeneous catalysts. An increasing use of zeolites for industrial purposes stimulates both experimental and theoretical studies aiming to understand the zeolite activity on the basis of the underlying microscopic processes. Recent results of such works can be found in Ref. [1].

Among the experimental techniques used for studies of zeolitic systems, the methods of vibrational spectroscopy play an important role in the characterization of these compounds and yield insight into the specific interactions between host lattice and sorbed guest molecules [2,3]. However, a complete interpretation of the zeolite vibrational spectra on the basis of experimental results is difficult due to the enormous number of atoms in the unit cell. This problem could be solved by the use of normal mode analysis (NMA) or molecular dynamics (MD) techniques which relate particular spectral features to specific atomic motions. Nevertheless, the reliability of the results obtained by these methods strongly depends on the set of potential functions employed in the calculations. As the bonds in zeolite frameworks have a partially covalent character, one can expect that sets of potential functions used in molecular mechanics (MM) or in NMA and which take the spatial orientation of the bonds explicitly into account, will be suitable for the description of both

* Corresponding author.

PII S0301-0104(96)00124-3

structure and dynamics of zeolite lattices. Indeed, MD calculations performed with the help of such force fields [4–6] led to a good agreement between experimental and calculated structural and dynamical characteristics of zeolite frameworks.

The application of the force fields in zeolite studies is often limited because of the lack of accurate parameters which can hardly be derived from experimental data due to the complexity of the zeolitic systems. Ab initio quantum chemical calculations provide a possible way for the parametrization of the potentials. A commonly accepted routine to perform the parametrization is the calculation of the potential energy hypersurface followed by the fitting of the surface by appropriate analytical functions. This approach has already been used for parametrization of ion pair [7–9] and shell model potentials [10]. Despite a reasonable agreement between the calculated and experimental structures, the computed vibrational spectra have revealed significant discrepancies with experimental data. Recently, Hill and Sauer have reported molecular mechanics force field parameters for silicates [11] and aluminosilicates [12] based on ab initio calculations of molecular models. The use of this force field in lattice energy minimization calculations of dense and microporous silicate and aluminosilicate compounds has shown a good agreement between calculated and experimental structural parameters. However, the application of this force field for the prediction of vibrational spectra was not mentioned.

In a previous paper we have presented parameters of a generalized valence force field (GVFF) for silicates on the basis of ab initio quantum chemical calculations of small molecular models [13]. The calculated spectra for a number of siliceous zeolites were in good agreement with the experimental ones and the obtained force field parameters were very close to those recently derived from experimental data. In the present paper we extend this approach to aluminosilicates with emphasis on zeolite Y as an experimental reference.

2. Method and computational procedure

Our approach implies that the dynamics of zeolite frameworks (as well as that of dense silicates and aluminosilicates) can be described in terms of vibrations of small building units such as TO_4 tetrahedra and oxygen sharing tetrahedra $O_3T\text{-}O\text{-}TO_3$ (T = Si, Al). These molecular models are treated with ab initio quantum chemical calculations resulting in a matrix of the second derivatives of the total energy with respect to Cartesian coordinates (F_x). However, as the matrix cannot be directly used in MD or NMA calculations, it is transformed into a matrix of second derivatives in internal coordinates (matrix of force constants, F_r) taking into account eventually existing redundancies between the coordinates. The obtained force field is tested with molecular dynamics calculations of zeolite vibrational spectra.

In order to derive the force field for aluminosilicates the following molecular models were considered in addition to $Si(OH)_4$ and $(OH)_3SiOSi(OH)_3$ already studied in Ref. [13]: $Al(OH)_4^-$, $H_3SiOHAlH_3$, $(OH)_3SiOAl(OH)_3^-$, $(OH)_3SiOHAl(OH)_3$. All these clusters were treated at the Hartree–Fock level with 3-21G* basis set. Reference calculations employing the DZP basis set at the MP2 level were performed for $Al(OH)_4^-$ and $H_3SiOHAlH_3$. Comparison of the results obtained with the help of these two levels of theory enables the derivation of a systematic difference between the 3-21G* results and those calculated at the more sophisticated DZP/MP2 level. The obtained scaling factors are then used to calculate the final force field from the results of 3-21G* calculations of larger models. Such an approach yields transferable GVFF parameters at reduced computational costs [13].

The quantum chemical calculations were carried out with the CADPAC package [14]. The transformation of the matrix F_x into F_r was performed with the REDONG program [15] using the set of internal coordinates defined in Fig. 1. As no symmetry constraints were applied in the calculations, distortion of symmetry of the molecules results in a set of force constants of the same type for all species and thus the procedure used in Ref. [13] was applied to deduce the force field for the Al derivatives. MD runs and spectra calculations were carried out with original programs developed in our group. Details of the computational procedures used can be found in Ref. [5,6]. The initial framework structure used in the MD calculations was that given in ref. [5] and was equilibrated for 20 ps at 300 K. The radial and angle

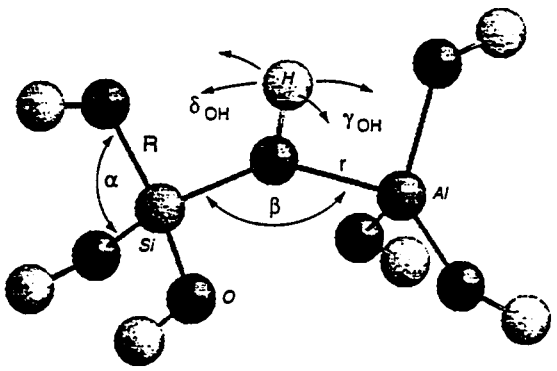

Fig. 1. Definition of the set of internal coordinates used in transformation F_x into F_r matrix.

distribution functions are in good agreement with the crystal experimental data.

As the electrostatic interactions are not considered in the present study no charge balancing cations were used for the calculation performed for non-protonated zeolite structures. The negative charge of the Si–O–Al bridges is implicitly taken into account via values of the force constants. The initial coordinates of the atoms were taken from Ref. [16,17]. The values of the equilibrium parameters are discussed in the subsequent section of the paper.

For the protonated samples NMA were performed in order to ascertain the assignment of the bands and to follow the couplings upon deuteration. These NMA were calculated on a cluster $(OH)_3SiOH–Al(OH)_3$ taken at the geometry defined later in this paper for the MD calculations.

3. Results and discussion

3.1. Ab initio force field

In the previous paper [13] it was shown that the force field in SiO_4 tetrahedra only weakly depends on the size of the clusters. Tables 1 and 2 summarize the force constants, excluding those for T–O bonds, obtained with a 3-21G* basis for SiO_4 and AlO_4^- tetrahedra in different molecules. These tables show two main effects for the off-diagonal and angle bending force constants. First, as already mentioned, the structures were optimized without symmetry constraints so that each type of interaction is spread over a certain range covering the geometrical differences in one molecule. The mean amplitude of variation of the force constants around the mean value for each molecule is about 20%. The second effect is the variation of the mean values when going from one molecule to another. In this case the mean variation is clearly smaller and of the order of $\pm 5\%$. These observations confirm that the size of the cluster is less important for the determination of the force constant than the actual geometry of the molecule considered. This means that the force field can be obtained with calculations employing a good quality

Table 1
The force constants in SiO_4 tetrahedra from 3-21G* calculations of different molecular models. Digits in brackets separated by a slash stand for maximum and minimum value among the force constants of this type. Units are mdyn/Å, mdyn Å/rad^2 and mdyn/rad

	$Si(OH)_4$	$(OH)_3SiOAl(OH)_3^-$	$(OH)_3SiOHAl(OH)_3$
R/α (R comm.)	0.156	0.160	0.163
	(0.091/0.260)	(0.111/0.190)	(0.114/0.298)
R/α (no R c.)	−0.156	−0.160	−0.157
	(−0.119/−0.197)	(−0.150/−0.183)	(−0.122/−0.219)
α/α (R comm.)	−0.135	−0.137	−0.130
	(−0.105/−0.177)	(−0.119/−0.172)	(−0.008/−0.197)
α/α (no R c.)	−0.382	−0.420	−0.380
	(−0.374/−0.390)	(−0.417/−0.427)	(−0.374/−0.391)
α	0.922	0.973	0.913
	(0.874/0.946)	(0.938/0.999)	(0.865/1.040)
R/R	0.243	0.297	0.267
	(0.220/0.254)	(0.265/0.322)	(0.246/0.302)

Table 2
The force constants in AlO_4 tetrahedra from 3-21G* calculations of different molecular models. Comments, see Table 1

	$Al(OH)_4^-$	$(OH)_3SiOAl(OH)_3^-$	$(OH)_3SiOHAl(OH)_3$
R/α (R comm.)	0.099	0.105	0.135
	(0.068/0.141)	(0.074/0.134)	(0.034/0.504)
R/α (no R c.)	−0.099	−0.104	−0.101
	(−0.073/−0.131)	(−0.090/−0.120)	(−0.055/−0.197)
α/α (R comm.)	−0.095	−0.091	−0.075
	(−0.075/−0.119)	(−0.042/−0.117)	(−0.235/0.208)
α/α (no R c.)	−0.289	−0.302	−0.240
	(−0.279/−0.309)	(−0.301/−0.303)	(−0.235/−0.251)
α	0.667	0.671	0.683
	(0.653/0.675)	(0.656/0.689)	(0.487/1.177)
R/R	0.180	0.213	0.196
	(0.174/0.183)	(0.201/0.224)	(0.128/0.323)

basis set for small models such as $Si(OH)_4$ and $Al(OH)_4^-$ clusters. The corresponding harmonic force constants calculated for these models at DZP/MP2 level are given in Table 3. By the way, this table is a nice subsequent confirmation of the validity of the factor 0.75 applied in Ref. [6] to silicon force constants in order to obtain the corresponding aluminium force constants in the treatment of zeolite A; the mean value of the factor calculated from the data of Table 3 is equal to 0.71.

On the contrary, the values of the T–O bond force constants vary over a larger interval and show a significant dependence on the surrounding. Table 4 lists the values of the T–O force constants and bond lengths calculated for different clusters with 3-21G* basis set. The most pronounced influence is observed for the $(OH)_3SiOHAl(OH)_3$ cluster. Indeed, protonation of the SiOAl bridge results in a small value of the Al–O force constant and in the lengthening of the Al–O bond to 1.915 Å in the Si–OH–Al linkage. Simultaneously this leads to a shortening of the other Al–O bonds and to an increase of the corresponding force constants. Similar trends are shown by the Si–O bonds: the force constant for the bond in the Si–OH–Al bridge decreases (bond length increases) whereas the force constants for other bonds increase (bond lengths decrease).

Fig. 2 displays the calculated values of the Si–O and Al–O bond stretching force constant versus the bond length. This plot suggests an hyperbolic relation between the force constant and the interatomic distance. In fact, a better fit is obtained with a function representing Badger's rule [18,19] expressed by the equation:

$$K_{TO} = A/(R_{TO} - B)^3$$

where A and B are parameters. The parameter A is a constant equal to 1.86 mdyn/Å^2, while the value of B depends on the nature of the atoms. A fit of the calculated data by the function indicated above yields $A = 1.824$ mdyn/Å^2 and $B = 0.966$ Å in good agreement with the value of the parameters A given above and B of 0.94 Å reported in Ref. [18,19]. The same curve fits the values of force constants for both SiO and AlO bonds as already mentioned in Ref.

Table 3
Force constants for $Si(OH)_4$ [3] and $Al(OH)_4^-$ clusters calculated at DZP/MP_2 level. Units see Table 1

	$Si(OH)_4$	$Al(OH)_4^-$
TO	5.38	3.20
TO/TO	0.19	0.15
OTO	0.78	0.56
OTO/OTO (TO common)	−0.11	−0.08
OTO/OTO(no TO common)	−0.32	−0.25
TO/OTO (no TO common)	−0.13	−0.08
TO/OTO (TO common)	0.13	0.08
OH	8.86	8.88
TOH	0.38	0.27
OH/TOH	0.21	0.20
TO/TOH	0.28	0.16

Table 4
Values of bond lengths R (in Å) and force constants K (in mdyn/Å) calculated with the 3-21G* basis set for disilicic acid [13] and its Al derivatives

		Si–O bonds		Al–O bonds	
		R	K	R	K
$(OH)_3SiOSi(OH)_3$	bridge	1.595	7.13		
	TO(H)	1.623	6.50		
$(OH)_3SiOAl(OH)_3^-$	bridge	1.549	9.04	1.749	3.58
	TO(H)	1.648	5.75	1.743	3.95
$(OH)_3SiOHAl(OH)_3$	bridge	1.653	5.74	1.915	1.82
	in plane TO(H)	1.615	6.75	1.714	4.62
	out of plane TO(H)	1.606	7.00	1.695	4.93

[18,20]. A possible reason for the difference between our parameters and those of the literature is that our data were obtained for calculated molecular models revealing large T–O bond lengths, whereas the values reported in Ref. [19] were derived from data of crystalline silicates and aluminosilicates spread over a narrower range of distances.

The large bond length and small value of the force constant for Al–O bond in the Si–OH–Al linkage are in line with data of Ref. [12], which shows that the Si–O(H)–Al bridge can be considered as a SiOH group bound to an AlO_3 Lewis acid site. As mentioned above, the force field inside of AlO_4 tetrahedron in the $(OH)_3SiOHAl(OH)_3$ cluster shows a larger range of values for force constants of the same type when compared to that for SiO_4 tetrahedra and for AlO_4 tetrahedra in other models (Tables 1 and 2). It is obviously due to the strong distortion from tetrahedral symmetry caused by the weak Al–O(H) bond. The analysis of the geometry shows that values of the O–Al–O angles between Al–O bonds not involved in the Al–O(H)–Si bridge are close to 120° (117°, 117°, 118°) thus pointing to the sp2-hybridization of the Al atom and to a weak bonding to the bridging oxygen.

Calculations of angle bending T–O–T force constants and interaction bond-angle and bond–bond force constants in a non-protonated Si–O–T bridge (T = Si, Al) show that their values weakly depend on the nature of the T atom and are very close to those calculated for the Si–O–Si bridge in [13]. For example, a value of 0.31 mdyn/Å was obtained for the SiO/SiO interaction force constant in the $(OH)_3SiOSi(OH)_3$ cluster while it is equal to 0.28 mdyn/Å for the $(OH)_3SiOAl(OH)_3^-$ model. For the T–O/T–O–T interaction force constant values of −0.07/0.02 and 0.09/0.03 mdyn/rad were obtained for disilicic acid and Al-substituted disilicic acid, respectively. The corresponding T–O–T angle bending force constants are of 0.01 and 0.02 mdynÅ/rad^2.

In order to derive force constants in the AlOHSi bridge from calculations of the $(OH)_3SiOHAl(OH)_3$ cluster with the 3-21G* basis set, the $H_3SiOHAlH_3$ cluster was calculated at both the 3-21G* and DZP/MP2 levels. The force constants obtained in these calculations for the Si–OH–Al bridge are listed

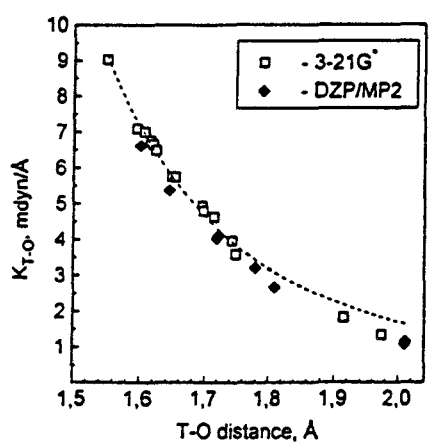

Fig. 2. Calculated dependence of the T–O stretching bond force constant on T–O bond length. Dashed line is the fit of the dependence by Eq. (1).

in the first two columns of Table 5. The values of the scaling factors for the transition from 3-21G* to DZP/MP2 force constants corresponding to the stretching coordinates without hydrogen atoms are equal to 0.81, 0.77 and 0.84; their mean value of 0.81 is in agreement with our previous data obtained from calculations of the $Si(OH)_4$ and $(OH)_3SiOSi(OH)_3$ clusters [13]. Thus, a scaling factor of 0.81 will be used to deduce the force constants for zeolites from a calculation of the $(OH)_3SiOHAl(OH)_3$ molecule at the 3-21G* level. This model has the advantage of saturating the T atoms with oxygen atoms as proposed in Ref. [21]. For the OH bond stretching force constant the calculated scaling factor is equal to 0.94 and exactly corresponds to the value obtained in Ref. [13]. Further, Table 5 shows that the other force constants for internal coordinates with H atom do not significantly vary with the basis set. Thus, it is suggested that the values of force constants for internal coordinates with H atom derived from 3-21G* calculation of the $(OH)_3SiOHAl(OH)_3$ cluster (column 3, Table 5) can be directly used in the force field for protonated zeolites.

The data presented above can be summarized as follows: (i) force constants in TO_4 tetrahedron (except T–O bond force constants) do not depend on the cluster size or on the nature of the T atom in adjacent tetrahedra and do only depend on the nature of the central T atom (Si or Al); they will therefore be transferred from the DZP/MP2 calculations of $Si(OH)_4$ and $Al(OH)_4^-$ (Table 3); (ii) values of the force constants in non-protonated Si–O–T linkage (T = Si,Al) do not depend on the nature of the T atom; they will be transferred from our previous calculations of purely silicic zeolites; (iii) for protonated bridges the force constants are given in the last column of Table 5; (iv) T–O bond stretching force constants largely vary with the environment and this variation is correlated to the bond length (Fig. 2).

Table 5
Force constants for Si–OH–Al bridge. Units see Table 1

	H_3-SiOHAl-H_3		$(OH)_3$-SiOHAl-$(OH)_3$	MD
	3-21G*	DZP/MP2	3-21G*	
SiO	4.79	4.03	5.74	4.65 [a]
AlO	1.33	1.07	1.82	1.47
SiO/AlO	0.30	0.23	0.22	0.17
SiOAl	0.18	0.19	0.14	0.14
SiOAl/SiO	0.03	0.05	0.00	
SiOAl/AlO	−0.01	0.01	−0.01	
OH	9.18	8.65	8.70	8.18
SiO/OH	0.03	−0.03	0.10	0.10
AlO/OH	0.07	0.05	0.22	0.22
SiOH	0.24	0.22	0.21	0.21
AlOH	0.18	0.16	0.19	0.19
SiOH/SiO	0.09	0.07	0.11	0.11
SiOH/AlO	−0.01	−0.01	0.00	
SiOH/OH	0.08	0.06	0.02	
AlOH/SiO	−0.12	−0.12	−0.11	−0.11
AlOH/AlO	0.01	0.00	0.01	
AlOH/OH	0.00	0.00	0.14	0.14
SiOAl/OH	−0.08	−0.07	−0.17	−0.17
SiOH/AlOH	−0.12	−0.10	−0.13	−0.13
SiOAl/SiOH	−0.12	−0.12	−0.08	−0.08
SiOAl/AlOH	−0.06	−0.07	−0.06	−0.06
Out-of-plane	0.02	0.02	0.03	0.03

[a] A value of 3.65 should be preferred to 4.65 in MD simulations (see text).

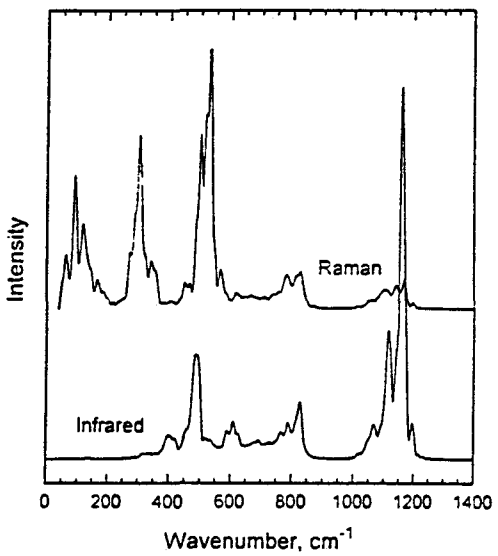

Fig. 3. Calculated infrared (a) and Raman (b) spectra of zeolite Y with Si/Al = 7.7.

The obtained results allow to form the GVFF for modelling the aluminosilicates. First, let us recall that the stretching force constant obtained in Ref. [13] for purely siliceous structures was 5.38 mdyn/A. Upon inserting the Al atoms into the framework the force field changes. However, these changes are limited by the relaxation of the bonds in the neighboring Si tetrahedra [12]. From the 3-21G* calculation of the $(OH)_3SiOAl(OH)_3^-$ cluster we obtain the force constants 9.04 and 5.75 mdyn/Å for the stretching SiO(Al) and the three SiO(Si) coordinates in the $(Si)_3O-Si-O(Al)$ linkage, respectively. The value 3.58 mdyn/Å for the AlO stretching force constant was also taken from this calculation (Table 4). Here we use the results of previous calculations for siliceous zeolites showing that the termination of the SiO_4 tetrahedron by the H atoms is a good model for the real crystalline system [12,13]. The previously discussed factor of 0.81 is then applied in order to obtain the force constants for MD and NMA calculations. These results are summarized by the following scheme:

$$\underset{}{Si}\underset{5.38}{---}O\underset{4.66}{---}Si\underset{7.32}{---}O\underset{2.90}{---}Al\underset{2.90}{---}O\underset{7.32}{---}Si$$

where the digits stand for values of the T–O bond stretching force constants (in mdyn/Å) among the bond in the tetrahedra.

The results of the calculations do not allow the correct assignment of the force constant for a possible structure where Al atoms would be the next nearest neighbours. This obviously requires the calculations of larger clusters with different distribution of the Al atoms over the T atoms positions. Thus, MD calculations were performed for a model where Al atoms in the framework are far enough apart and thus corresponds to a high Si/Al ratio. According to the results discussed above the other force constants inside the tetrahedra were transferred from DZP/MP2 calculations of $Si(OH)_4$ and $Al(OH)_4^-$ clusters (Table 3). The angle bending and TO/TO interaction force constants in T–O–T linkages were taken from Ref. [13]. The equilibrium TO bond lengths used were equal to 1.61 Å and 1.72 Å for SiO and AlO bonds, respectively [12]. The equilibrium value of the T–O–T angles was set to 143° [16,17].

In the case of protonated zeolites we are mainly interested in the dynamics of hydrogen atoms. Obviously, the vibrational motion of the H atoms mainly depends on the force field in the SiOHAl bridge, whereas changes of the force constants in the next coordination spheres has a less pronounced effect. In addition, Table 4 shows that the relaxation of the

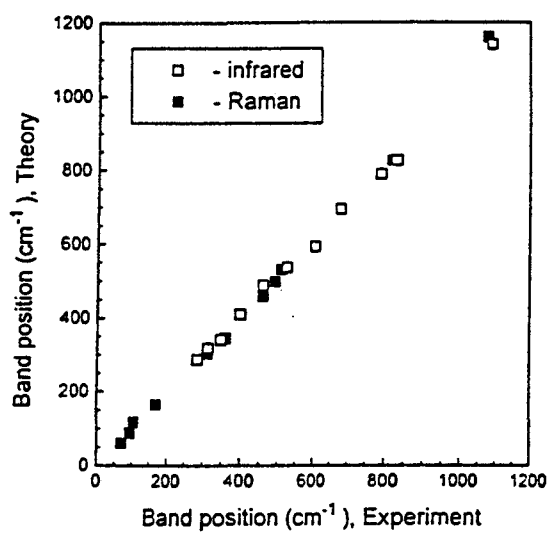

Fig. 4. Plot of calculated positions of the bands in infrared and Raman spectra of zeolite Y with Si/Al = 7.7 vs. experimental positions. The optimal linear regression leads to a line with equation $\nu_{calc} = 0.9875\nu_{exp} + 6.057$ (in cm^{-1}) with a correlation coefficient of 0.9991. Under 900 cm^{-1} the mean square deviation is smaller than 12 cm^{-1}.

bonds in the next coordination sphere caused by the formation of the protonated bridge is weaker than that in the case of its non-protonated analogue. Thus, for a model used in the MD calculations of protonated structures, the values 5.38 and 2.90 mdyn/Å were assigned to all SiO and AlO bond stretching force constants in non-protonated T–O–T bridges, respectively. The values for SiO(H) and AlO(H) bonds were taken from the 3-21G* calculation of the $(OH)_3SiOHAl(OH)_3$ cluster and scaled by the factor 0.81. The force constants for internal coordinates involving the hydrogen atom in the SiOHAl bridge are reported in the last column of Table 5. The distribution of the T–O bond stretching force constant (in mdyn/Å) is presented in the following scheme together with the equilibrium values of the T–O bond lengths (in Å) transferred from Table 8 in Ref. [12]:

	Si —· O —· Si		H —· O —· Al		Al —· O —· Si	
Force constant	5.38	5.38	4.65	1.47	2.90	5.38
Bond length	1.61	1.61	1.66	1.97	1.72	1.61

As before, data of Table 3 and Ref. [13] were used to assign force constants in TO_4 tetrahedra and non-protonated Si–O–T linkages, respectively. Equilibrium values of 143°, 117°, and 106° obtained from the quantum chemical calculations were assigned to the T–O–T, Si–O–H, and Al–O–H angles, respectively.

3.2. Molecular dynamics test

Calculated infrared and Raman spectra of dehydrated faujasite structure with the Si/Al ratio equal to 7.7 are presented in Fig. 3; the positions of the bands in the spectra as compared with those measured experimentally [22,23] are shown in Fig. 4. In the spectral region below 900 cm^{-1} our model reproduces the experimental data well, all observed bands have their counterparts in the calculated spectra. For this region the mean square deviation of the calculated and observed band positions is less than 12 cm^{-1}. A discrepancy between the spectra appears only for the region above 900 cm^{-1} that is characteristic for T–O–T asymmetric stretching vibrations. The positions of the calculated bands are shifted upwards as compared with those in the experimental spectrum. Such an overestimation of the vibrational frequencies for asymmetric stretching vibrations, while the positions of all other bands are well reproduced, has already been discussed in our previous paper [13].

The relaxation of T–O bonds upon formation of the Si–O–Al and Si–OH–Al linkages is not an artefact of the present work (Table 4) that could be due to a small size of the models used. Such a relaxation has also been calculated in Ref. [12] for larger clusters. Moreover, it should be noted that this relaxation gives an explanation for the observed high-frequency shift of the asymmetric T–O–T vibrations band upon protonation of the bridges [22]. The shift was explained as a result of coupling between T–O stretching and OH in-plane bending vibrations [22]. In fact, the formation of an OH group results in the weakening of one T–O bond in the tetrahedra while three other bonds become stronger. This results in a larger mean value of the force constant in the tetrahedra near a protonated bridge than in other tetrahedra and leads to the observed blue shift of the T–O–T asymmetric stretching vibration.

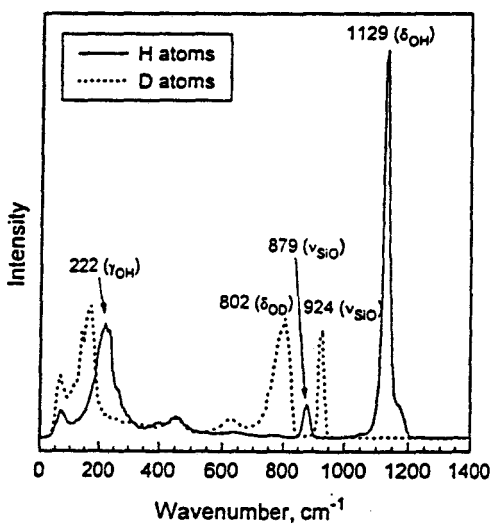

Fig. 5. Power spectrum of H atoms (solid line) and D atoms (dotted line) calculated for H-zeolite Y with Si/Al = 7.7 using values force constants defined in Table 5 and in Fig. 1.

As the chemical reactivity of zeolites originates from Brönsted acidity of the bridging hydroxyl groups, knowledge of the dynamics of these groups plays an important role in understanding their activity. Fig. 5 shows power spectra for H and D atoms calculated with the force field developed in this work for protonated zeolites. These spectra can be directly compared with inelastic neutron scattering (INS) data (the latter are weighted by the cross section, which is much higher for light H atoms). In the region of the OH stretching vibrations above 3000 cm^{-1} only one broad band without noticeable structure is calculated. Two modes usually termed HF and LF are expected in this region, which are assigned for example in faujasite to the O_1 and O_2–O_3 sites, respectively [24]. This discrepancy is not surprising because our model developed from small clusters cannot take interactions at longer range into account and in the calculations the electrostatic interactions which could lead to this band splitting for the different sites has been neglected. The following discussion will treat only the region under 1200 cm^{-1}. The most prominent peaks in the calculated proton spectrum occur at 1129 cm^{-1} and 222 cm^{-1}. NMA calculations enable us to assign the peaks to in-plane (δ) and out-of-plane (γ) OH bending vibrations, respectively. The position of the δ_{OH} vibration is in good agreement with the position of the peak at 1090 cm^{-1} observed in INS spectra [25] and the value of 1100 cm^{-1} computed for this vibration in Ref. [26]. In different zeolites the γ_{OH} mode is always observed between 350 and 400 cm^{-1} (see Ref. [25]). Calculations performed at different levels on several clusters yield the γ_{OH} vibration between 222 and 460 cm^{-1} [27,28]. In all the calculations we obtained frequencies between 100 and 150 cm^{-1} for the γ_{OH} mode. This frequency corresponds to the value of 0.02 mdyn/Å^2 for the out-of-plane force constant reported in Table 5 and leads to the 222 cm^{-1} frequency obtained in the MD calculation of the zeolite, whereby the frequency shift is probably due to the environment in the solid. A discrepancy of roughly 150 cm^{-1} is observed between the calculated and experimental spectra for the three main patterns of the density of vibrational states in the region below 500 cm^{-1}. The low-frequency motion of the light particle with a large amplitude requires the knowledge of the whole potential hypersurface to take into account the couplings with the modes of the solid. This fact concerning the dynamics of the proton recalls the problem encountered by Fillaux et al. in the treatment of *N*-methyl-acetamide by NMA [29], but can be mastered by an empirical correction of the constant as in Ref. [26] where a value of 0.12 was proposed. Obviously the value of the force constant is at the limit of the possibilities of the method we used because the error on this value is of the order of the force constant as can be estimated from Table 5. Two additional peaks at 879 and 450 cm^{-1} are present in the calculated spectrum. On the basis of NMA calculations the former band mainly originates from localized Si–O vibration in the Si–OH–Al bridge, while the latter is due to coupling between framework and proton motions.

Substitution of the H atoms by deuterium results in the downward shift of the spectrum (Fig. 5). NMA analysis indicates that the low-frequency peak at 802 cm^{-1} results from the δ_{OD} vibration, while the high-frequency peak at 924 cm^{-1} is mainly (65% of potential energy) due to the Si–O vibration. These two peaks result from a mechanical coupling in the system and could be described in terms of splitting caused by the resonance interaction of the in-plane OD and the localized Si–O vibration that is present in the spectrum of H atoms at 879 cm^{-1}. Nearly equivalent intensities of the peaks, indicating that the motion of D atoms participates in both vibrations, also support this conclusion. The δ_{OD} frequency is conversely lowered as compared to the expected value of 822 cm^{-1} that could be estimated from the mass effect. The experimental position for the in-plane OD bending vibration is ca. 870 cm^{-1} [26] and it is shifted upwards by comparison with both the value of 800 cm^{-1} calculated in the same work, and the expected position estimated from the mass effect. The shift was explained as a Fermi resonance between the δ_{OD} mode and lattice vibrations [26].

In our mind the discrepancy between the calculated and observed positions of δ_{OD} vibration (802 vs. 870 cm^{-1}) is due to the fact that the Si–O(H) stretching force constant in the model is still overestimated. Indeed, the use of a lower value for the force constant will result in a low-frequency shift of the localized Si–O mode in the Si–OH–Al bridges. In this case, due to the resonance interaction of the Si–O(D) and δ_{OD} vibrations, the former will un-

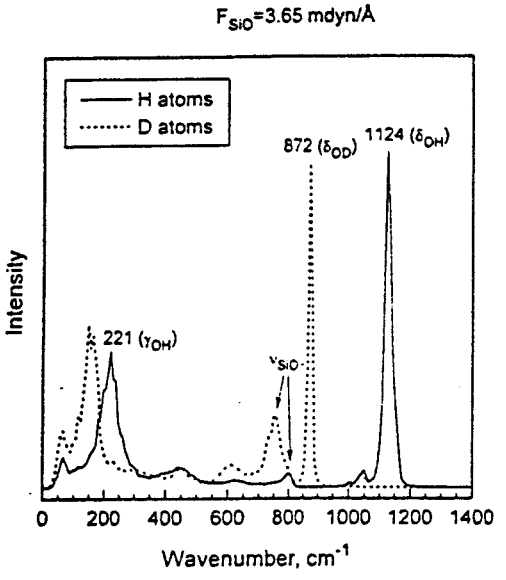

Fig. 6. Power spectrum of H atoms (solid line) and D atoms (dotted line) calculated for H-zeolite Y with Si/Al = 7.7 with value of Si–O(H) stretching bond force constant is equal to 3.65 mdyn/Å. All values of other force constants used are the same as in Table 5.

dergo a low-frequency shift, while the latter will be shifted to higher wavenumbers in good agreement with the experimental data. In this case the Si–O(D) vibration cannot clearly be observed in the infrared spectra because of the overlap by the band of symmetric T–O–T stretching vibrations at 800 cm^{-1}. One supplementary argument for this explanation is obtained from the analysis of the SiO(H) bond lengths in calculations of clusters of different sizes [12]. While a value of 1.663 Å was computed for the Al-substituted disilicic acid, Si–O(H) bond lengths in the range 1.708–1.726 Å were obtained for large clusters modelling Al-rich zeolite (Table 2 and Fig. 8 in Ref. [12]). Making use of Badger's rule formula one can estimate that the elongation of the bond length by 0.05 Å will result in decreasing the force constant by 1.0 mdyn/Å.

The power spectra presented in Fig. 6 is a nice confirmation of the above hypothesis. In this calculation the stretching force constant for the SiO(H) bond was changed to a value of 3.65 mdyn/Å. In the spectrum of H atoms the SiO band calculated before at 879 cm^{-1},is shifted down to 800 cm^{-1}. The D atoms spectrum shows two peaks at 872 and 754 cm^{-1} which can be attributed with the help of the NMA calculations to the δ_{OD} and SiO(D) vibrations, respectively. The former band corresponds very well to the band observed in the IR spectrum [26], while the latter might be responsible for the changes in the region 700–800 cm^{-1} [26]. It should be noted that a band at 758 cm^{-1} has been observed in INS spectra of H-Y zeolites [25]. Thus we recommend the use of the value 3.65 mdyn/Å for the SiO(H) stretching force constant and these results show that the main features in the IR and INS spectra and the dynamics of the protonated (deuterated) zeolites can be explained in the frames of the vibrational mechanics without resort to additional effects such as Fermi resonance.

4. Concluding remarks

A GVFF developed in our previous work for calculation of the vibrational spectra of siliceous zeolites [13] has been extended for aluminosilicates.

As mentioned in the introduction, a molecular mechanics force field for aluminosilicates has recently been developed by Hill and Sauer [11,12] on the basis of ab initio cluster calculations. However, a direct comparison of the force field obtained in the present work with that of Ref. [12] is difficult because of different numbers of parameters used to determine the force fields. As many as about 300 force constants are used in Ref. [12], while it is supposed that only about 35 force constants are sufficient to derive the force field that is able to describe the dynamics of zeolite lattices. The empirical force fields developed in [19] and [30] are destined for the case of the Al-substituted zeolites with the low Si/Al ratio that does not correlate with the model used in the present study.

The systematic way of deriving the force constants developed in this and previous [13] papers allows to express the rich information obtained in the output of a quantum-chemical calculation in clear chemical terms. It can of course be applied to a variety of other systems. Further improvements should include the corrections caused by the long-range interactions. For Al-substituted zeolites the use

of larger clusters is obviously required to calculate the relaxation of stretching force constants. However, the results of MD modelling show that the main experimental features are reproduced, and the force field derived from the first principles is able to describe correctly the complicated spectra of the zeolitic framework.

Acknowledgements

The authors would like to acknowledge financial support of NATO (Contract HTECH.CRG 941422), computer time at IDRIS (Project 940148) and support of Russian Fondation for Basic Research (RFBR, grant no. 95-03-9551a). V.A.E. thanks the Ministère des Affaires Etrangères for a grant.

References

[1] J. Weitkamp, H.G. Karge, H. Pfeifer and W. Holderich, eds., Stud. Surf. Sci. Catal. 84 (1994).
[2] E.M. Flaningen, H. Khatami and H.A. Szymanski, Adv. Chem. Ser. 101 (1971) 201.
[3] C. Brémard and D. Bougeard, Adv. Mater. 7 (1995) 10.
[4] J.B. Nicholas, A.J. Hopfinger, F.R. Trouw and L.E. Iton, J. Am. Chem. Soc. 113 (1991) 4792.
[5] K.S. Smirnov and D. Bougeard, J. Phys. Chem. 97 (1993) 9434.
[6] K.S. Smirnov, M. Le Maire, C. Brémard and D. Bougeard, Chem. Phys. 179 (1994) 445.
[7] S. Tsuneyuki, M. Tsukada, H. Aoki and Y. Matsui, Phys. Rev. Lett. 61 (1988) 869.
[8] B.W.H. van Beest, G.J. Kramer and R.A. van Santen, Phys. Rev. Lett. 64 (1990) 1955.
[9] G.J. Kramer, N.P. Farragher, B.W.H. van Beest and R.A. van Santen, Phys. Rev. B 43 (1991) 5068.
[10] K. de Boer, A.P.J. Jansen and R.A. van Santen, Stud. Surf. Sci. Catal. 84 (1994) 2083.
[11] J.-R. Hill and J. Sauer, J. Phys. Chem. 98 (1994) 1238.
[12] J.-R. Hill and J. Sauer, J. Phys. Chem. 99 (1995) 9536.
[13] V.A. Ermoshin, K.S. Smirnov and D. Bougeard, Chem. Phys. 202 (1996) 53.
[14] R.D. Amos and J.E. Rice, CADPAC: The Cambridge analytical derivatives package, issue 4.0 (Cambridge, 1987).
[15] A. Allouche and J. Pourcin, Spectrochim. Acta 49A (1993) 571; A. Allouche, REDONG, QCPE 628.
[16] A.N. Fitch, H. Jobic and A. Renouprez, J. Phys. Chem. 90 (1986) 1311.
[17] M. Czjzek, H. Jobic, A.N. Fitch and T. Vogt, J. Phys. Chem. 96 (1992) 1535.
[18] R.M. Badger, J. Chem. Phys. 2 (1934) 128.
[19] C.S. Blackwell, J. Phys. Chem. 83 (1979) 3251; ibid. 83 (1979) 3257.
[20] J. Sauer, Chem. Rev. 89 (1989) 199.
[21] B.J. Teppen, D.M. Miller, S.Q. Newton and L. Schäfer, J. Phys. Chem. 98 (1994) 12545.
[22] W.P.J.H. Jacobs, J.H.M.C. Wolput and R.A. van Santen, J. Chem. Soc., Faraday Trans. 89 (1993) 1271.
[23] C. Brémard, M. Le Maire, J. Phys. Chem. 97 (1993) 9695.
[24] P.A. Jacobs and J.B. Uytterhoeven, J. Chem. Soc., Faraday Trans. 1 69 (1973) 359; 373.
[25] H. Jobic, J. Catal. 131 (1991) 289.
[26] W.P.J.H. Jacobs, J.H.M.C. Wolput, R.A. van Santen and H. Jobic, Zeolites 14 (1994) 117.
[27] J. Sauer J. Mol. Catal. 54 (1989) 312.
[28] J. Sauer, P. Ugliengo, E. Garrone and V.R. Saunders, Chem. Rev. 94 (1994) 2095.
[29] F. Fillaux, J.P. Fontaine, M.-H. Baron, G.J. Kearley and J. Tomkinson, Chem. Phys. 176 (1993) 249.
[30] E. Geidel, H. Böhlig and P. Birner, Z. Phys. Chem. 171 (1991) 121.

5.4. Vibrations des OH de surface.

Article publié dans Surface Science, sous presse

ELSEVIER

Surface Science 0 (1996) 000–000

surface science

Molecular dynamics calculation of the vibrational spectra of OH groups in zeolites and on silica surfaces

V.A. Ermoshin [a,b,*], K.S. Smirnov [a], D. Bougeard [b]

[a] *LASIR-CNRS, Université des Sciences et Technologies de Lille, Bât. C5, F59655 Villeneuve d'Ascq Cedex, France*
[b] *Institute of Physics, St. Petersburg State University, St. Petersburg 198904, Russia*

Received 1 May 1996; accepted for publication 1 May 1996

Abstract

Ab initio calculations on small clusters were used to derive a potential for OH groups, permitting the study of their vibrational behavior in zeolites and on silica surfaces. The spectra calculated with the help of molecular dynamics are in good agreement with experimental data for the zeolites. In the case of surface hydroxyls, the Si–O stretching band and the angle bending modes are assigned.

Keywords: XXX;

1. Introduction

Dynamics of surface hydroxyls of silica and bridging OH groups in microporous alumino-silicates (zeolites) is of importance for the application of these compounds in heterogeneous catalysis. Several experimental and theoretical studies have been undertaken in order to elucidate the vibrational motion of the hydroxyls [1,2]. Nevertheless, the problem is still far from being resolved, especially for the bending hydroxyl vibrations.

Information on the dynamics of surface species is usually obtained by means of vibrational spectroscopy. However, a reliable interpretation of the vibrational spectra necessitates the use of theoretical methods which are able to assign spectral features to a specific atomic motion. The present work reports results of a theoretical study of the vibrational spectra of OH groups in zeolites and on silica surfaces which uses an approach recently developed for deriving parameters of a generalized valence force field suitable for the simulation of the spectra of complicated inorganic compounds [3,4]. As the bending vibrations of the OH groups were the main subject of this study, the stretching modes are not considered in the present paper.

2. Computational procedure

The approach used implies that the dynamics of silicates and aluminosilicates can be described in terms of vibrations of small building units such as TO_4 tetrahedra and $O_3T–O–TO_3$ shared tetrahedra. Models of these units present in the molecules $Si(OH)_4$, $(OH)_3SiOSi(OH)_3$, $Al(OH)_4^-$, $H_3SiOHAlH_3$, $(OH)_3SiOAl(OH)_3^-$ and $(OH)_3SiOHAl(OH)_3$ were treated with ab initio quantum chemical calculations employing the 3-21G* basis set at HF level and the DZP basis set within the MP2

* Corresponding author.

PII S0039-6028(96)01043-6

perturbation formalism [5]. These calculations resulted in a matrix of the second derivatives of the total energy with respect to the Cartesian coordinates, which was transformed into the matrix of second derivatives of the energy in internal coordinates (matrix of force constants) under consideration of the redundancies existing between the internal coordinates [6].

The obtained sets of force constants [3,4] were used in molecular dynamics (MD) simulations of the vibrational spectra of hydrated and dehydrated microporous silicates and aluminosilicates (zeolites), as well as for OH groups on silica surfaces. The potential energy V for the torsion internal coordinate ϕ was assumed periodic and represented by the function $V = V_0 \cos 3\phi$, whereby V_0 was set equal to 0.053 kcal mol^{-1} in order to reproduce the observed frequencies. Additional normal mode analyses (NMA) were performed to assign the bands in the spectra to specific vibrational modes. Zeolitic hydroxyl groups were created by adding H atoms to one of the four oxygens bound to Al atoms in the faujasite lattice, taking into account the Lowenstein rule. Although the structure of surfaces is different for different silica polymorphs, the local structure around the OH groups is the same for all of them, i.e. three SiO_4 tetrahedra bound to the OH group. Hydroxyl groups of silica surface were formed by cutting the sodalite structure [7] along the (100) plane and completing the unsaturated Si atoms with OH groups. The internal coordinates are defined in Fig. 1. The description of the MD procedures as well as those used to derive the vibrational spectra from an MD runs can be found in Refs. [8,9].

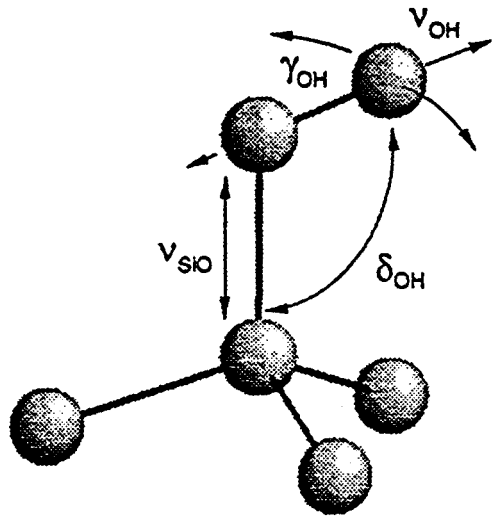

Fig. 1. Definition of the internal coordinates of for the calculations of the surface OH groups on silica.

3. Results and discussion

3.1. Silicates and dehydrated aluminosilicates

The application of the force field developed by the procedure described above to the calculation of the vibrational spectra of siliceous zeolites [3] and dehydrated aluminosilicates [4] has shown that the RMS deviation of the calculated and experimental position of bands in the IR and Raman spectra does not exceed 20 cm^{-1}, and for some systems approaches 12 cm^{-1}. Taking into account that no experimental information was used in the calculations, and that the experimental data also have an uncertainty of up to 10 cm^{-1}, the agreement can be considered as very satisfactory.

3.2. Hydrated aluminosilicates

The comparison of the force constants calculated for Si–O and Al–O bonds in the zeolitic OH groups shows that the Si–O force constant has significantly larger value than that of the Al–O bond (3.65 versus 1.47 mdyn $Å^{-1}$). This is accompanied by a lengthening of the Al–O bond as compared to its value in dehydrated structures. The analysis of the geometry of the models shows that values of the O–Al–O angles between Al–O bonds not involved in the Al–OH–Si bridge are close to 120°. Thus the bridging OH group can be considered as an Si–OH group bound to an AlO_3 Lewis acid site. Such an interpretation is in line with a recent intensive ab initio study of aluminosilicate clusters reported in Refs. [10,11].

The calculated frequencies of the vibrations of the OH and OD groups are listed in Table 1. The computed value of the in-plane bending vibration is in good agreement with the experimental IR and INS data. It is interesting to notice that for this

Table 1
Calculated end experimental frequencies (in cm^{-1}) of the bending vibrations of OH groups in zeolites and on silica surface

Mode	Zeolites		Silica surface	
	MD	Exp.	MD	Exp.
γ_{OH}	221	450[a]	131	100[c] 125[d]
γ_{OD}	156	—	95	75[c] 94[d]
γ_{OH}	1124	1090[a]	870	840[c,f] 770[e,f]
γ_{OD}	872	870[b]	642	620[c,f] 605[e]

[a] Ref. [17]. [b] Ref. [1]. [c] Ref. [13]. [d] Ref. [14]. [e] Ref. [15]. [f] Ref. [16].

mode the ratio δ_{OH}/δ_{OD} differs from the estimation on the basis of mass effect. This is due to the fact that the δ_{OD} vibration interacts with the Si–O vibration in the bridge, resulting in a high-frequency shift of the former mode and a low-frequency shift of the latter one. Therefore the high-frequency position of the in-plane OD vibration is accounted for as the result of a mechanical coupling without invoking Fermi resonance, as was proposed in Ref. [1].

Table 1 also shows a discrepancy of about 230 cm^{-1} between the calculated and experimental positions of the out-of-plane OH bending mode. Results of our quantum-chemical calculations employing different basis sets and cluster sizes have always resulted in frequencies in the range 150–250 cm^{-1}, as compared to the experimental value of 450 cm^{-1} [17]. A possible reason for this discrepancy is that the value of the force constant obtained for this coordinate is close to the limit of the method, as the error on this value is of the order of the magnitude of the value itself.

3.3. OH groups of the silica surface

Fig. 2 shows the calculated power spectra of the H atoms and of the O atoms in the OH groups and in the bulk of the system. The calculated values of the frequencies for the modes are gathered in Table 1. A wide band with a maximum at 130 cm^{-1} belongs to the out-of-plane OH vibration

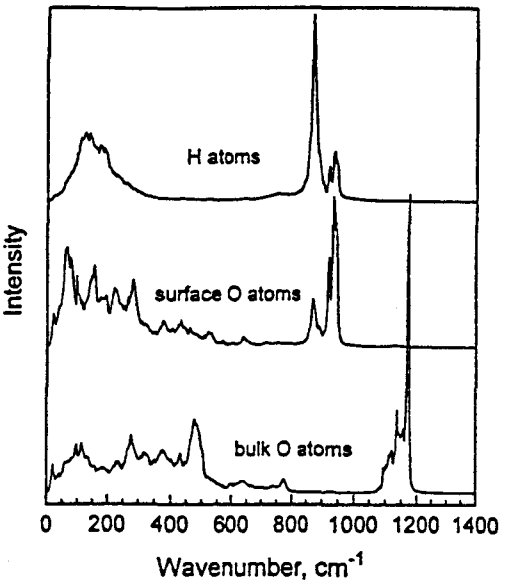

Fig. 2. Density of vibrational state of the hydrogen and oxygen atoms in the bulk and on the surface.

(γ_{OH}). On the basis of NMA calculations, the two bands at 870 and 935 cm^{-1} are assigned to the in-plane OH bending (δ_{OH}) and Si–OH stretching vibrations, respectively. The latter vibration appears as a strong peak in the power spectrum of O atoms in the OH groups, while it is absent in the spectrum of the atoms in the bulk. The substitution of H atoms by D atoms leads to a shift of the γ_{OH} band to 95 cm^{-1} and δ_{OH} to 642 cm^{-1}, whereas the Si–OH mode undergoes a smaller shift of 10 cm^{-1} to lower frequency.

Fig. 3 displays the Raman spectra calculated for sodalite and for the system with the OH groups on the (100) sodalite surface. One stronger peak is present in the spectrum of the surface model at 935 cm^{-1}, which can unambiguously be assigned to the Si–OH vibration. The position of this band agrees well with a band at 980 cm^{-1} in Raman spectra of silica, which has been assigned to the Si–O mode [12]. Experimentally this band shifts by 20 cm^{-1} upon H/D isotope substitution, in good agreement with the results of the present work.

Experimental data on the position of the out-of-plane OH vibration were obtained from the analysis of IR combination bands of silica surface

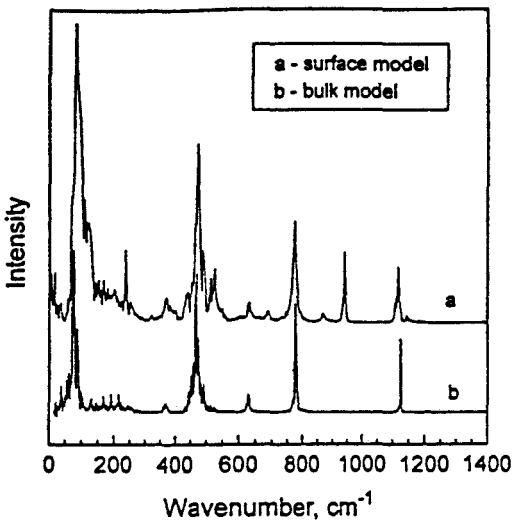

Fig. 3. Calculated Raman spectra of the silica models: (a) sodalite surface, (b) sodalite bulk.

OH groups [13] and from direct far-infrared measurements [14]. They led to values of 100 [13] and 127 cm^{-1} [14]. The frequency calculated for the γ_{OH} vibrations in the present work agrees well with both experimental values. A direct observation of the δ_{OH} vibration is difficult because of a strong absorption of silica itself in the spectral region below 1300 cm^{-1}. Information on the frequency of this vibration was obtained from an analysis of combination bands [13,15]. One band at 4550 cm^{-1} is observed in the IR spectrum of silica samples at room temperature, which splits into two peaks at 4515 and 4590 cm^{-1} at 77 K [13]. The splitting disappears after the substitution of the H atoms by deuterium. The author [13] attributes the two peaks in the spectra of hydroxylated samples to the combination of the OH stretching vibration with OH in-plane bending and Si–OH stretching vibrations, respectively, whereas the opposite attribution is proposed in Ref. [15].

The results of the present calculations yield values of 870 and 642 cm^{-1} for δ_{OH} and δ_{OD} vibrations, respectively. They confirm the assignment of the vibration at 840 cm^{-1} (610 cm^{-1}) to the in-plane OH(OD) mode, as proposed in Ref. [13]. Our calculations unambiguously indicate that the Si–OH stretching mode has a frequency above 900 cm^{-1}, which agrees with the Raman measurements [12]. Several NMA of isolated and geminal OH groups on surfaces performed with the diagonal force constants derived from the $Si(OH)_4$ cluster have shown that the frequency difference is only of some wavenumbers. Different trials to introduce reasonable electrostatic couplings between geminal groups also could not generate a large splitting. Further such electrostatic interactions do not appear in the form of unusually large interaction force constants between non-bonded parts of the molecule. Finally, as the couplings are very small between geminal groups, it seems unlikely that vicinal groups at larger distance will be able to cause such a large frequency difference, as proposed in Ref. [16]. Thus, it is probable that the modes at 840 and 770 cm^{-1} are due to different angle bending motions which differ in their diagonal force constants; the study of these variations necessitates the study of larger clusters in order to derive the influence of the environment on the bending force constant of the surface OH groups.

4. Conclusion

The dynamics of hydroxyl groups in zeolites and on silica surfaces was studied by the molecular dynamics method using a general valence force field derived from ab initio calculations on small clusters. The results account for the dependence of the in-plane bending vibration frequency of the OH groups in zeolites upon isotopic H/D substitution. In the case of OH groups on silica surfaces, the SiO stretching mode and the in-plane OH bending modes are assigned.

Acknowledgements

The authors gratefully acknowledge financial support of NATO (contract HTECH.CRG 941422) and RFBR (grant No. 95–03–09551) and allocation of computing time at IDRIS (project 940148). V.A.E. thanks the Ministère des Affaires Etrangères for a grant.

References

[1] W.P.J.H. Jacobs, J.H.M.C. Wolput and R.A. van Santen, J. Chem. Soc., Faraday Trans. 89 (1993) 1271, and references therein.

[2] A.A. Tsyganenko, K.S. Smirnov, E.P. Smirnov and A.Yu. Pavlov, Chem. Phys. Technol. Surf. 1 (1993) 65, and references therein.

[3] V.A. Ermoshin, K.S. Smirnov and D. Bougeard, Chem. Phys. 202 (1996) 53.

[4] V.A. Ermoshin, K.S. Smirnov and D. Bougeard, Chem. Phys., in press.

[5] R.D. Amos and J.E. Rice, CADPAC: Cambridge Analytical Derivatives Package, issue 4.0 (Cambridge, 1987).

[6] A. Allouche and J. Pourcin, Spectrochim. Acta 49A (1993) 571;
A. Allouche, REDONG, QCPE 628.

[7] J.W. Richardson, J.J. Pluth, J.V. Smith, W.J. Dytrych and D.M. Bibby, J. Phys. Chem. 92 (1988) 243.

[8] K.S. Smirnov and D. Bougeard, J. Phys. Chem. 97 (1993) 9434.

[9] K.S. Smirnov and D. Bougeard, J. Raman Spectrosc. 24 (1993) 255.

[10] J.-R. Hill and J. Sauer, J. Phys. Chem. 98 (1994) 1238.

[11] J.-R. Hill and J. Sauer, J. Phys. Chem. 99 (1995) 9536.

[12] B.A. Morrow and A.J. MacFarlan, J. Non-Cryst. Solids 120 (1990) 61.

[13] A.A. Tsyganenko, Russ. J. Phys. Chem. 56 (1982) 2330.

[14] P. Hoffmann and E. Knozinger, Surf. Sci. 188 (1987) 181.

[15] L.M. Kustov, V.Yu. Borovkov and V.B. Kazanski, Z. Fiz. Khim. 59 (1985) 2213.

[16] B.A. Morrow and A.J. McFarlan, J. Phys. Chem. 96 (1992) 1395.

[17] H. Jobic, J. Catal. 131 (1991) 289.

5.5. Conclusion

La modélisation des vibrations dans les aluminosilicates a été effectuée à l'aide d'un champ de forces de valence développé à partir de calculs *ab initio* de petites molécules choisies comme modèles: $Si(OH)_4$, $(OH)_3SiOSi(OH)_3$, $Al(OH)_4^-$, $H_3SiOHAlH_3$, $(OH)_3SiOAl(OH)_3^-$ et $(OH)_3SiOHAl(OH)_3$. Ces molécules ont été traitées au niveau Hartree - Fock avec la base 3-21g* et au niveau MP2 avec la base DZP.

La matrice des constantes de force en coordonnées cartésiennes, obtenue par un calcul de chimie quantique, a été transformée en coordonnées internes en utilisant le programme REDONG [1] qui prend en compte les conditions de redondance.

Ce champ de force a été appliqué dans la simulation par la dynamique moléculaire des vibrations du réseau de quelques zéolithes siliciques (sodalite, faujasite et silicalite), dans l'étude de l'influence de la substitution de Si par Al dans la faujasite, et dans l'étude des vibrations des groupes OH dans les zéolithes et sur la surface de la silice. Les spectres vibrationnels infrarouge, Raman et de densité d'états ont été calculés par la transformée de Fourier des fonctions d'autocorrélation du moment dipolaire, du tenseur de polarisabilité et de la vitesse.

Pour les zéolithes siliciques, le champ de forces *ab initio* est très proche du champ de forces dérivé de l'ajustement aux données expérimentales [2]. Les deux champs de forces donnent une bonne correspondance avec les spectres expérimentaux. L'erreur moyenne entre les positions des maxima des spectres calculés et expérimentaux est de $20cm^{-1}$.

L'étude de la substitution de Si par Al montre aussi une bonne correspondance entre les spectres calculés et expérimentaux. La relaxation des liaisons SiO autour de l'atome de Si proche d'un atome d'Al a une influence importante sur la dynamique du réseau.

Le champ de force *ab initio* a été appliqué dans l'étude de la dynamique des zéolithes hydratées, en particulier à la dynamique des groupes OH et OD du centre acide de Brönsted. L'application du champ de force dérivé de calculs *ab initio* permet l'attribution des maxima des spectres infrarouges et de diffusion de neutrons sur la base des couplages

mécaniques. L'effet isotopique du mode de déformation de l'angle $SiOH$ est expliqué dans notre modèle par l'interaction du mode de déformation de l'angle $SiOD$ avec le mode d'élongation de la liaison de $SiO(D)$.

L'analyse des constantes de force nous permet de dire que le pont $SiOHAl$ peut être considéré comme la liaison du groupe $SiOH$ à un site acide de Lewis AlO_3 . L'analyse de la géométrie optimisée montrant l'hybridation sp^2 de l'atome d'aluminium confirme également cette hypothèse.

Nous avons aussi appliqué le champ de force *ab initio* dans l'étude du comportement vibrationel des groupes OH sur la surface de la silice. Les spectres obtenus par dynamique moléculaire et par l'analyse en coordonnées normales nous permettent d'attribuer les maxima des spectres Raman et infrarouges de combinaison.

REFERENCES

1. A.Allouche and J.Pourcin, Spectrochim.Acta **49A** (1993) 571; A.Allouche, QCPE 628

2. M.Bärtsch, P.Bornhauser, G.Calzaferri, and R.Imhof J.Phys.Chem. **98** (1994) 2817

CHAPITRE 6

RELAXATION DE L'ENERGIE VIBRATIONELLE DES ADSORBATES: ETUDE THEORIQUE DU SYSTEME H/SI(111)

Article publié dans Journal of Chemical Physics, sous presse

VIBRATIONAL ENERGY RELAXATION OF ADSORBATE VIBRATIONS: A THEORETICAL STUDY OF THE H/Si(111) SYSTEM.

V.A.Ermoshin[1,2], A.K.Kazansky [1], K.S.Smirnov[1], and D.Bougeard[2]

[1] *Institute of Physics, St.Petersburg State University, St.Petersburg, 198904, Russia*

[2] *LASIR-CNRS, Bât. C5, 59655, Villeneuve d'Ascq Cedex, France*

ABSTRACT

The energy relaxation rate for the first excited stretching vibration of hydrogen atoms adsorbed on an $Si(111)$ surface is calculated treating the motions of the H atoms quantum–mechanically and computing the substrate phonon spectrum by molecular dynamics. The relaxation occurs through excitation of three bending modes and emission of a 188 cm^{-1} phonon.

The intensive development of the laser "pump-and-probe" experiments is a good means to draw direct information on the population dynamics of vibrations in condensed matter [1]. In these experiments the lifetime of the excited vibrational level is measured from the dependence of the probe pulse transmission on the time delay with respect to the pump pulse. Such studies are especially important for systems where the pumped oscillators are embedded in a dielectric medium with its Debye frequency much lower than the energy of the vibrational transition under investigation. The energy relaxation in this case proceeds via the excitation of few vibrational quanta of accepting modes and a very low transition rate is usually observed [2-4]. Population dynamics of vibrationally excited states in such systems is difficult to study with conventional spectroscopic experiments because of a significant contribution of the dephasing and inhomogeneous broadening to the absorption band width [5-7].

In particular, much attention has been given to the vibrational energy relaxation dynamics of the $Si-H$ stretching vibration of hydrogen atoms on an $Si(111)$ surface [4,8,9]. Recent experimental studies for the relaxation of the v=1 level of the Si-H stretching modes yielded a lifetime of about 1 ns [4,10].

The theoretical study of the dynamics of the excited vibrational $v = 1$ level for the $Si - H$ stretching vibrations on a silicon surface was started with a Langevin classical dynamics simulation carried out by Tully *et al* [11]. The authors obtained an estimation $\tau_H \geq 2 \times 10^{-8} s$ for the lifetime of the $Si - H$ stretch on an $Si(100)$ surface. An attempt to treat this problem within the perturbation theory was undertaken by Gai *et al* [12]. The method they used combined the Bloch-Redfield theory [13] and the molecular dynamics method: the quantum dynamics of $Si - H$ stretching oscillator was described with a set of differential equations for the reduced density matrix elements. The quantum correlation function, which appears in the transition matrix elements, was substituted by a classical one [14] computed by molecular dynamics calculations with constraint of the $Si - H$ bond. The authors of Ref. 12 claim that the dominant damping term for the $v = 1$ state probability ρ_{11} corresponds to the transition into the ground state. Therefore, conventional two-level perturbation theory [15] can be applied. Based on an

analysis of the power spectrum of the fluctuating force acting on the $Si-H$ bond, the dominant energy relaxation was found to occur via kinetic coupling to a state with three $Si-Si-H$ quanta plus one phonon.

Although this approach has led to a reasonable value for the transition rate, it seems doubtful that the highly localised bending vibrations of the H atom can be treated as bath modes. The method using a quantum-mechanical description of a one-dimensional oscillator interacting with a classical bath seems to be more convenient for the study of the vibrational relaxation of diatomic molecules in solution [16], where it was first applied within the Landau-Teller approach [17].

An attractive method to study the vibrational relaxation of polyatomic molecules in solutions was proposed in an investigation of HOD dynamics in D_2O solution [18]. It is based on a quantum-mechanical treatment of the intramolecular transitions induced by forces resulting from the intermolecular interactions. The method uses a linear form for the oscillator-bath coupling which is written as the product of the harmonic normal coordinates of solute molecule and of the intermolecular forces due to the solvent.

In the present paper we report results of a theoretical study of the lifetime and of the relaxation channels of the $Si-H$ stretching vibration in the $H/Si(111)$ system. As in Ref. 18, the dynamics of the H atom on an Si surface is governed by the 3-dimensional quantum Hamiltonian. Considering the motion of the H atom in the non-inertial coordinate system related to the top Si atom, the Hamiltonian for this motion can be written as:

$$H = -\frac{1}{2M_H}\Delta + U(\vec{r}) + V_{int}(\vec{r},t). \tag{1}$$

where M_H is the mass of hydrogen atom. The potential $U(\vec{r})$ describes the interaction of the H atom with all the surface Si atoms being fixed at their equilibrium positions. The term $V_{int}(\vec{r},t)$ arises because of our treatment of the H dynamics from the non-inertial reference frame. It describes the time-dependent interaction of the H oscillator with the substrate modes:

$$V_{int}(\vec{r},t) = -\vec{r}\vec{F}(t) \tag{2}$$

where the force $\vec{F}$ is directly related to the acceleration $a_{Si}(t)$ of the top Si atom

$$\vec{F}(t) = -M_H \vec{a}_{Si}(t). \tag{3}$$

Equation (2) is a good approximation as long as the displacements of all other Si surface atoms from their equilibrium positions are small compared to the distance between the neighboring $Si - Si$ atoms. This equation also implies that the motion of the light H atom does not affect the dynamics of the much heavier top Si atom.

With this linear form for the coupling between the three-dimensional $H-Si$ oscillator and the bath, the Fermi Golden Rule expression for the rate of the decay of the initial vibrational level $|i>$ reads [18,19]

$$r = \sum_f \gamma_{if} \sum_{s=x,y,z} |<i|s|f>|^2 \int_{-\infty}^{\infty} d\tau <F_s(\tau)F_s(0)> exp(\imath\omega_{if}\tau), \tag{4}$$

where

$$\omega_{if} = (E_i - E_f)/\hbar \tag{5}$$

is the frequency of the transition between the states $|i>$ and $|f>$ of the oscillator. The first sum runs over all possible final states $|f>$. In the equation (4) we neglected the correlation terms between two different Cartesian coordinates. The Fourier transform of the x, y, z - components of the classical autocorrelation function of force

$$\zeta(\omega) = \int_{-\infty}^{\infty} d\tau <F_s(t)F_s(0)> \exp(\imath\omega\tau) \tag{6}$$

can be calculated by the classical molecular dynamics simulation for pure Si surface. $<i|s|f>$ is the matrix element of the corresponding coordinates. The prefactor

$$\gamma_{if} = \begin{cases} \beta\omega_{if}\,(1-\exp(-\beta\omega_{if}))^{-1} & \omega_{if} > 0: \\ \beta\omega_{if}\,(\exp(\beta\omega_{if})-1)^{-1} & \omega_{if} < 0 \end{cases} \tag{7}$$

makes it possible to adapt results of classical molecular dynamics calculations to the description of the corresponding quantum system. It is obtained by the direct comparison of the classical and quantum correlation functions for a harmonic lattice. Although it is valid for the harmonic bath only, the anharmonicity of substrate vibrations obviously induces weaker effects on the relaxation rate. It is noteworthy, that the product of commonly used prefactor from Ref. 19 and quantum correction for this quantity from Ref. 20 directly leads to our expression for γ_{if} in the case of phonon emission ($\omega_{if} > 0$).

In our study the potential energy surface (PES) $U(x,y,z)$ was obtained from an *ab initio* quantum chemical calculations of the SiH_4 molecule. The calculations were performed with the CADPAC package [21]. The Dunning DZP basis set was employed and the electronic correlations were taken into account at the MP2 level.

As anharmonicity of the PES plays an important role in the investigation of the relaxation rate, large regions of the coordinate space have to be explored in the calculation of the PES. In the present study the z-coordinate was varied in the [-0.6 $a.u.$, 0.8 $a.u.$] interval, and the x,y-coordinate in the [0.0 $a.u.$, 1.6 $a.u.$] interval (assuming radial symmetry) with 0.2 $a.u.$ step. The computed PES shown in Fig.1 was fitted with a polynomial of the sixth degree:

$$U(x,y,z) = \frac{1}{2}\alpha_\rho \rho^2 + \frac{1}{2}\alpha_z z^2 + \sum_{i,j} a_{ij} z^i \rho^j, \quad \rho = \sqrt{x^2+y^2}. \tag{8}$$

The numerical values of the coefficients in (8) obtained by a least-square process are listed in Table 1. It is worth noting that fitting the potential surface with a polynomial of the fourth degree [22] results in an unphysical behaviour of the PES in the regions where the wave-functions under study are still non-negligible.

It is well known that the force constants obtained with the methods of quantum chemistry are overestimated by about 5-10 percent because of insufficient treatment of the correlation energy [23], whereas the problem of relaxation requires the knowledge of the precise values of the frequencies of the vibrational transitions. Fortunately, the anharmonic coefficients only weakly depend on the level of theory, while a standard scaling procedure can be applied to the harmonic coefficients [23]. The harmonic coefficients in (8) were scaled to $\alpha_z = 0.18260\, a.u.$ and $\alpha_\rho = 0.01491\, a.u.$ in order to reproduce the experimental frequencies of the $0 \rightarrow 1$ transitions in the stretching SiH mode [9] $\omega_z^{10} = 2083.7\, cm^{-1}$ and bending $Si-Si-H$ vibrations [24] $\omega_\rho^{10} = 637.1\, cm^{-1}$ in the procedure of diagonalisation described below. The calculation of the anharmonicity of the stretching $Si-H$ vibration has resulted in the value $\omega_{21} - \omega_{10} = -75.8\, cm^{-1}$ which is close to previous theoretical [22] and experimental data [8]. The scaled values of the harmonic coefficients were used in this study of $Si-H$ vibrational relaxation.

The Hamiltonian

$$H_0 = -\frac{1}{2M_H}\Delta + U(x,y,z) \tag{9}$$

was diagonalised in the basis consisting of the eigenfunctions of a three-dimensional harmonical oscillator with force constants α_ρ, α_ρ and α_z. The eigenenergies and the eigenvectors for the few lowest oscillator states are shown to converge for a basis consisting of nine states for each one-dimensional oscillator.

For the relaxation process we consider the states with an energy mismatch less than the Debye frequency of the solid (ω_D *ca.* $500\,cm^{-1}$). Further, we are interested in the transitions which couple the state that is pumped in the "pump-and-probe" experiments and has a predominantly $(0,0,1)$ character to the states which have a $(a,b,0)$ character ((n_x,n_y,n_z) means the basis function occupation number). This strongly limits possible relaxation channels. Analysis of the transition matrix elements has only shown one possible state which could be regarded as an accepting mode for the initial state with the energy of $3788.3\,cm^{-1}$ which includes the zero-point energy. It is the double-degenerated linear combination with four principal terms $|f\rangle = c_1(3,0,0) + c_2(1,2,0) + c_3(2,1,0) + c_4(0,3,0)$ with the eigen energy 3600.3 cm^{-1}. Thus, the frequency mismatch which is important for further calculations is equal to $\omega_{if} = 188.0\,cm^{-1}$. Only the following expressions have a physical meaning

$$\begin{aligned} &c_1^2 + c_4^2 = 0.616; \\ &c_2^2 + c_3^2 = 0.210. \end{aligned} \tag{10}$$

Note that the difference between the sum of these numbers and unity is due to a contribution of other basis states. The non-zero component of the corresponding dipole matrix element is directed parallel to the surface and has the following numerical value:

$$2(|<f|x|i>|^2 + |<f|y|i>|^2) = 1.38 \times 10^{-4} a.u. \tag{11}$$

where the coefficient 2 arises from the double-degeneracy of the accepting state.

In order to calculate the classical force autocorrelation function $< F_s(0)F_s(t) >$, a molecular dynamics simulation was performed. The pure $Si(111)$ surface was modelled

with a slab of $8 \times 8 \times 16$ Si atoms in x, y, and z directions, respectively. The interaction potential among Si atoms was taken from Ref. 25. The equations of motion were integrated with the velocity Verlet algorithm using a time step of 2 fs. The first 24 ps of the run were used for equilibration while data were collected during the 40.96 ps following the equilibration stage. $\zeta(\omega)$ was computed as the average of the Fourier transformations of the autocorrelation functions [26] of acceleration of the top Si atoms in the direction parallel to the surface and was multiplied by the square of the hydrogen mass, according to (6). The results of these calculations are shown in Fig.2 for three values of the temperature. The computed values of $\zeta(\omega)$ for $\omega_{if} = 188.0\,cm^{-1}$ are presented in the first column of Table 2.

The calculation with equations (4) and (11) gives the theoretical rates of relaxation of the $Si - H$ vibration. These are gathered in Table 2 together with the experimental data[10] for three temperatures. Table 2 shows that both the absolute values and temperature dependence of the relaxation rate are in good agreement with the experiment. The absolute value is only slightly sensitive to the substrate potential because the force autocorrelation function curve is rather flat in the region studied, but it should be sensitive to the PES because of the small value of the transition dipole moment. The relaxation is shown to proceed via the excitation of three vibrational quanta of the bending $Si - Si - H$ vibration accompanied by the emission of a phonon at $188\,cm^{-1}$. This conclusion agrees with the results obtained in Ref. 12. It is also in line with the experimental data of Ref. 27 where the temperature dependence of the frequency of the $Si - H$ stretching vibration, its width and intensity were accounted for by a *strong* anharmonic coupling to the $Si - H$ bending mode and by a *weak* anharmonic coupling to a silicon surface phonon (at *ca.* $210\,cm^{-1}$).

In summary we would like to note that the approach presented here introduces the natural form of the unperturbed Hamiltonian and of the coupling to a bath for light particles adsorbed on surfaces. It takes the quantum mechanical effects on the bath motion into account and provides the correct temperature dependence. This approach singles out the main relaxation channels and permits to calculate the corresponding rates.

ACKNOWLEDGMENTS

We would like to acknowledge the financial support of NATO (Contract HTECH.CRG 941422), computing time at IDRIS (Project 940148) and support by RFFI (Russian Foundation for Basic Researches) (Grant No 95-03-09551). VE acknowledges a grant from the Ministère des Affaires Etrangères.

1. A.Laubereau and W.Kaiser Rev.Mod.Phys. **50**, 607 (1978).

2. M.P.Casassa, E.J.Heilweil, J.C.Stephenson, and R.R.Cavanagh J.Chem.Phys. **84**, 2361 (1986).

3. M.J.P.Brugmans, H.J.Bakker, and A.Lagendijk J.Chem.Phys. **104**, 64 (1996).

4. P.Guyot-Sionnest, P.Dumas, Y.J.Chabal, and G.S.Higashi Phys.Rev.Lett. **64**, 2156 (1990).

5. B.N.J.Persson, F.M.Hoffmann, and R.Ryberg, Phys.Rev.B **34**, 2266 (1986).

6. B.N.J.Persson, Phys.Rev.B **46**, 12701 (1992).

7. Yu.A.Tsyganenko, V.A.Ermoshin, M.R.Keyser, K.S.Smirnov, and A.A.Tsyganenko, Vibr.Spectr.,*in press*

8. P.Guyot-Sionnest Phys.Rev.Lett. **67**, 2323 (1991).

9. G.S.Higashi, Y.J.Chabal, G.W.Trucks, and K.Raghavachari, Appl.Phys.Lett. **56**, 656 (1990).

10. P.Guyot-Sionnest, P.Dumas, Y.J.Chabal, and G.S.Higashi, J.Electron Spectrosc. Relat. Phenom. **54/55**, 27 (1990).

11. J.C.Tully, Y.J.Chabal,K.Raghavachari,J.M.Bowman, and R.R.Lucchese Phys.Rev.B **31**, 1184 (1985).

12. H.Gai and G.Voth, J.Chem.Phys. **99**, 740 (1993).

13. A.G.Redfield, IBM J.Res.Devel. **1**, 19 (1957).

R.K.Wangness and F.Bloch Phys.Rev. **89**, 728 (1953).

14. F.E.Figuerido and R.M.Levy J.Chem.Phys. **97**, 703 (1992).

15. R.Zwanzig, J.Chem.Phys. **34**, 1931 (1961).

16. R.M.Whitnell,K.R.Wilson, and J.T.Hynes J.Phys.Chem. **94**, 8625 (1990).

17. L.Landau, E.Teller, Z.Sowjetunion **10**, 34 (1936).

18. R.Rey and J.T.Hynes J.Chem.Phys. **104**, 2356 (1996).

19. D.W.Oxtoby, Adv.Chem.Phys. **47**, 487 (1981).

20. J.S.Bader and B.J.Berne J.Chem.Phys. **100**, 8359 (1994).

21. R.D.Amos and J.E.Rice, CADPAC: The Cambridge Analytical Derivatives Package,

Issue 4.0, Cambridge, 1987.

22. X.-P.Li and D.Vanderbilt Phys.Rev.Lett. **69**, 2543 (1992).

23. R.J.Bartlett and J.F.Stanton, p.65, in *Reviews in Computational Chemistry*, vol.5 edited by K.B.Lipkowitz and D.B.Boyd (VCH Publishers, New York, 1994).

24. H.Froitzheim, U.Köhler, and H.Lammering, Surf.Sci. **149**, 537 (1985).

25. B.M.Rice, L.M.Raff, and D.L.Thompson, Surf.Sci. **198**, 360 (1988).

26. W.H.Press, B.P.Flannery, S.A.Teukolsky, and W.T.Vettering, *Numerical Recipes* (Cambridge University Press, 1986).

27. P.Dumas, Y.J.Chabal, and G.S.Higashi, Phys.Rev.Lett. **65**, 1124 (1990).

Table 1: The coefficients (in *a.u.*) of the polynomial expansion (eqn.(8)) of the calculated potential energy surface for the H atom motion.

Coefficient	*Value*	*RMS error*
α_z	0.20669	0.00260
α_ρ	0.02044	0.00104
a_{30}	-0.08343	0.00101
a_{40}	0.04583	0.00342
a_{04}	0.00378	0.00067
a_{12}	0.02959	0.00064
a_{22}	-0.05860	0.00204
a_{14}	-0.00750	0.00026
a_{32}	0.02755	0.00129
a_{42}	-0.01743	0.00294
a_{24}	0.01365	0.00060
a_{06}	-0.00099	0.00017

Table 2: Fourier transform of the autocorrelation function $\zeta(\omega)$ (in *a.u.*) of the component parallel to the surface of the force on the top Si atom of the $Si(111)$ surface computed for $\omega_{if} = 188\,cm^{-1}$. The calculated and experimental [8] relaxation rates (in ns^{-1}) of the $v = 1$ level of the $Si - H$ stretching vibration.

T, K	$\zeta(\omega_{if})$	r_{calc}	r_{exp}
95	0.3×10^{-4}	0.52	0.69
300	0.9×10^{-4}	0.77	1.0
460	1.5×10^{-4}	1.14	1.82

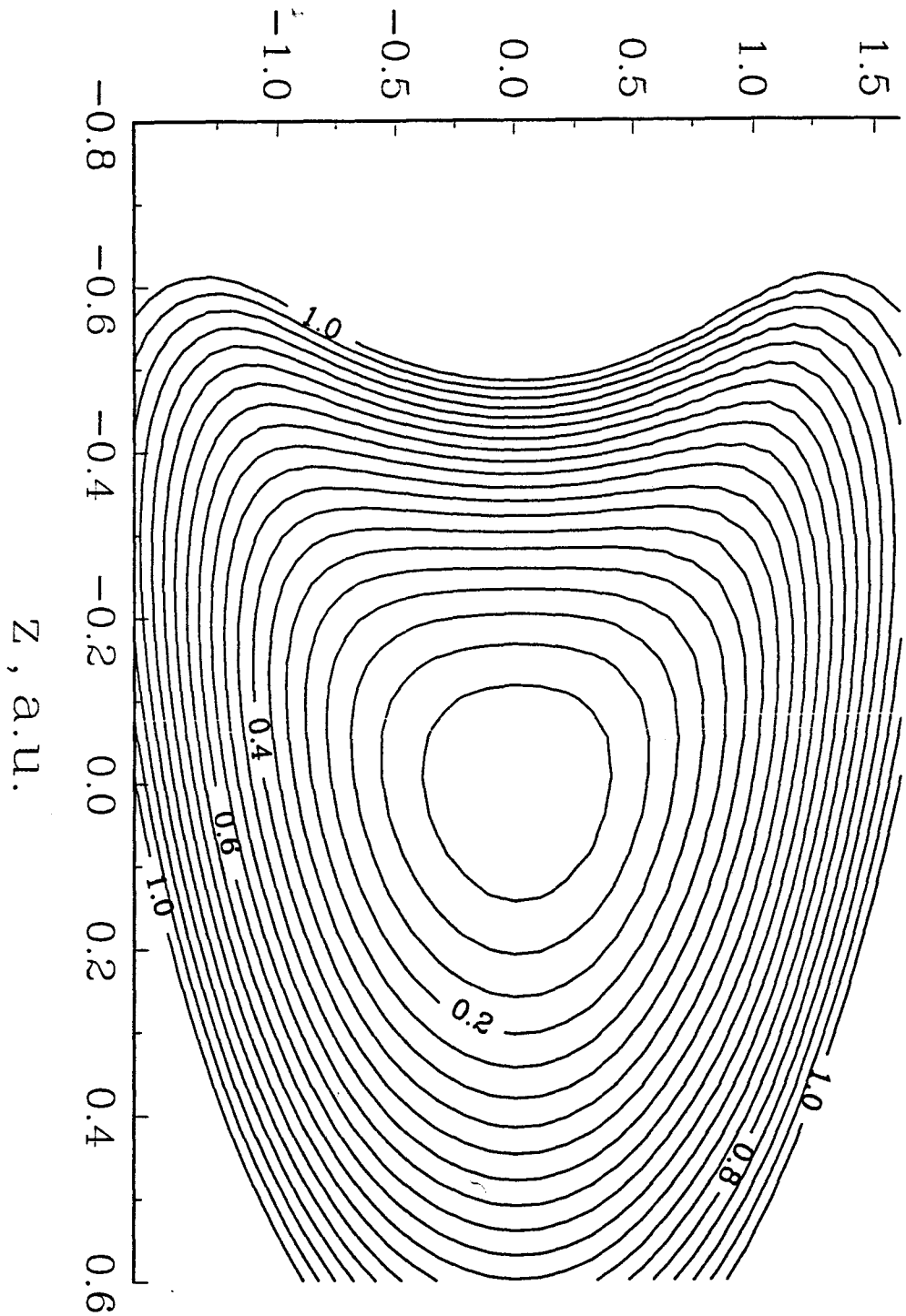

Fig.1 The potential energy surface (in eV) for the H atom motions computed with *ab initio* quantum-chemical calculation of SiH_4 molecule.

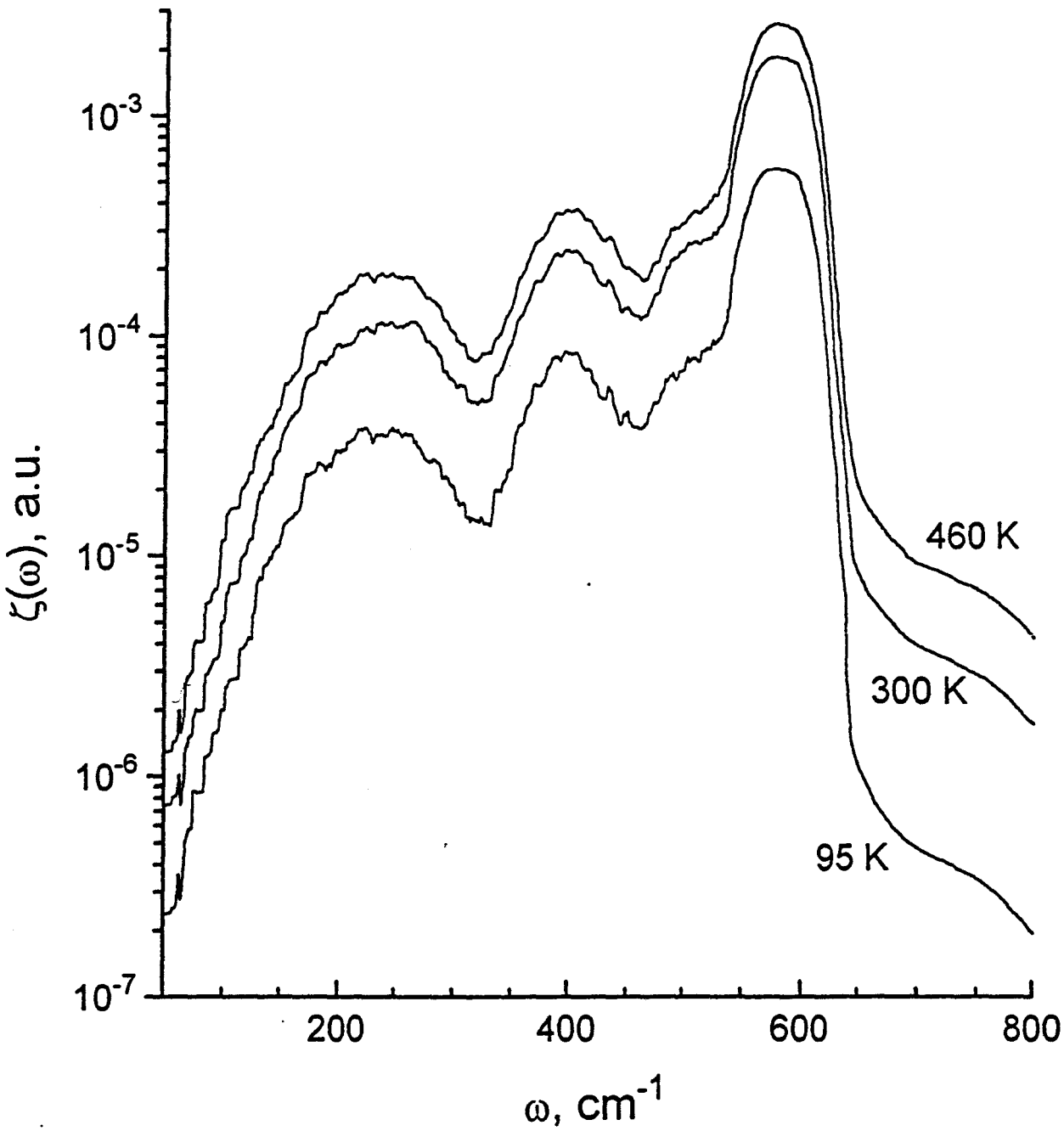

Fig.2 Fourier transform of the autocorrelation function $\zeta(\omega)$ of the component parallel to the surface of the force on the top Si atoms of the $Si(111)$ surface calculated with the molecular dynamics method for three different temperatures. The curves were smoothed with averaging over 32 neighboring points.

CHAPITRE 7
CONCLUSION

Les calculs de la structure électronique au niveau *ab initio* fourmillent dans les différentes branches de la science. A cause de la complexité des matériaux composés de Si et d'Al, les seules méthodes expérimentales (analyse chimique, spectroscopies vibrationnelle et résolue dans le temps) sont insuffisantes pour interpréter les mécanismes des processus étudiés. Aussi une étude théorique devient indispensable. Dans ce travail nous avons appliqué des méthodes de chimie quantique à l'étude des propriétés chimiques et spectroscopiques des aluminosilicates.

Dans la première partie les étapes élémentaires du processus sol-gel et de la synthèse hydrothermale de zéolithes sont étudiées par les calculs *ab initio* effectués sur des modèles moléculaires représentant les réactifs et des intermédiaires réactionnels possibles afin d'identifier les chemins de réaction. Les calculs ont montré que dans les solutions basiques les espèces anioniques sont plus stables que les composés neutres correspondants. Nous proposons donc comme mécanisme de réaction une polycondensation faisant intervenir les espèces anioniques avec la formation ultérieure de chaînes linéaires et de cycles. Les résultats des calculs montrent aussi que l'énergie de stabilisation dans le processus d'hydroxylation est plus élevée pour les composés aluminés. L'analyse des recettes de fabrication des zéolithes mises en oeuvre dans les laboratoires de synthèse associée aux résultats de chimie quantique suggère l'assemblage de tétraèdres $Al(OH)_4^-$ et $Si(OH)_4$ comme mécanisme le plus probable dans la synthèse hydrothermale de zéolithes.

La dynamique des matériaux microporeux et, en particulier, des groupes OH qui sont connus comme centres catalytiques est le sujet de la deuxième partie de ce travail. Avec l'aide de la chimie quantique nous avons développé un champ de forces de valence pour la modélisation des vibrations de la silice et des aluminosilicates. La matrice des constantes de force en coordonnées cartésiennes, obtenue par calcul *ab initio* de petites molécules modèles, a été transformée en coordonnées internes en tenant compte des conditions de redondance.

Nous avons appliqué ce champ de force dans la simulation par dynamique moléculaire des vibrations du réseau de quelques zéolithes siliciques (sodalite, faujasite et silicalite) et dans l'étude de l'influence de la substitution de Si par Al dans la faujasite.

Pour les zéolithes siliciques, le champ de force *ab initio* donne une bonne correspondance avec les spectres expérimentaux. L'erreur moyenne entre les positions des maxima des spectres calculés et expérimentaux est de $20cm^{-1}$. La comparaison de nos résultats avec les champs de force développés par d'autres groupes montre que la méthode proposée est une approche cohérente, systématique, précise et relativement simple.

L'étude de la substitution par Al présente aussi une bonne correspondance entre les spectres calculés et expérimentaux. La relaxation des liaisons SiO autour d'un atome Si proche d'un atome Al a une influence importante sur la dynamique du réseau.

Le champ de forces *ab initio* a été appliqué dans l'étude de la dynamique des zéolithes hydratées, en particulier à la dynamique des groupes OH et OD du centre acide de Brönsted. L'application du champ de forces dérivé de calculs *ab initio* permet d'attribuer les maxima des spectres infrarouges et de diffusion de neutrons sur la base de couplages mécaniques. L'effet isotopique du mode de déformation de l'angle $SiOH$ est expliqué dans notre modèle par l'interaction du mode de déformation de l'angle $SiOD$ avec la vibration de valence de la liaison $SiO(D)$, sans faire appel à des résonances de Fermi comme cela avait été proposé antérieurement.

L'analyse des constantes de force nous permet de dire que les ponts $SiOHAl$ peuvent être considérés comme des groupes $SiOH$ liés à des sites acides de Lewis AlO_3 et l'analyse de la géométrie calculée montrant l'hybridation sp^2 de l'atome d'aluminium confirme également ce résultat.

Nous avons enfin appliqué le champ de force *ab initio* à l'étude du comportement vibrationel des groupes OH sur la surface de silice. Les spectres obtenus par dynamique moléculaire et par analyse en coordonnées normales nous permettent d'attribuer les maxima des spectres Raman et infrarouges de combinaison expérimentaux.

Le champ de forces développé dans ce travail décrit correctement la dynamique à

l'équilibre des groupes hydroxyles. Or les processus chimiques mettant en jeu la participation de ces groupes OH sont essentiellement des processus hors-équilibre. Par conséquent, l'étude d'un nouveau modèle de la dynamique hors-équilibre de parti-cules sur des surfaces fait l'objet de la troisième partie. Le modèle développé est destiné à terme à l'étude de la relaxation vibrationnelle des groupes OH sur des surfaces. On a choisi le système $H/Si(111)$ pour comprendre les mécanismes élémentaires de la dynamique hors-équilibre et tester cette approche théorique. Celle-ci combine les mécaniques classique et quantique sur la base de la théorie des perturbations et est développée pour les études de surface. Le mouvement de l'atome d'hydrogène est traité quantiquement, et la fonction d'autocorrélation de force a été calculée par la dynamique moléculaire. Les effets quantiques de vibrations du solide sont pris en compte par une renormalisation de la fonction d'autocorrélation classique. Nous avons trouvé que la relaxation se produit par l'excitation de trois quanta du mode de déformation $Si-Si-H$ et d'un phonon de 188 cm^{-1}. La vitesse de la relaxation et sa dépendance en fonction de la température sont en bonne correspondance avec les résultats expérimentaux.

L'information sur le temps de relaxation du niveau $v = 1$ du mode d'élongation de la liaison OH obtenue dans les expériences "pump-and-probe" est riche pour ce système, mais il n'existe pas de théorie permettant d'expliquer tous les faits expérimentaux sur la même base. Nous pensons que le champ de force développé dans ce travail et l'approche qui combine les mécaniques classique et quantique pour la dérivation de la vitesse de transition entre les niveaux vibrationnels peuvent être les premiers pas dans la construction d'un modèle plus élaboré. Les résultats du Chapitre 6 montrent que le travail réalisé pour l'obtention des coefficients d'anharmonicité correspondants est nécessaire.

En conclusion, l'application de la chimie quantique dans l'étude des différents aspects de la chimie et de la spectroscopie des aluminosilicates met en évidence la puissance de cet outil. Il permet d'obtenir des conclusions intéressantes concernant les processus microscopiques étudiés et apporte une aide notable à l'interprétation des données expérimentales.